TISSUE COMPARTMENTALIZATION AND TROPISM OF HIV-1

A Dissertation Presented

By

ROBIN LEIGH BRESE

Submitted to the Faculty of the
University of Massachusetts Graduate School of Biomedical Sciences, Worcester
in partial fulfillment of the requirements for the degree of

DOCTOR OF PHILOSOPHY

August 10, 2016

IMMUNOLOGY AND VIROLOGY PROGRAM

TISSUE COMPARTMENTALIZATION AND TROPISM OF HIV-1

A Dissertation Presented By

Robin Leigh Brese

This work was undertaken in the Graduate School of Biomedical Sciences

Immunology and Virology Program

The signature of the Thesis Advisor signifies validation of Dissertation content

_____
Paul Clapham, Ph.D., Thesis Advisor

The signatures of the Dissertation Defense Committee signify completion and approval as to style and content of the Dissertation

_____
Heinrich Gottlinger, M.D., Ph.D., Member of Committee

_____
Timothy Kowalik, Ph.D., Member of Committee

_____
Maria Zapp, Ph.D., Member of Committee

_____
Manish Sagar, M.D., External Member of Committee

The signature of the Chair of the Committee signifies that the written dissertation meets the requirements of the Dissertation Committee

_____
Trudy Morrison, Ph.D., Chair of Committee

The signature of the Dean of the Graduate School of Biomedical Sciences signifies that the student has met all graduation requirements of the School.

_____
Anthony Carruthers, Ph.D., Dean of the Graduate School of Biomedical Sciences

August 10, 2016

ACKNOWLEDGEMENTS

I would like to thank Paul Clapham and the members of the Clapham Lab. I am especially thankful for the friendship of Olivia O'Connell.

I am sincerely grateful for the members of my thesis and dissertation committees: Heinrich Gottlinger, Tim Kowalik, Trudy Morrison, Mohan Somasundaran, and Maria Zapp. Thank you for all of the mentorship, advice, and scientific discussions over the past few years. I truly appreciate it. I would also like to thank my external committee member, Manish Sagar.

I would like to thank my family, friends, and fellow graduate students for their support.

Thank you to my husband, Joseph Libutti, for everything.

ABSTRACT

Despite the development of effective antiretroviral treatments, there is still no cure for HIV-1. Major barriers to HIV-1 eradication include the diversity of intrapatient viral quasispecies and the establishment of reservoirs in tissue sanctuary sites. A better understanding of these populations is required for targeted treatments. While previous studies have examined the relationship between brain and blood or immune tissues, few have looked at and compared the properties of viruses from other tissue compartments. In this study, 75 full length HIV-1 envelopes were isolated from the frontal lobe, occipital lobe, parietal lobe, colon, lung, and lymph node of an HIV-1 infected subject. No envelopes could be amplified from the plasma or serum. Envelopes were subjected to genotypic and phenotypic characterization. Of the 75 envelopes, 53 were able to infect HeLa TZM-bl cells. The greatest proportion of non-functional envelopes was from the lung, a result of APOBEC-induced hypermutation. Lower frequencies of hypermutation were also observed in the occipital lobe and colon. Envelopes from regions of the brain were almost all macrophage tropic, while those from the body were predominantly non-macrophage tropic. All envelopes used CCR5 as a coreceptor. Phylogenetic analyses showed that sequences were compartmentalized inside the brain. These findings were also observed using PacBio next generation sequencing to examine 32,152 full length sequences. Envelopes from tissues of the body displayed greater variation in sequence length,

charge, and number of potential N-linked glycosylation sites in comparison to envelopes from tissues of the brain. Increased variation was also observed in IC50s for inhibition and neutralization assays using sCD4, maraviroc, b12, PG16, 17b, and 447-52D. The increased variation observed in envelopes from tissues outside the brain suggests that different pressures may be influencing the evolution of these viruses and emphasizes the importance of further studies in these tissue sites.

TABLE OF CONTENTS

LIST OF FIGURES

LIST OF TABLES

LIST OF THIRD PARTY COPYRIGHTED MATERIAL

Figure Number	Publisher	License Number
Figure 1.1	Springer	3897640362491
Figure 1.2	Elsevier	3897340639413
Figure 1.5	Nature Publishing Group	3897341478479

The following figures were reproduced from journals: No permission required

Figure Number	Publisher
Figure 1.3	AVERT
Figure 1.4	Annual Reviews

LIST OF ABBREVIATIONS

AIDS	Acquired Immune Deficiency Syndrome
amfAR	The Foundation for AIDS Research
APOBEC	apolipoprotein B mRNA editing enzyme catalytic polypeptide-like
AZT	azidothymidine
BBB	blood brain barrier
BC	blood cells
bnAb	broadly neutralizing antibody
bp	base pairs
C	colon
CA	capsid
CCR5	C-C chemokine receptor type 5
CD4bs	CD4 binding site
CDC	Centers for Disease Control
CRF	circulating recombinant form
CSF	cerebrospinal fluid
CXCR4	C-X-C chemokine receptor type 4
DMEM	Dulbecco's Modified Eagle Medium
DNA	deoxyribonucleic acid
EMBOSS	European Molecular Biology Open Software Suite
Env	envelope protein

env	envelope gene
ER	endoplasmic reticulum
ESCRT	endosomal sorting complex required for transport
FDA	Food and Drug Administration
FFU	focus forming units
FL	frontal lobe
Gag	group specific antigen
GALT	gut-associated lymphoid tissue
gp120	envelope surface glycoprotein
gp160	envelope polyprotein
gp41	envelope transmembrane glycoprotein
GPCR	G protein–coupled receptors
HAD	HIV-Associated Dementia
HIV	Human Immunodeficiency Virus
HR1	heptad repeat 1
HR2	heptad repeat 2
HTLV-III	Human T-Lymphotrophic Virus type III
IC50	concentration of inhibitor or antibody at which infection is reduced by 50%
IN	integrase
kb	kilobases
kD	kilodalton
L	lung

LANL	Los Alamos National Laboratory
LAV	Lymphadenopathy-Associated Virus
LN	lymph node
LTR	long terminal repeat
MA	matrix
MEGA	Molecular Evolutionary Genetics Analysis
MPER	membrane proximal external region
MSM	men who have sex with men
M-Tropic	macrophage tropic
NC	nucleocapsid
NCBI	National Center for Biotechnology Information
NDRI	National Disease Research Interchange
Nef	negative factor
NIH	National Institutes of Health
NNRTI	non-nucleoside reverse transcriptase inhibitor
NRTI	nucleoside reverse transcriptase inhibitor
NSI	non-syncytia inducing
OL	occipital lobe
PacBio	Pacific Biosciences
PBMC	peripheral blood mononuclear cell
PBS	phosphate-buffered saline
PCR	polymerase chain reaction

PIC	pre-integration complex
PL	parietal lobe
PNGS	potential N-linked glycosylation sites
PR	protease
R5	CCR5
Rev	regulator of virion expression
RLU	relative light units
RNA	ribonucleic acid
RRE	Rev response element
RT	reverse transcriptase
RT-PCR	reverse transcriptase polymerase chain reaction
sCD4	soluble CD4
SERINC	serine incorporator
SI	syncytia inducing
SIV	Simian Immunodeficiency Virus
SP1	spacer peptide 1
SP2	spacer peptide 2
STR	Short Tandem Repeat
TAR	trans-activation response region
Tat	trans-activator of transcription
T-Tropic	T cell tropic
UNAIDS	The Joint United Nations Programme on HIV/AIDS

Vif	viral infectivity factor
Vpr	viral protein r
Vpu	viral protein u
VSVG	Vesicular Stomatitis Virus G protein
WHO	World Health Organization
X4	CXCR4

CHAPTER I: INTRODUCTION

1.1 HIV and AIDS

1.1.1 Natural History and Discovery

On June 5, 1981, the Centers for Disease Control and Prevention (CDC) published a report documenting *Pneumocystis carinii* pneumonia in five healthy, young men who were homosexuals (CDC, 1981; Gottlieb et al, 1981). Doctors discovered that these patients also suffered from cytomegalovirus and mucosal candidiasis infections. This was surprising given that these types of opportunistic infections were usually limited to individuals with known immunocompromising diseases. Soon additional cases were described and doctors observed that these individuals had impaired T cell responses (Siegal et al, 1981). Initial reports concluded that this was an epidemic of the gay community, however similar patterns of opportunistic infections and acquired immunodeficiency emerged in other populations, including heterosexual men, women, and children (Masur et al, 1981; CDC, 1982a; CDC, 1982b; CDC, 1982c; CDC, 1982d; CDC, 1983). On September 24, 1982 the CDC called the disease Acquired Immune Deficiency Syndrome (AIDS) (CDC, 1982e). This was the start of a public health crisis and researchers began searching for the etiological agent responsible for the disease.

Luc Montagnier's group from the Pasteur Institute was the first to publish a paper describing the Lymphadenopathy-Associated Virus (LAV) as the probable cause of AIDS (Barre-Sinoussi et al, 1983). This was followed by papers from

Robert Gallo and colleagues at the National Cancer Institute describing the isolation of Human T-Lymphotrophic Virus type III (HTLV-III) from patients with AIDS (Gallo et al, 1984; Gelmann et al, 1984; Popovic et al, 1984). Soon it was determined that they, as well as many other groups, were describing the same virus, which became known as the Human Immunodeficiency Virus (HIV) (Coffin et al, 1986a; Coffin et al, 1986b).

HIV is a *lentivirus* and a member of the *Retroviridae* family. Its origins can be traced back to West Central Africa where two viruses, HIV-1 and HIV-2, arose from separate zoonotic events. HIV-1 is found throughout the world and is responsible for the global HIV pandemic, while HIV-2 is endemic only to regions of West Africa. Using phylogenic analyses and archived tissue and blood samples, the origins of HIV-1 have been mapped to Kinshasa, formerly Leopoldville, in the Democratic Republic of the Congo in the early part of the 20th century, no later than 1933 (Zhu et al, 1998; Korber et al, 2000; Worobey et al, 2008). From there HIV-1 strains spread across the globe. By the 1960s HIV-1 had arrived in the United States, though it would take almost twenty more years to be discovered (Gilbert et al, 2007).

HIV-1 is divided into four groups, which resulted from separate transmission events: M (Major or Main), N (New or non-M, non-O), O (Outlier), and P (Pending) (De Leys et al, 1990; Gurtler et al, 1994; Simon et al, 1998; Plantier et al, 2009; Vallari et al, 2010; Vallari et al, 2011). Genetic analyses have determined that HIV-1 group M and N viruses originated from Simian Immunodeficiency Virus (SIV) in

chimpanzees (Huet et al, 1990; Gao et al, 1999; Corbet et al, 2000; Keele et al, 2006). HIV-1 group P strains are most closely related to gorilla SIV, while the origin of group HIV-1 group O strains are unclear and may have come from chimpanzees or gorillas (Van Heuverswyn et al, 2006; Plantier et al, 2009; Takehisa et al, 2009; D'Arc et al, 2015). HIV-2 strains are genetically most similar to SIV from Sooty Mangabeys (Hirsch et al, 1989; Gao et al, 1992).

HIV-1 Group M viruses are responsible for the majority of HIV infections in the world and are grouped into nine subtypes, or clades: A, B, C, D, F, G, H, J, and K. Each clade is genetically distinct and dominant in specific geographic regions (Figure 1.1). In areas where more than one clade is present, viruses can recombine to create circulating recombinant forms (CRFs).

1.1.2 Transmission and Disease Progression

HIV-1 infection is acquired through three major modes of transmission: sexual contact, vertical transmission, or intravenous drug use. In the United States, approximately 63% of new infections, and 78% of new infections in men, are the result of men who have sex with men (MSM) (CDC, 2016). In contrast, 70% of new infections globally occur in sub-Saharan Africa, where the majority of infections arise from heterosexual sex (WHO, 2016). In about 80% of the transmissions, infection is established by a single viral variant. However, in the remaining cases two or more variants are transmitted (Keele et al, 2008). Once established, infection proceeds through acute, chronic, and late-stage phases (Figure 1.2).

During acute infection, the HIV-1 infected individual may experience flu-like symptoms. There is an initial spike in plasma HIV-1 RNA copies as the virus infects CD4+ T cells at infection sites and in immune tissues (Zhang et al, 1999). Virus then spreads to gut-associated lymphoid tissue (GALT) where large numbers of CD4+ T cells reside, become infected, and die (Veazey et al, 1998; Douek et al, 2003; Guadalupe et al, 2003; Brenchley et al, 2004; Li et al, 2005). Viral load drops to a stable setpoint during the chronic phase. At this time, the infected individual is asymptomatic and the virus remains latent. CD4+ T cell counts may briefly rebound, but eventually decline over a period of several years until the count is below 200 cells/mm^3. At this point the infected individual has entered the late-stage phase and is said to have Acquired Immune Deficiency Syndrome (AIDS). Plasma viremia will increase and the individual will become unable to mount an immune response to opportunistic infections and cancers, such as *Pneumocystis carinii* pneumonia, Kaposi's Sarcoma, and mucosal candidiasis, which will ultimately lead to death.

1.1.3 Global Health

The World Health Organization (WHO) reported that in 2014 there were approximately 37 million people living with HIV globally, with 2 million new infections that year (WHO, 2016). The Foundation for AIDS Research (amfAR) estimates that an additional 5,753 people contract HIV each day, around 240 every hour, with those in developing countries and members of minority populations

disproportionally affected (Figure 1.3) (amfAR, 2016; WHO, 2016). The impact of the HIV epidemic has most severely affected sub-Saharan Africa and infections in this region account for the majority of new infections globally (UNAIDS, 2016). Despite this, there have been dramatic improvements in HIV rates with new infections declining 35% since 2000 and HIV-related deaths declining 42% since a peak in 2004 (UNAIDS, 2016).

In efforts to continue towards the goal of ending the HIV/AIDS epidemic, the Joint United Nations Programme on HIV/AIDS (UNAIDS) has proposed an ambitious 90-90-90 plan with three objectives to be accomplished by the year 2020: 1) 90% of infected people will know their HIV positive status, 2) 90% of infected people will receive antiretroviral treatment, and 3) 90% of those on treatment will have viral suppression (UNAIDS, 2016). Presently, it is estimated that 54% of those who are infected do not know they are infected and only 41% of those infected are receiving antiretroviral treatment (amfAR, 2016; WHO, 2016).

Antiretroviral treatments were established soon after the onset of the HIV crisis with monotherapies as the first treatments. The first drug approved by the Food and Drug Administration (FDA) was azidothymidine (AZT) on March 19, 1987 (FDA, 2016a). Others soon followed. However monotherapies did not perform well, as rapidly replicating HIV-1 was able to acquire resistance mutations and drug failure and viral rebound would follow. In the mid-1990s, new reverse transcriptase inhibitors and protease inhibitors were discovered and for the first time

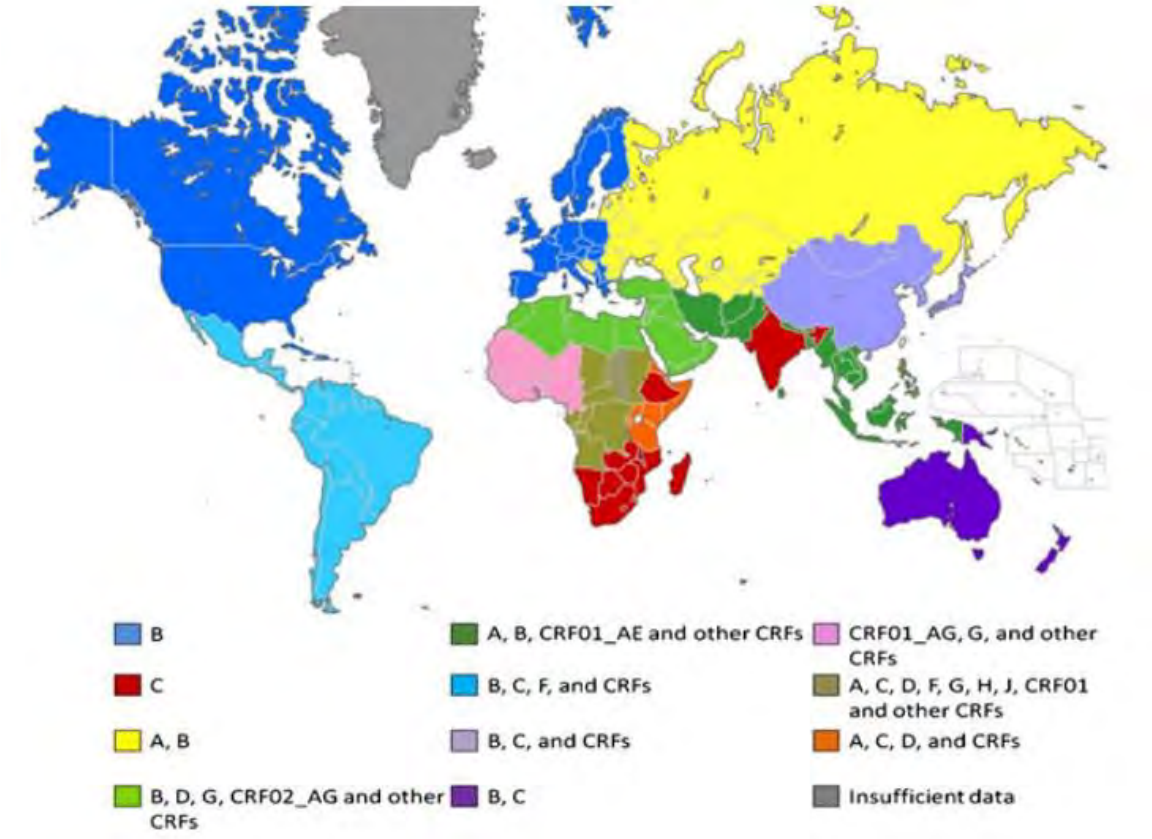

Figure 1.1 Global distribution of HIV-1 subtypes and circulating recombinant forms (CRFs) While subtype B is predominate in developed countries, subtype C and CRFs are more prevalent in developing countries and are responsible for the largest number of HIV-1 infections. (Reproduced from Tyor et al, 2013 with permission)

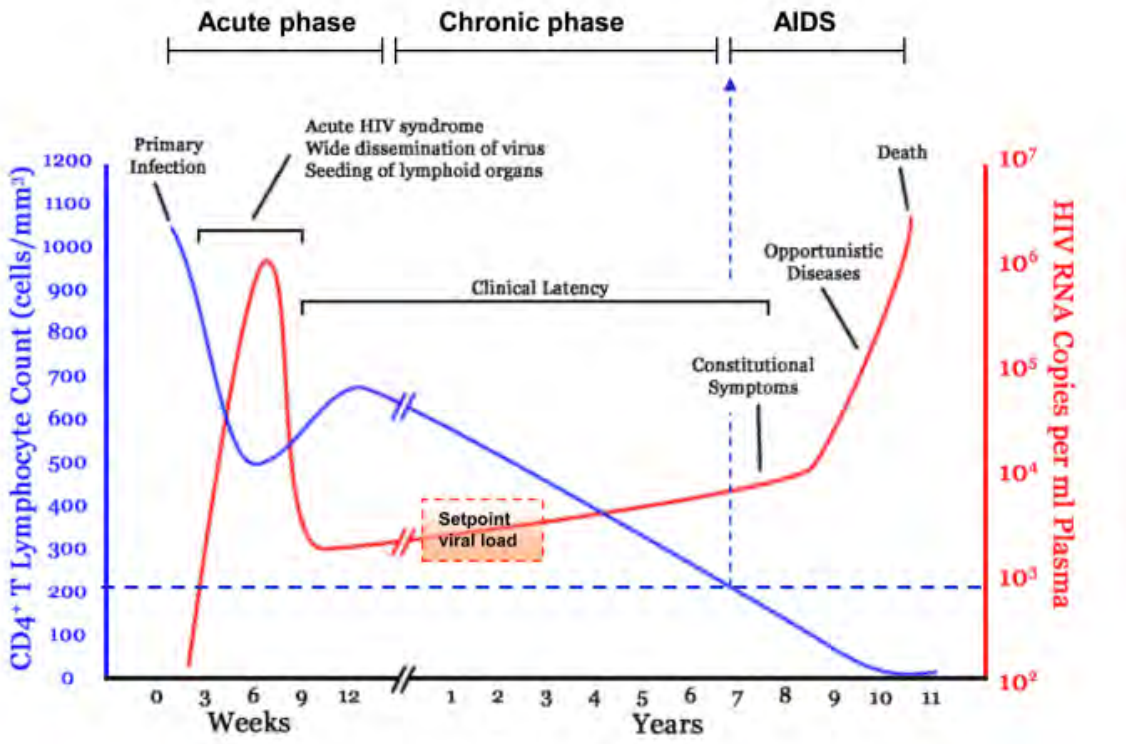

Figure 1.2 Course of typical HIV-1 infection During the acute phase of HIV-1 infection, there is an initial spike in viral RNA copies in the plasma and a decline in CD4+ T cells, which may be accompanied by flu-like symptoms. This is followed by the chronic phase, where the infected individual is asymptomatic, viral load drops to a setpoint, and the CD4+ T cell count may be stable for a long period before it begins to decline. Late stage infection, or AIDS, is defined by a CD4+ T cell count that has dropped below 200 cells/mm^3. This is when opportunistic infections occur, resulting in a rapid decline in health and eventually death. (Reproduced from An and Winkler, 2010 with permission)

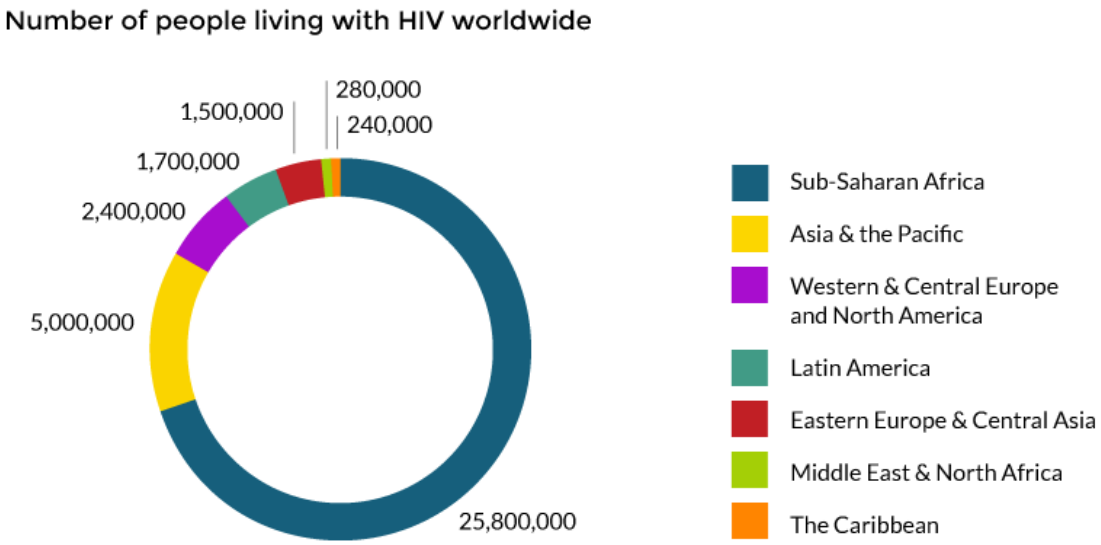

Figure 1.3 Number of HIV cases per region Sub-Saharan Africa accounts for the majority of HIV infections, with approximately 70% of the total global infections. (Reproduced from AVERT, 2016 with no permission required)

administered in combination, which greatly improved treatment outcomes (Collier et al, 1996; D'Aquila et al, 1996; Staszewski et al, 1996). Mathematical modeling was used to determine that three drugs in combination would provide sufficient protection against drug resistance (Frost and McLean, 1994; Coffin 1995; Nowak et al, 1997; Stengel, 2008). Currently, the FDA has 39 medications approved for the treatment of HIV (FDA, 2016b; NIH, 2016). These include Nucleoside Reverse Transcriptase Inhibitors (NRTIs), Non-nucleoside Reverse Transcriptase Inhibitors (NNRTIs), Integrase Inhibitors, Protease Inhibitors, Entry Inhibitors, Fusion Inhibitors, Pharmacokinetic Enhancers, and Combination Drugs (FDA, 2016b; NIH, 2016).

Antiretroviral treatments have improved the health and extended the lifespans of HIV-1 infected individuals. However a vaccine is needed to eradicate the virus and thus vaccine development has become a priority of global HIV research. However, vaccine design has been challenging and traditional methods have not worked (Kwong et al, 2002; Wei et al, 2003; Burton et al, 2004; Lu, 2006). There have been six HIV-1 vaccine phase IIb/III clinical trials, with all but one having no efficacy (Schiffner et al, 2013). Only RV144, known as the Thai Trial, experienced a modest 31.2% efficacy using a two vaccine prime boost model using the ALVAC HIV and AIDSVAX B/E vaccines (Rerks-Ngarm et al, 2009). A successful vaccine will likely require both T cell responses and the generation of broadly neutralizing antibodies (bnAbs). Progress has been hampered by several factors, including the highly glycosylated structure of the HIV-1 envelope protein,

which shields it from antibodies, the high diversity of HIV-1, which contributes to the emergence of escape mutants, and the fact that effective HIV-1 immunogens have not been established.

1.2 Genome and Viral Proteins

1.2.1 Genome Organization

The HIV-1 genome is approximately 9.7 kb and consists of a positive sense single stranded RNA genome which is packaged as a dimer within the virion. (Figure 1.4). The integrated proviral DNA genome is flanked by 5' and 3' long terminal repeats (LTRs), which contain sites important for regulating viral transcription and the replication cycle.

1.2.2 Enzymatic Proteins

The polymerase gene (*pol*) encodes the three enzymatic proteins of HIV-1: protease (PR), reverse transcriptase (RT), and integrase (IN). Pol is synthesized along with Gag as $Pr160^{gag\text{-}pol}$ polyprotein, resulting from a ribosomal frameshift, which is then cleaved by protease (Jacks et al, 1988).

Protease (PR)

PR is responsible for the cleavage of HIV-1 polyproteins Gag-Pol ($Pr160^{gag\text{-}pol}$), Gag ($Pr55^{Gag}$), Pol, and Env (gp160) into their constituent proteins.

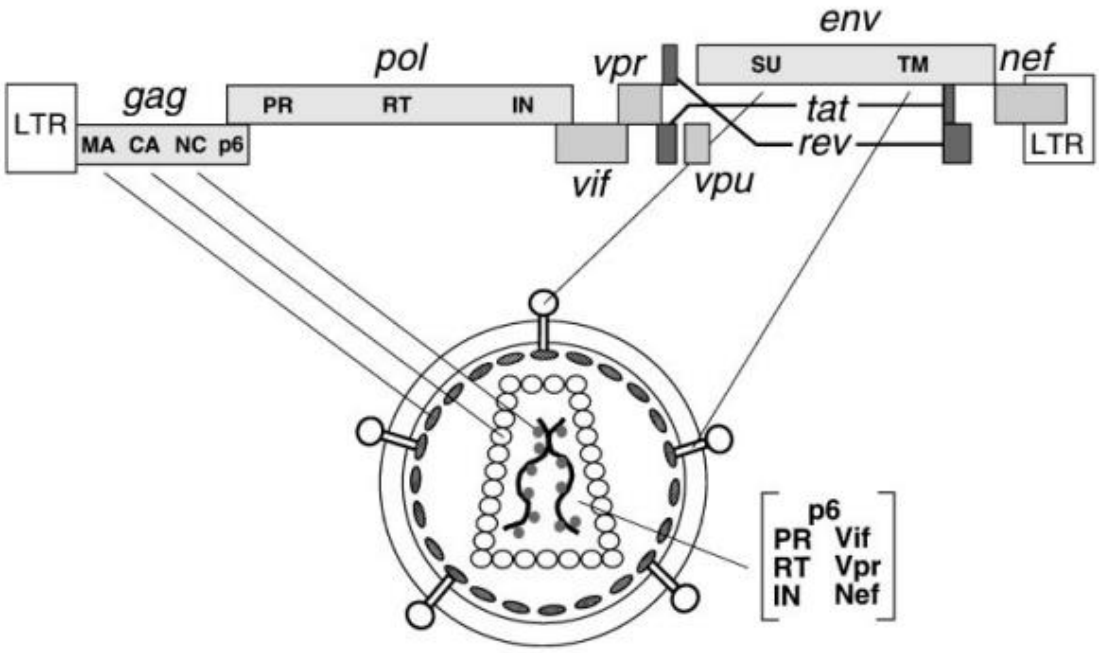

Figure 1.4 HIV-1 genome and virion structure Genome diagram depicts the organization of the HIV-1 genome with polyproteins and cleavage products noted. The locations of HIV-1 proteins are shown on the virion structure illustration. (Reproduced from Frankel and Young, 1998 with no permission required)

Reverse transcriptase (RT)

Retroviral reverse transcriptases function to convert the viral RNA template into DNA (Baltimore, 1970; Mizutani et al, 1970). In HIV-1 RT accomplishes this using RNA-dependent DNA polymerase activity, ribonuclease H, and DNA-dependent DNA polymerase activity. RT has a high error rate around 3 X 10^{-5}, which contributes to the diversity of HIV-1 (Preston et al, 1988; Mansky and Temin, 1995).

Integrase (IN)

Integrase is involved with mediating the incorporation of HIV-1 DNA into the host cell genome by facilitating the formation of the pre-integration complex (PIC) and insertion into the target chromosomal DNA (Bushman et al, 1990).

1.2.3 Structural Proteins

HIV-1 structural proteins include group-specific antigen (Gag) and envelope (Env) polyproteins and the proteins resulting from their cleavage by PR.

Group-specific antigen (Gag)

Gag is produced as polyprotein $Pr55^{Gag}$, which is cleaved into p17 matrix (MA), p24 capsid (CA), p7 nucleocapsid (NC), p6, and spacer peptides SP1 and SP2 by protease during maturation (Gottlinger et al, 1989). Gag is membrane associated in part via an N-terminal myristylation signal and recruits viral RNA and proteins to facilitate viral budding.

Matrix (MA)

MA is located at the N-terminal region of $Pr55^{Gag}$ and plays a role in incorporation of Env into virions (Dorfman et al, 1994a; Freed and Martin, 1995b; Freed, 1998; Kiernan et al, 1998). Following cleavage by protease, it remains associated with the plasma membrane in the virus particle.

Capsid (CA)

CA proteins surround the viral core in the virion, protecting the nucleocapsid, and are involved with assembly during the replication cycle (Dorfman et al, 1994b; Franke et al, 1994; Thali et al, 1994; Ganser-Pornillos et al, 2007). CA is involved in Gag oligomerization and plays a role in the uncoating process (Gamble et al, 1996; Luban, 1996; Gamble et al, 1997).

Nucleocapsid (NC)

NC is associated with the genomic RNA dimer and is flanked by SP1 and SP2 in the Gag and Gag-Pol precursors, which allow proper processing. An important function of NC is facilitating the packaging of viral RNA into new virus particles by recognizing the packaging signal (Poznansky et al, 1991; Harrison and Lever, 1992). NC also mediates reverse transcription (Lapadat-Tapolsky et al, 1993; Levin et al, 2005).

p6

p6 facilitates incorporation of Vpr into the virion and release of virus particles from the plasma membrane through interactions with the host ESCRT pathway

(Gottlinger et al, 1991; Paxton et al, 1993; Huang et al, 1995; Kondo et al, 1995; Strack et al, 2003).

Envelope (Env)

Env is synthesized as polyprotein gp160, which is then cleaved by host furin and furin-like proteases into the gp120 surface glycoprotein and gp41 transmembrane domain. Env interacts with the CD4 receptor and a coreceptor, typically CCR5 or CXCR4, to initiate membrane fusion and host cell infection (Maddon et al, 1986; McDougal et al, 1986; Deng et al, 1996; Feng et al, 1996; Berger et al, 1998).

1.2.4 Regulatory Proteins

Two proteins play essential regulatory roles in HIV-1 replication, trans-activator protein (Tat) and regulator of virion expression (Rev).

Trans-activator protein (Tat)

Tat is an RNA binding protein that is required for replication (Feng and Holland, 1988; Ruben et al, 1989; Roy et al, 1990). It enhances HIV-1 transcription through binding the trans-activation response region (TAR) on RNA stem-loops at the start of HIV-1 transcripts and promotes elongation of full length transcripts (Dayton et al, 1986; Fisher et al, 1986; Kao et al, 1987; Feinberg et al, 1991).

Regulator of virion expression (Rev)

Rev regulates HIV-1 protein expression by binding the Rev response element (RRE) on viral mRNAs and exporting them out of the nucleus (Felber et al, 1989;

Zapp and Green, 1989; Malim et al, 1989a; Malim et al, 1989b; Malim et al, 1990; Bartel et al, 1991).

1.2.5 Accessory Proteins

HIV-1 has four accessory proteins: Vif, Vpu, Vpr, and Nef. These proteins were originally labeled as “accessory” because they are not required for infection in many cell lines. However, they have now been found to play important roles in HIV-1 infection in vivo.

Virus infectivity factor (Vif)

Vif is an HIV-1 protein that enhances infectivity and is required for replication in primary cells, but not all cell lines (Gabuzda et al, 1992; von Schwedler et al, 1993; Hoglund et al, 1994; Liu et al, 1995). Vif counteracts human apolipoprotein B mRNA editing enzyme catalytic polypeptide-like 3G (APOBEC3G) (Sheehy et al, 2002; Harris et al, 2003; Lecossier et al, 2003; Mangeat et al, 2003; Zhang et al, 2003). It does this by ubiquitin mediated targeting of APOBEC3G to the proteasome, which results in its subsequent degradation (Marin et al, 2003; Sheehy et al, 2003; Yu et al, 2003).

Viral protein U (Vpu)

Vpu is a membrane protein that enhances virion release from the host cell surface (Cohen et al, 1988; Strebel et al, 1988, Klimkait et al, 1990; Gottlinger et al, 1993). This is accomplished by degrading CD4 molecules, which trap Env proteins in the

ER, and by counteracting host cell tetherin/BST-2, which retains budding virions on the cell surface (Willey et al, 1992; Neil et al, 2008; Van Damme et al, 2008).

Viral protein R (Vpr)

Vpr is a virion-associated protein that aids in the nuclear import of HIV-1 preintegration complexes (Cohen et al, 1990; Heinzinger et al, 1994). It is also involved with cell cycle arrest and replication in non-dividing cells (Jowett et al, 1995; Rogel et al, 1995; Cohen et al, 1996).

Negative factor (Nef)

Nef is an HIV-1 gene that is expressed early and enhances viral infectivity (Kim et al, 1989; Kestler et al, 1991; Miller et al 1994). Nef decreases immune cell recognition of infected cells by downregulating MHC class I molecules along with CD4, which also enhances Env incorporation and viral budding (Garcia and Miller, 1992; Aiken et al, 1994; Schwartz et al, 1996). In addition, the Gottlinger and Pizzato labs recently discovered that Nef prevents serine incorporator 3 and 5 (serinc3 and serinc5) from being included in the HIV-1 virion and that this correlates with enhanced infectivity (Rosa et al, 2015; Usami et al, 2015).

1.3 HIV-1 Replication Cycle

1.3.1 Replication

The HIV-1 replication cycle (Figure 1.5) can be divided into early and late phases. During the first steps of the early phase, HIV-1 enters host cells through receptor binding and membrane fusion, though there is some evidence that

endocytosis may also play a role (Miyauchi et al, 2009). The Env polyprotein gp160 is post translationally cleaved to surface protein gp120 and transmembrane protein gp41, which are non-covalently linked and are arranged in trimers on the viral surface (McCune et al, 1988; Lu et al, 1995). When a virus encounters a permissive cell, the Env trimers bind the host cell CD4 receptor through the CD4 binding site on gp120 (Maddon et al, 1986; McDougal et al, 1986; Kwong et al, 1998). Following engagement with the CD4 receptor, the Env undergoes a conformational change which allows interaction with a coreceptor (Kwong et al, 1998; Chen et al, 2005). C-C chemokine receptor type 5 (CCR5) and C-X-C chemokine receptor type 4 (CXCR4) are G protein–coupled receptors (GPCRs) and are the two main coreceptors for HIV-1 infection (Berger et al, 1998). They are expressed on HIV-1 target CD4+ T cells, macrophages, and dendritic cells. The Env then experiences another conformational change and a fusion pore begins to form (Markosyan et al, 2003). During this conformational change, N-terminal heptad repeat 1 (HR1) and C-terminal heptad repeat 2 (HR2) of gp41 interact forming a stable six helix bundle structure (Chan et al, 1997; Weissenhorn et al, 1997; Melikyan et al, 2000). Membrane fusion proceeds, allowing the viral core to enter the cytoplasm of the host cell.

Once inside the host cell, the viral core goes through an uncoating process to expose a reverse transcription complex (RTC) consisting of viral RNA, MA, CA, NC, RT, IN, and Vpr. HIV-1 genomic RNA is then bound by tRNA primer Lys3 at a primer binding site approximately 180 nucleotides from the 5’ end to initiate

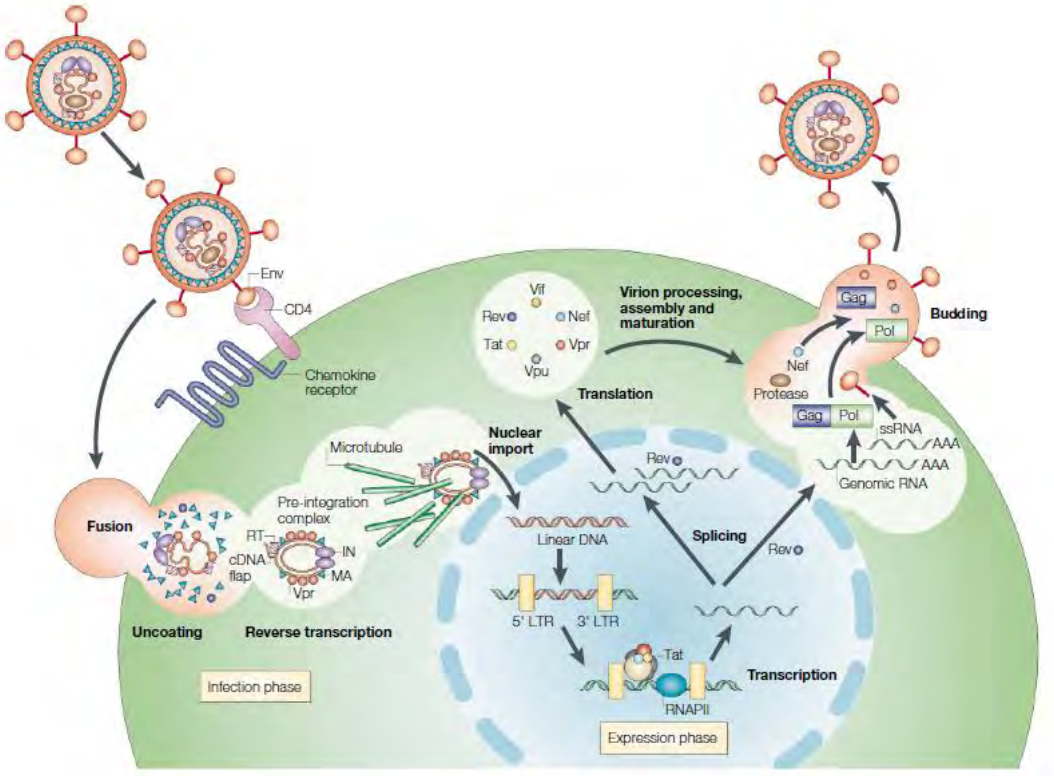

Figure 1.5 HIV-1 replication cycle HIV-1 binds to the host cell CD4 receptor and a coreceptor, usually CCR5 or CXCR4. Following membrane fusion, the viral core enters the cell and an uncoating process occurs. Reverse transcriptase synthesizes cDNA from viral RNA, which then becomes part of a pre-integration complex that is shuttled into the nucleus. Viral cDNA is integrated into the host cell DNA and then gives rise to HIV-1 proteins from unspliced genomic RNA, singly spliced mRNAs (ssRNA), and fully spliced mRNAs. These proteins, along with HIV genomes, are assembled and packaged into new virions, which bud off from the plasma membrane. Finally, polyproteins are cleaved by protease during the maturation process. (Reproduced from Peterlin and Trono, 2003 with permission)

DNA synthesis (Robert et al, 1990). An RNA-DNA hybrid molecule is formed, providing a substrate for RNase H, which then degrades the RNA strand. Finally, a second strand of DNA is synthesized via the RT DNA-dependent polymerase activity.

After a cDNA copy of the viral genome has been made, the pre-integration complex (PIC) is formed and is imported into the nucleus (Bowerman et al, 1989). IN facilitates the incorporation of viral DNA into the host's genome through DNA cutting, joining, and repair mechanisms (Brown et al, 1987; Fujiwara and Mizuuchi, 1988; Brown et al, 1989). The integrated HIV-1 genome, called a provirus, is now a permanent part of the host cell's genome and can be replicated using host cell machinery.

The late phase of replication begins after integration and includes the expression of viral genes, viral budding, and maturation. Viral RNAs are exported to the cytoplasm, proteins are translated and trafficked to the plasma membrane where they are then assembled, and virus particles bud off from the cell. This process is completed using the endosomal sorting complex required for transport (ESCRT) pathway of the host cell, which is recruited by the p6 domain of the Gag polyprotein. After budding occurs, the Gag polyprotein is cleaved by PR during the maturation process.

1.3.2 Evolution and Diversity

HIV-1 has extraordinary genetic diversity based on several aspects of its replication cycle. HIV-1 RT lacks proofreading mechanisms and has an error rate of 3 x 10^{-5} (Preston et al, 1988; Mansky and Termin, 1995). This allows for mutations to arise in every replication cycle. During replication, recombination also occurs allowing for more genetic diversity (Jetzt et al, 2000; An and Telesnitsky, 2002; Rhodes et al, 2003; Charpentier et al, 2006; Chen et al, 2006; Mild et al, 2007; Zhang et al, 2010; Brown et al, 2011; Immonen et al, 2015; Sanborn et al, 2015). Considering that an infected cell can produce between 3.5 x 10^3 and 2.4 x 10^5 virus particles during the course of infection, it is clear how quickly genetic changes can accumulate (Ho et al, 1995; Wei et al, 1995; Althaus et al, 2014). Other factors shaping viral evolution include pressures from neutralizing antibodies, host restriction factors, antiretroviral drug treatment, and coinfections.

In a recent study examining full length genomic sequences, it was estimated that average nucleotide diversity was approximately 50% between HIV-1 and HIV-2, 37.5% between HIV-1 groups, 14.7% between HIV-1 subtypes, 8.2% within a single subtype, and less than 1% within an individual (Li et al, 2015). However, these numbers could be lower or higher in specific cases. For example, the *env* gene is particularly polymorphic and viruses within a single individual can change over 10% of their *env* sequence during an HIV-1 infection (Wolinsky et al, 1996; Shankarappa et al, 1999). The result of this genetic diversity is that a single HIV-1 positive individual is infected by populations of related but genetically distinct viral

variants called quasispecies (Goodenow et al, 1989). These quasispecies can have different properties, such as coreceptor use and cell tropism, discussed further below.

1.4 HIV-1 Envelope

The Env glycoprotein is synthesized on the rough endoplasmic reticulum (RER) from a bicistronic mRNA encoding both Env and Vpu (Hunter and Swanstrom, 1990; Freed and Martin, 1995a). Env gp160 polyprotein is targeted to the RER membrane by an N-terminal signal sequence, which is cotranslationally cleaved. Env then remains anchored to the membrane by a hydrophobic sequence in the gp41 domain (Berman et al, 1988; Haffar et al, 1988). Glycosylation occurs during translation, adding predominately N-linked oligosaccharides, but some O-linked oligosaccharides as well (Leonard et al, 1990; Bernstein et al, 1994). The gp160 polyproteins oligomerize into trimers and traffic to the Golgi where they are cleaved by furin and furin-like proteases into gp120 and gp41 proteins at a conserved K/R-X-K/R-R sequence (McCune et al, 1988; Freed et al, 1989; Hallenberger et al, 1992; Sen et al, 2007). The gp120 and gp41 proteins, associated by non-covalent interactions, are then trafficked to the plasma membrane where they are incorporated into virions and are essential for infectivity. Trimer conformation dynamics are not well understood, but trimers may adopt more open or closed states, or oscillate between these two, which could affect

receptor binding and antibody neutralization (Kwong et al, 2002; Davenport et al, 2013; Julien et al, 2013; Lyumkis et al, 2013; Guttman et al, 2015).

The gp120 glycoprotein is composed of five regions of variable sequences (V1-V5) and five regions of comparatively constant sequences (C1-C5) (Starcich et al, 1986; Willey et al, 1986). Amino acids in different constant regions of gp120 are responsible for CD4 binding (Kowalski et al, 1987; Lasky et al, 1987; Olshevsky et al, 1990). Crystal structures have shown CD4 making contact with gp120 at 26 different residues (Kwong et al, 1998). The V3 loop region of gp120 confers coreceptor specificity (Hwang et al, 1991; Shioda et al, 1991; Cann et al, 1992).

The gp41 transmembrane glycoprotein plays an important role in mediating fusion of the viral and host cell membranes to allow the viral core to enter the host cell. It contains an extracellular domain with an N-terminal fusion peptide, two heptad repeat regions (HR1 and HR2), and a membrane proximal external region (MPER) (Bosch et al, 1989; Freed et al, 1990; Muñoz-Barroso et al, 1999; Salzwedel et al, 1999). In addition, gp41 has a transmembrane domain, which anchors Env in the membrane, and a long C-terminal cytoplasmic tail.

1.5 Tropism

Initial efforts to classify HIV-1 isolates by tropism were based on the ability of variants to induce syncytia in T cell lines, such as MT-2 cells. Syncytia inducing (SI) variants were defined as T cell tropic (T-tropic) and the non-syncytia inducing (NSI) variants were defined as macrophage tropic (M-tropic) (Gartner et al, 1986;

Tersmette et al, 1988). Studies aimed at identifying potential coreceptors on permissive cell types found that the chemokines RANTES, MIP-1 alpha, and MIP-1 beta could inhibit HIV-1 infection (Cocchi et al, 1995). This gave researchers clues that lead to the discovery of the coreceptors. The CXCR4 receptor, originally called LESTR or fusin, was the first to be identified and was defined as the predominant coreceptor for T-tropic HIV-1 variants (Feng et al, 1996). Soon after, it was discovered that the reason that RANTES, MIP-1 alpha, and MIP-1 beta inhibited infection was because they were binding to the CCR5 coreceptor and this was presumed to be the coreceptor for M-tropic HIV-1 variants (Deng et al, 1996).

This, however, turned out to be an incomplete story and variants described as NSI on cell lines were observed forming syncytia on primary CD4+ T cells and replicating in MT-2 cells (Forte et al, 1994; Todd et al, 1995; Berger et al, 1998; Goodenow and Collman, 2006). The syncytia induction tests being used to categorize viral variants were performed using the MT-2 cell line, which only expressed the CXCR4 coreceptor and not CCR5, though this was not known at the time (Koot et al, 1992). Thus this test had really been a test of coreceptor use and not cell tropism. A new definition of tropism was proposed based on coreceptor use with CCR5-using variants (R5), CXCR4-using variants (X4), and dual-tropic variants (R5X4) (Berger et al, 1998). In addition, these variants could be defined as T-tropic or M-tropic. Current tropism tests now include genotype analyses using prediction algorithms, such as WebPSSM and Geno2Pheno (Jensen et al, 2003; Sing et al, 2007), that predict whether an Env uses CCR5 or CXCR4, and

phenotype analyses, such as testing infection on primary cells or cell lines expressing one or both coreceptors.

T-tropic R5 variants are almost always the transmitted/founder viruses in a new infection (Keele et al, 2008; Salazar-Gonzalez et al, 2009; Wilen et al, 2011; Ochsenbauer et al, 2012). Tropism may then switch during disease progression and X4 variants emerge in approximately 50% of patients. There is some evidence that R5X4 strains represent an intermediate in the evolution of X4 variants (Yi et al, 1999; Huang et al, 2007; Irlbeck et al, 2008).

Coreceptor use has been mapped mainly to the V3 region of gp120 (O'Brien et al, 1990; Hwang et al, 1991; Shioda et al, 1991; Milich et al, 1997; Nelson et al, 1997; Nelson et al, 2000; Hoffman et al, 2002; Jensen et al, 2003). Accordingly, R5- and X4-using variants have V3 loops with different properties. For example, X4 variants have an overall higher positive charge compared to R5 variants (Fouchier et al, 1992). This may be in part due to changes to basic amino acids at positions 11 or 25 in the V3 region, which is associated with X4 tropism (Resch et al, 2001).

Once X4 variants are established in the HIV-1 population, disease prognosis is poor (Tersmette et al, 1989; Koot et al, 1993; Richman and Bozzette, 1994; Connor et al, 1997; Blaak et al, 2000). The reason for a rapid decline of CD4+ T cells and acceleration to AIDS and death is not known. One hypothesis is that as variants gain the ability to use the X4 receptor, they are able to rapidly deplete previously non-permissive T cell populations.

While the T cell population expresses both R5 and X4, there is a significant difference in the expression of R5 and X4 in T cell subsets: memory T cells express both R5 and X4 and naïve T cells only express X4 (Blaak et al, 2000). This means that in the overall T cell population, up to 90% of the T cells may be expressing X4, but only 15-35% may be expressing the R5 receptor (Bleul et al, 1997; Berkowitz et al, 1998; de Roda Husman et al, 1999). Given the abundance of permissive cells, it is unclear why X4 variants do not emerge sooner during the course of infection. It is possible that R5 variants out compete X4 variants by infecting CCR5+ CD4+ T cells recruited to the sites of infection or that immune pressures select against X4 variants. This is supported by the observation that X4 variants are more sensitive to CD4 binding site (CD4bs) antibodies and that they emerge later in disease progression when immune competence wanes (Bunnik et al, 2007). However, this explanation does not account for why X4 variants would not be transmitted and be present at earlier time points.

Cell tropism may also change as disease progression occurs, allowing viral variants within an individual to have different cell tropisms (Koyanagi et al, 1987). Though transmitted variants are usually T-tropic, M-tropic variants often arise and may predominate in some tissues. For example, R5 variants from the brain have higher frequency of M-tropism than R5 variants from blood and immune tissues do (Gorry et al, 2002; Peters et al, 2004; Peters et al, 2006; Peters et al, 2007). Macrophage tropism is associated with the ability to use low levels of CD4 and may become more prevalent in late stage infection (Li et al, 1999; Tuttle et al, 2002;

Gray et al, 2005; Thomas et al, 2007). Though they are often R5-using, macrophage tropic R5X4 and X4 variants have been isolated (Simmons et al, 1996; Simmons et al, 1998; Yi et al, 2003; Gray et al, 2009).

Several regions of gp120 have been implicated in the development of macrophage tropism, including regions flanking the CD4bs, V1V2, C2, and V4 (Koito et al, 1994; Imamichi et al, 2002; Walter et al, 2005; Dunfee et al, 2006; Dunfee et al, 2007; Duenas-Decamp et al, 2009; Musich et al, 2011). Specifically, an asparagine at position 283, loss of an N-linked glycosylation site at 386, and an E153G substitution have been identified as determinants of macrophage tropism (Dunfee et al, 2006; Dunfee et al, 2007; Musich et al, 2011). It has also been observed that macrophage tropic variants isolated from brain tissue have gp120s with lower charges in comparison with non-macrophage variants from immune tissues from the same patient (Gonzalez-Perez et al, 2012).

1.6 Compartmentalization

As discussed above, HIV-1 has extreme genetic diversity and this allows populations of viral quasispecies to arise with mutations that allow them to use different coreceptors, have different cell tropisms, develop drug resistance, and escape antibody neutralization, among other viral properties. Quasispecies may be particular to a specific tissue site, or compartment, and are said to be compartmentalized.

Compartmentalization may be the result of the availability of particular cell types in a specific tissue compartment, the presence or absence of antibodies (e.g., the brain is immune privileged), tissue specific coinfections (e.g., tuberculosis in the lungs), or the concentrations of antiretroviral drugs within in a tissue. Several studies have shown that HIV drugs do not penetrate tissues uniformly. This has been well documented in the brain, where drugs may be unable to cross the blood brain barrier (BBB), allowing the brain to potentially serve as a sanctuary site with continued replication despite controlled viremia in the plasma (Nowacek and Gendelman, 2009; Varatharajan and Thomas, 2009; Gomes et al, 2014). Recent studies have also shown that antiretroviral treatments can be lower in lymphatic tissues than blood, which similarly allows for continued replication even in patients on therapy (Fletcher et al, 2014; Lorenzo-Redondo et al, 2016). Yet another study reported that patients with undetectable viral loads in their plasma had virus detected in their semen and this correlated with lower semen drug concentrations (Lorello et al, 2009). This could have important implications for HIV-1 transmission.

The HIV-1 Env is particularly susceptible to selection pressures due to its position on the virion surface, and thus exposure to antibodies, tissue microenvironments, and host target cells. HIV-1 envelope compartmentalization has been observed in peripheral blood mononuclear cells (PBMCs), brain tissues/cerebrospinal fluid (CSF), immune tissues, male and female genital tracts, lung, and possibly other tissues (reviewed in Blackard, 2012).

1.7 Scope of Thesis

The emergence of diverse populations of intrahost viral quasispecies is a hallmark of HIV-1 infection. Understanding how these population behave and their ability to evade immune responses, infect different cell types, and establish reservoirs is essential to producing effective antiretroviral drugs, as well the development of curative treatments and a vaccine. To this end, the HIV-1 envelope remains a critically important target. Despite this, there have been no studies to date looking at full length envelopes from multiple tissues from a single HIV-1 infected individual with both genotype and phenotype characterization.

In this study, 75 full length envelopes were examined from the frontal lobe, occipital lobe, parietal lobe, colon, lung, and lymph node of an HIV-1 positive subject who died from end stage AIDS. Genetic studies were conducted where sequences were characterized based on the presence of features known to disrupt function (e.g., insertions, deletions, and premature stop codons) and examined for mutations known to change tropism (e.g., N283, loss of an N-linked glycosylation site at 386, E153G, changes to V3 loop, etc). In addition, length, charge, and number of potential N-linked glycosylation sites (PNGS) were calculated for specific *env* regions. Sequences were analyzed for hypermutation and recombination and assembled into phylogenetic trees to assess compartmentalization. Functional studies were used to characterize phenotypes of each Env, including functionality, coreceptor use, cell tropism, and susceptibility to inhibition by a panel of inhibitors and monoclonal antibodies. Finally, state of the

art Pacific Biosciences next generation sequencing was used to examine thousands of full length *envs* from each tissue, the first time this has been done with full length proviral HIV-1 *env*.

The results of this study provide new insights into HIV-1 populations in different tissue compartments, an area of HIV research that has not been adequately addressed. Analyzing these populations will provide a better understanding of infection in different tissues and how viral variants at these sites evolve differently. This could lead to more targeted drug regimens and aid in vaccine development.

CHAPTER II: MATERIALS AND METHODS

2.1 HIV-1 Positive Subject and Tissues

HIV-1 positive tissue was obtained from the National Disease Research Interchange (NDRI; Philadelphia, PA). Tissue was harvested postmortem and stored at -80°C until use. For this study, six tissues were examined from Subject 162, along with blood plasma and serum (Table 2.1). These included three brain lobes (frontal lobe (FL), occipital lobe (OL), and parietal lobe (PL)), colon (C), lung (L), and lymph node (LN). Subject 162 died of end stage AIDS.

2.2 Nucleic Acid Extraction

DNA was harvested from tissues and cells from plasma and serum using the QIAamp DNA Mini Kit (QIAGEN) as described by the manufacturer's protocol. DNA was eluted in 300 µl nuclease free, PCR grade water and stored at -80°C.

RNA was isolated from plasma and serum using the High Pure Viral RNA Kit (Roche), eluted in 40 µl nuclease free, PCR grade water, and stored at -80°C.

2.3 PCR

Limiting Dilution Amplification

Nested PCR reactions were performed using limiting dilution amplification of HIV-1 proviral DNA. For the first PCR, outer primers RevenvA and EnvN were used (Table 2.2). Inner primers RevenvB_TOPO and Env-lo were used for the

Subject	A/R/S	Tissues	Plasma Viral Load	CD4 Count	HIV Treatment
162	53/B/F	Brain - Frontal Lobe Brain - Occipital Lobe Brain - Parietal Lobe Colon Lung Lymph Node Plasma Serum	undetectable (<40 copies/ml)	733 cells/µl (5 months prior to death)	Emtricitabine Tenofovir Lopinavir Ritonavir Kaletra

Table 2.1 Subject 162 data Tissue was obtained from the National Disease Research Interchange (NDRI; Philadelphia, PA). A/R/S = age/race/sex. Viral load testing was performed at the Ann & Robert H. Lurie Children's Hospital of Chicago.

Primer	Use	Sequence	Reference
EnvN	LD/RT-PCR/PacBio outer	CTG CCA ATC AGG GAA GTA GCC TTG TGT	Gao et al, 1996
RevenvA	LD/PacBio outer	TAG AGC CCT GGA AGC ATC CAG GAA G	Salazar-Gonzalez et al, 2008
RevenvB_TOPO	LD inner	CAC CTA GGC ATC TCC TAT GGC AGG AAG AAG	Clapham Lab
Env-lo	LD inner	GTT TCT TCC AGT CCC CCC TTT TCT TTT AAA AAG	Revilla et al, 2011
SG3-up	RT-PCR	TAC AGT GCA GGG GAA AGA AT AATA GAC ATA ATA	Revilla et al, 2011
SG3-lo	RT-PCR	AGA CCC AGT ACA GGC RAR AAG C	Revilla et al, 2011
Vif-2fw	RT-PCR	TAG GGA TTA TGG AAA ACA GAT GGC AG	Clapham Lab
TAT-1	RT-PCR	CCT AAA CTA GAG CCC TGG AAC CAT CC	Lee et al, 2000
T7*	sequencing/colony screen	TAA TAC GAC TCA CTA TAG GG	GENEWIZ universal primer
BGHR*	sequencing	TAG AAG GCA CAG TCG AGG	GENEWIZ universal primer
GP41F1	sequencing	GAG CAG CAG GAA GCA CTA T	Clapham Lab
GP41F2	sequencing	TGA ATA GAG TTA GGC AGG G	Clapham Lab
GP41R1	sequencing	ATA GTG CTT CCT GCT GCT C	Clapham Lab
GP41R1Yang	sequencing	AAC GAC AAA GGT GAG TAT CCC TGC CTA A	Yang et al, 1999
M5	sequencing	CCA ATT CCC ATA CAT TAT TGT GCC CCA GC	Takehisa et al, 1998
M5R	sequencing/colony screen	CCA GCC GGG GCA CAA TAA TGT ATG GG	Takehisa et al, 1998
GP41R2	sequencing	CCC TGC CTA ACT CTA TTC A	Clapham Lab
V1V2A1F	sequencing	CAG ATG CTA AAG CAT ATG	Clapham Lab
V1V2A2F	sequencing	TCA AAG CCT AAA GCC ATG	Clapham Lab
V1V2A3F	sequencing	CCC ATA CAT TAT TGT GCC	Clapham Lab
V1V2A4F	sequencing	TCA ACT CAA CTG CTG TTA	Clapham Lab
FL3F	sequencing	GCT GTG GAA AGA TAC CTA	Clapham Lab
4VF	sequencing	GAC CCA GAA ATT GTA ATG C	Clapham Lab
470F	sequencing	CTT TCA ATG TCA CCA CAG GC	Clapham Lab
1200F	sequencing	AGT TTT AAT TGT GGA GGG G	Clapham Lab
2240F	sequencing	GAA GAA GAA GGT GGA GAG	Clapham Lab
2310F	sequencing	TCT AGA TCG ACC TGA AGA GC	Clapham Lab
2470F	sequencing	TCT AGA TCG ACC TGA AGA GC	Clapham Lab
2170R	sequencing	GGT GAG TAT CCC TGC CTA ACT C	Clapham Lab
2180R	sequencing	CGG GTC TGA AAC GAT AAT GG	Clapham Lab
2320R	sequencing	GGC TCT TCA GGT CGA TCT AG	Clapham Lab
2850R	sequencing	CCT CTT GTG CTT CTA GCC AGG C	Clapham Lab
PacBioF-long	PacBio inner	GAG CAG AAG ACA GTG GCA ATG AGA GTG A	Clapham Lab
PacBioR-long	PacBio inner	TTG ACC ACT TGC CAC CCA TCT TAT AGC A	Clapham Lab

Table 2.2 HIV-1 *env* primers Primers were used for limiting dilution PCR (LD), RT-PCR, to colony screen, for sequencing (Sanger), and PacBio sequencing. Primers marked with an asterisk were used for *env* sequencing, but were located in the pcDNA 3.1D/V5-His-TOPO plasmid.

second PCR (Table 2.2). The Phusion High-Fidelity DNA Polymerase Kit (New England BioLabs) was used according to the manufacturer's protocol for 50 µl PCR reactions using "Phusion" thermocycler program with 40 cycles (Table 2.3). DNA was serially diluted to determine the concentration at which less than 30% of the reactions were positive. At this concentration, there is a >80% chance of PCR products being derived from single genomes and thus avoiding the generation of PCR generated recombinants during the amplification (Salazar-Gonzalez et al, 2008). Recent studies have demonstrated that there are minimal differences between products of limiting dilution PCR and bulk PCR (Etemad et al, 2015). However, limiting dilution PCR was used to be consistent with previously used methods and because recombination analyses were performed. PCR reactions were checked for positives by running 5 µl out on a 1.0% agarose gel with 0.5 µg/ml ethidium bromide in TAE buffer. Positive bands were approximately 3 kb, as determined using a 1 kb ladder for reference (New England BioLabs).

RT-PCR

RT-PCR was used to amplify *env* from viral RNA isolated from Subject 162 plasma and serum. SuperScript III One-Step RT-PCR System with Platinum Taq DNA Polymerase (Invitrogen) was used to synthesize cDNA and amplify *env* in a one-step PCR using primers SG3-up, SG3-lo, Vif2F, TAT1, and EnvN (Table 2.2) and the "RT-PCR" thermocyler program with 40 cycles (Table 2.3). RNA dilutions were used to achieve limiting dilution conditions, as described above. The second PCR was the same as described above, using primers RevenvB_TOPO and

Phusion		
Step	**Temperature**	**Time**
1	98°C	30 seconds
2	98°C	10 seconds
3	70°C	30 seconds
4	72°C	1.5 minutes
5	Repeat steps 2-4	40x
6	72°C	7 minutes
7	4°C	∞

RT-PCR		
Step	**Temperature**	**Time**
1	42°C	60 minutes
2	94°C	2 minutes
3	94°C	20 seconds
4	60°C	30 seconds
5	72°C	4 minutes
6	Repeat steps 3-5	40x
7	72°C	10 minutes
8	4°C	∞

General		
Step	**Temperature**	**Time**
1	95°C	5 minutes
2	95°C	1 minute
3	55°C	1 minute
4	72°C	1 minute
5	Repeat steps 2-4	40x
6	72°C	7 minutes
7	4°C	∞

PacBio		
Step	**Temperature**	**Time**
1	95°C	1 minute
2	95°C	30 seconds
3	68°C	3 minutes
4	Repeat steps 2-3	35x
5	70°C	10 minutes
6	4°C	∞

Table 2.3 Thermocycler programs used for PCR Programs were used for amplifying *envs* from patient tissues (Phusion), for RT-PCR to amplify *envs* from plasma and serum (RT-PCR), for colony screening to detect *env*+ clones (General), and to produce amplicons for Pacific Biosciences sequencing (PacBio).

Env-lo (Table 2.2), along with the Phusion High-Fidelity DNA Polymerase Kit (New England BioLabs) and Phusion thermocycler program with 40 cycles (Table 2.3).

2.4 Cloning

When PCR reactions had fewer than 30% of the reactions positive, the positive reactions were run out on a 1.0% agarose gel with 0.8% crystal violet in TAE buffer. Bands were purified using the QIAquick Gel Extraction Kit (QIAGEN) as described by the manufacturer. PCR products were eluted in 30 µl nuclease free, PCR grade water and stored at -20°C until use.

Eluted PCR products were ligated into pcDNA 3.1D/V5-His-TOPO using TA Expression Kit (Invitrogen). Ligation reactions were performed as directed by the manufacturer using the following reaction mix:

1 µl PCR product
1 µl pcDNA 3.1D/V5-His-TOPO vector
1 µl salt solution
3 µl water

Ligation products were transformed into TOP10 chemically competent cells (Invitrogen) and then plated on LB plates with 100 µg/ml carbenicillin to select positive clones.

Clones were checked for positive inserts using Go Taq Green Master Mix (Promega) with primers T7 and M5R (Table 2.2) using the “General” thermocycler program with 40 cycles (Table 2.3). PCR reactions were run on a 1.0% agarose gel with 0.5 µg/ml ethidium bromide in TAE buffer and compared to a 100 kb ladder (New England BioLabs) for confirmation of an approximately 1 kb product.

2.5 Sanger Sequencing

Positive colonies were grown in LB with 100 µg/ml ampicillin cultures overnight, pelleted by centrifugation, and plasmid DNA was isolated using the QIAprep Miniprep Kit (QIAGEN). DNA was eluted in 50 µl nuclease free, PCR grade water and stored at -20°C until use.

Each clone was sequenced in both directions using a series of primers directed to conserved regions of the *env* sequence (Table 2.2). Sanger sequencing was performed by GENEWIZ (South Plainfield, NJ). The first eight sequencing primers in Table 2.2 were used for every clone and then additional primers were used as needed until the DNA was sequenced completely in both directions.

2.6 Sequence Analyses

Alignments were constructed for each envelope using SeqMan Pro (DNASTAR) and sequence traces were checked for quality using FinchTV (Geospiza). They were assembled into consensus sequences and checked against the BLAST databases at the National Center for Biotechnology Information (NBCI) and Los Alamos National Laboratory (LANL) to ensure that they were not generated from laboratory contamination.

Sequences were then examined for mutations known to affect tropism (e.g., N283, loss of an N-linked glycosylation site at 386, E153G, changes to V3 loop, etc), length and charge of *env* regions, and changes in potential N-linked glycosylation sites (PNGS). PNGS were counted using the LANL N-Glycosite

program (Zhang et al, 2004). The WebPSSM program (Jensen et al, 2003) was used to predict coreceptor use for each envelope based on the amino acid sequence of the V3 loop. Sequences were also checked for characteristics of non-functional *envs*, including insertions, deletions, and premature stop codons.

Sequences were analyzed for hypermutation and recombination by Thomas Leitner at LANL. Hypermutation was assessed using the Hypermut program (Rose and Korber, 2000). The Hypermut program detects G to A mutations that are likely the result of APOBEC3G or APOBEC3F activity of based on the context of the mutations in comparison to a reference sequence. Recombination was predicted using a hierarchical PHI test (Bruen et al, 2006; Immonen and Leitner, 2014). The PHI test measures the pairwise homoplasy index for sequences to predict recombination based on convergent mutations.

2.7 Phylogenetics

The *env* sequences from each tissue were aligned in GeneDoc (Pittsburgh Supercomputing Center) using manual adjustments with gaps excluded. Four HIV-1 group M subtype B reference sequences from LANL were included as well to be used as an outgroup:

Ref.B.FR.83.HXB2_LAI_IIIB_BRU.K03455
Ref.B.US.98.1058_11.AY331295
Ref.B.NL.00.671_00T36.AY423387
Ref.B.TH.90.BK132.AY173951

Maximum likelihood phylogenetic trees were then constructed using Molecular Evolutionary Genetics Analysis (MEGA) software version 5 (Tamura et al, 2011). Trees were constructed for the following regions of *env*: gp160, gp120, gp41, V1-V2, V1-V5, V1, V2, V3, V4, V5, C1, C2, C3, C4, and C5. For full length *env*, the General Time Reversible Substitution Model with Gamma distribution was used and compartmentalization was confirmed using the Slatkin-Maddison test (Slatkin and Maddison, 1989). MEGA was used to select the best models for trees of individual *env* regions. In all cases, bootstrap analyses were used with 1,000 replicates and values ≥70% were noted on the trees.

2.8 Cell Culture

Three cell lines were used in this study: HEK 293T cells (American Type Culture Collection), HeLa TZM-bl cells (NIH AIDS Reagent Program), and HeLa HIJ cells (Platt et al, 1998). The HEK 293T cell line is a human embryonic kidney cell line containing the SV40 Large T-antigen and was used for the generation of pseudotyped viruses, or pseudoviruses (Graham et al, 1977; DuBridge et al, 1987; Pear et al, 1993). HeLa TZM-bl cells are indicator cells that express high levels of CD4, CCR5, and CXCR4 and have HIV-inducible luciferase and β-galactosidase genes (Platt et al, 1998; Derdeyn et al, 2000; Wei et al, 2002; Takeuchi et al, 2008; Platt et al, 2009). These were used to determine pseudovirus titers and for inhibition and neutralization assays. HeLa HIJ cells are a HeLa cell line that express CD4 and CXCR4, but not CCR5, and therefore can be used to evaluate

CXCR4 coreceptor tropism (Kabat et al, 1994; Platt et al, 1998). Cell lines were maintained in Dulbecco's Modified Eagle Medium (DMEM) (Gibco) with 10% fetal bovine serum and 10 µg/ml gentamicin.

Macrophages were isolated from leuopaks (New York Biologics) using Ficoll separation. Following purification, cells were resuspended at 6.5 x 10^6 cells/ml in DMEM with 10% human plasma and 10 ug/ml gentamicin and plated on 150 mm non-tissue culture treated plates. Cells were incubated overnight and then washed with media the next day to remove non-adherent cells. Cells were allowed to incubate for an additional 6 days (7 days total) and then macrophages were replated for tropism experiments.

2.9 Pseudovirus Production

Pseudoviruses were constructed using *env*+ pcDNA 3.1D/V5-His-TOPO plasmids, carrying patient derived *env* genes, and an *env*- pNL4.3Δenv plasmid, an HIV-1 clone with a premature stop codon in the *env* gene (Bhattacharya et al, 2004). For each patient *env*, 1.25 µg of *env*+ plasmid and 1.25 µg of *env*- plasmid were cotransfected into 293T cells using the ProFection Mammalian Transfection System (Promega) as described by the manufacturer. Supernatants were harvested 48 hours post transfection and clarified by centrifugation. Cell free pseudovirus stocks were removed, aliquoted, frozen in liquid nitrogen, and stored at -152°C until use.

2.10 Viral Titer and Tropism

TZM-bl and HIJ cells were used to determine Env functionality and ability to use CXCR4 as a coreceptor, respectively. For each infectivity assay, cells were diluted to 4.0 x 10^4 cells/ml and 500 µl/well were added to 48-well plates the day prior to infection. The day of infection, pseudovirus stocks were thawed at room temperature and then serially diluted in media to yield four concentrations: stock, 1/10, 1/100/ and 1/1000. In addition, several laboratory strains were used as controls. For TZM-bl infection, B33, JRFL, and JRCSF were used as positive controls and L411 *env*- plasmid and L411 *env*- plasmid + pSVIII plasmid were used as negative controls. For HIJ infection, NL4.3 was used as a positive control and B33, JRFL, JRCSF, L411 *env*- plasmid, and L411 *env*- plasmid + pSVIII plasmid were used as negative controls.

Cells were infected by removing media and adding 100 µl of pseudovirus dilution. Plates were incubated for 3 hours at 37°C and then 400 µl of media were added to each well. Plates were incubated at 37°C for 48 hours. TZM-bl cells were fixed with 0.5% glutaraldehyde in phosphate-buffered saline (PBS). Cells were stained by rinsing twice in 1 x PBS and then adding 500 µl X-gal substrate (0.5 mg/ml 5-bromo-4-chloro-3-indolyl-β-D-galactopyranoside, 3 mM potassium ferrycyanide, 3 mM potassium ferrocyanide, 1 mM magnesium chloride). Plates were incubated at room temperature overnight and then β-galactosidase expressing cells were counted to determine the focus forming units (FFU)/ml of each pseudovirus stock. HIJ cells were fixed in cold 1:1 methanol:acetone,

washed, and immunostained for p24 using monoclonal antibodies 365 and 366 (UK Centre for AIDS Research), followed by an IgG-β-galactosidase conjugate (Southern Biotech), and then X-gal substrate. Plates were incubated overnight at room temperature and FFU were counted.

To determine macrophage tropism, 500 µl of macrophages at 2.5 x 10^5 cells/ml were plated in 48-well plates the day prior to infection. On the day of infection, media was removed from cells and 100 µl of 10 µg/ml DEAE dextran were added to each well and plates were incubated at 37°C for 30 minutes. Following incubation, 100 µl of serially diluted pseudovirus stocks, described above, were added to each well. Laboratory strains B33 and JRFL were used as positive controls and JRCSF, L411 *env*- plasmid and L411 *env*- plasmid + pSVIII plasmid were used as negative controls. Macrophages were spinoculated for 45 minutes at 1200 rpm in a benchtop centrifuge, incubated for 3 hours at 37°C, and then 300 µl media were added to each well. Plates were incubated for one week, adding additional media as needed. Macrophages were fixed, stained, and counted as described above for HIJ cells.

For viral titer and tropism experiments, a titer of 10^3 FFU/ml was used as a cutoff to determine whether a pseudovirus was functional on TZM-bl cells or could infect macrophages or HIJ cells. This titer was selected because it is sufficiently high to use the pseudovirus for inhibition and neutralization experiments. Below this value, it is difficult to observe changes in infection. However, it should be noted that while pseudoviruses below this value are categorized as “non-functional” for

the purpose of this study, they may still be infectious at a lower level. Likewise, they may be able to infect macrophages and HIJ cells at lower levels.

2.11 Inhibition and Neutralization Assays

Inhibition and neutralization assays were carried out as previously described to determine IC50 values, or the concentration of inhibitor or antibody at which infection is reduced by 50% (Peters et al, 2008). Two inhibitors and four monoclonal antibodies were tested: sCD4 (prepared in house), maraviroc (NIH AIDS Reagent Program), b12 (provided by Dennis Burton, The Scripps Research Institute), PG16 (Polymun Scientific), 17b (provided by George Lewis, Institute of Human Virology) and 447-52D (Polymun Scientific) (Table 2.4). Inhibitions were performed using HIV-1 inducible HeLa TZM-bl cells, which were diluted to 1.6 x 10^5 and plated at 50 µl/well in 96-well white-sided luminometer plates the day prior to the assay. The day of the assay, pseudovirus stocks were thawed at room temperature and diluted to 8000 FFU/ml. Several laboratory strains were used as controls for each experiment. Vesicular Stomatitis Virus G protein (VSVG) was used as a resistant control for all inhibitions and neutralizations. For sCD4, maraviroc, and b12, JRFL and JRCSF were used as sensitive controls. For PG16, JRFL was used as a resistant control and JRCSF was used as a sensitive control. In the 17b and 447-52D neutralization experiments, NL4.3 was used as a sensitive control and JRFL and JRSCF were used as resistant controls.

Eleven twofold serial dilutions were used for each inhibitor or antibody along with a media only, no inhibitor/antibody sample (Table 2.4). For each well of maraviroc inhibition, 25 µl serially diluted maraviroc were added to each well and incubated for 30 minutes at 37°C. Then 25 µl (200 FFU) pseudovirus were added to each well. For each well of inhibition or neutralization with sCD4, b12, PG16, 17b, and 447-52D, 25 µl (200 FFU) pseudovirus and 25 µl serially diluted inhibitor or antibody were combined, incubated for 1 hour at 37°C, and then added to TZM-bl cells. Plates were incubated at 37°C overnight and media was changed in the morning. The following day, media was removed via aspiration, 100 µl media without phenol red was added to each well and infection was detected with a luciferase readout using Beta-Glo (Promega). To each well, 100 µl Beta-Glo were added and plates were incubated at room temperature in the dark for 30 minutes. Plates were read using a BioTek Clarity luminometer (Winooski, VT) to obtain Relative Light Units (RLU).

2.12 Next Generation Sequencing

Full length *envs* were amplified for Pacific Biosciences (PacBio) next generation sequencing. DNA was isolated from tissues as described above and a nested PCR approach was used to amplify a 2.6 kb product. Outer primers RevenvA and EnvN and inner primers PacBioF-long and PacBioR-long were used (Table 2.2). The Advantage 2 PCR Kit (Clontech) was used as described in the manufacturer's protocol for 50 µl reactions. The thermocylcer program "PacBio"

was used with 35 cycles (Table 2.3). PCR products were cleaned up by running them out on a 2% E-Gel EX Agarose Gel (ThermoFisher Scientific) and purified with a QIAquick Gel Extraction Kit (QIAGEN). PCR products were eluted in 50 µl nuclease free, PCR grade water. Samples were sent to the Deep Sequencing Core Labs at the University of Massachusetts Medical School for sequencing using the PacBio RS II instrument. One SMRT Cell was analyzed for DNA from each tissue with 6-hour collection times.

Bioinformatics analyses were performed by Bioinfoexperts, LLC (Thibodaux, LA). The V3 loop nucleic acid sequences were isolated and aligned using Geneious software version 9 (Kearse et al, 2012) and Gene Cutter (Los Alamos National Laboratory), respectively. Any V3 amino acid sequence containing an ambiguous position was removed from the alignment. Tropism prediction was performed using WebPSSM (Jensen et al, 2003) and the x4r5 matrix. A python script was generated to randomly select 250 sequences from each tissue. Maximum likelihood phylogenies were generated with phyML (Guindon et al, 2010) using the HKY85 substitution model, the NNI tree improvement method, and the approximate likelihood ratio test (Anisimova and Gascuel, 2006). A midpoint rooted tree was graphed and colored according to tissue type using FigTree software (http://tree.bio.ed.ac.uk/software/figtree/).

Inhibitor	Epitope	Starting Concentration
sCD4	CD4 binding site	50 µg/ml
Maraviroc	CCR5	100 ng/ml

Antibody	Epitope	Starting Concentration
b12	CD4 binding site	50 µg/ml
PG16	V2&V3	10 µg/ml
447-52D	V3	50 µg/ml
17b	CD4i	50 µg/ml

Table 2.4 Inhibitors and antibodies A panel of HIV-1 inhibitors and neutralizing antibodies were tested for their ability to block infection of TZM-bl cells using pseudoviruses with patient derived Envs.

CHAPTER III: GENETIC CHARACTERIZATION OF HIV-1 ENVELOPES FROM TISSUES OF AN HIV-1 INFECTED SUBJECT

3.1 Introduction

A number of studies have addressed the diversity of HIV-1 *env* quasispecies. However one caveat of these studies is that they often look at only a particular region of the *env* (e.g., V1-V2 or V3), which may not be representative of the overall *env* sequence and may not be sufficient to infer phenotypes. Furthermore, these studies typically only examine a few tissue sites, such as brain, immune tissue, and plasma. In the first part of this study, *envs* were amplified from multiple tissues of an HIV-1 positive subject. They were then compared for compartmentalization, sequence variation, length, charge, possible N-linked glycosylation sites (PNGS), hypermutation, and recombination.

Previous studies have shown genetic compartmentalization in the brain compared to plasma and immune tissue, but there is limited data on compartmentalization in other tissues (Wong et al, 1997; van't Wout et al, 1998; Wang et al, 2001; Caragounis et al, 2007; Schnell et al, 2010; Gonzalez-Perez et al, 2012; Sturdevant et al, 2015). Similarly, studies have been conducted to examine the overall charge of *env* regions, but they have been restricted to only a few tissue compartments. Nevertheless, it has been reported that CCR5-using envelopes carried an increased overall positive charge as disease progressed (Repits et al, 2008; Seclen et al, 2011; Gonzalez-Perez et al, 2012). In AIDS patients with neurological complications, envelopes in immune tissue carried a

higher positive charge in the V1-V5 region compared to those in brain tissue (Gonzalez-Perez et al, 2012).

Mutations in the HIV-1 genome can impact quasispecies diversity. These include mutations that result in amino acid substitutions as well as loss or addition of PNGS. Together with insertions and deletions, they play an important role in diversity and phenotypes of viral variants. Several groups have examined the relationship between sequence length and PNGS and disease progression. These studies have found that variants with shorter V1-V2 lengths and less PNGS may be selected for at transmission, but that length expanded and number of PNGS increased over the course of infection (Pollakis et al, 2001; Derdeyn et al, 2004; Chohan et al, 2005; Sagar et al, 2006; Liu et al, 2008; Curlin et al, 2010; Huang et al, 2012; Wang et al, 2013; Pollakis et al, 2015).

HIV-1 diversity can also be affected by human restriction factors, aimed at protecting host cells. Hypermutation resulting from the activity of APOBEC3G and F results in defective virus. Vif protects HIV-1 from APOBEC activity by inducing its degradation (Sheehy et al, 2002). However, in cells that express higher amounts of APOBEC or following a *vif* mutation, hypermutation can result (Lecossier et al, 2003). Previous studies have shown that APOBEC genes are differentially expressed in tissue compartments and that this can result in different levels of hypermutation (Koning et al, 2009; Refsland et al, 2010; Fourati et al, 2014).

Finally, recombination has been shown to increase genetic diversity in HIV-1 populations and increase the rate of evolution (Jetzt et al, 2000; An and Telesartsky, 2002; Rhodes et al, 2003; Charpentier et al, 2006; Chen et al, 2006; Mild et al, 2007; Zhang et al, 2010; Brown et al, 2011; Immonen et al, 2015; Sanborn et al, 2015).

To effectively treat HIV-1 and develop a vaccine, it is essential to understand its genetic variability and how this may be different in tissue compartments. This study represents the first time that full length *env* sequences have been amplified and analyzed from multiple tissue sites within an infected individual. In addition, all of the envelopes were functionally characterized, which is discussed in Chapter IV.

3.2 Results

3.2.1 Envelopes were amplified from all tissues except for plasma and serum

Limiting dilution PCR was used to amplify full length envelopes from proviral DNA at end point dilution from frontal lobe, occipital lobe, parietal lobe, colon, lung, and lymph node tissues, as well as from residual cellular material in plasma and serum of Subject 162 (Table 2.1). Envelopes were successfully amplified from all tissues, except plasma and serum, and used for further analyses (Table 3.1). Envelopes were named as follows: number of the PCR reaction – number of the PCR tube – number of the clone that was sequenced. A total of 8 envelopes were

Tissue	Envelope
Brain - Frontal Lobe (FL)	
8 envelopes	17-53-4
	52-19-3
	53-30-5
	53-53-3
	65-15-1
	68-59-1
	70-14-2
	74-14-2
Brain - Occipital Lobe (OL)	
10 envelopes	19-94-2
	19-108-2
	52-59-21
	54-32-6
	75-28-2
	76-35-5
	76-59-4
	76-72-1
	86-131-1
	86-167-2
Brain - Parietal Lobe (PL)	
5 envelopes	51-77-2
	52-79-17
	49-74-1
	83-34-4
	88-68-2
Colon (C)	
11 envelopes	2-2-1
	3-1-4
	3-4-2
	4-3-1
	4-5-1
	4-8-1
	4-13-2
	4-15-2
	4-22-1
	4-38-12
	4-39-3

Tissue	Envelope
Lung (L)	
29 envelopes	6-10-1
	7-7-16
	7-20-1
	7-22-1
	7-34-15
	7-38-3
	7-43-5
	8-3-6
	8-8-1
	58-1-2
	58-7-4
	58-13-1
	58-15-1
	59-12-1
	59-51-1
	98-11-1
	98-22-1
	98-36-1
	98-51-1
	98-59-1
	98-60-2
	99-35-2
	101-12-2
	101-23-1
	101-25-1
	101-35-1
	101-54-1
	101-60-1
	101-66-1
Lymph Node (LN)	
12 envelopes	17-84-1
	17-89-1
	56-13-4
	56-43-7
	56-57-2
	56-67-3
	62-16-1
	62-30-1
	62-37-6
	62-41-3
	62-43-1
	62-47-1

Table 3.1 Subject 162 HIV-1 envelopes isolated from different tissues HIV-1 *envs* were isolated from three brain regions (frontal lobe, occipital lobe, and parietal lobe), colon, lung, and lymph node using nested PCR and DNA at limiting dilution.

isolated from frontal lobe, 10 from occipital lobe, 5 from parietal lobe, 11 from colon, 29 from lung, and 12 from lymph node for a total of 75 envelopes. Additional PCR reactions were performed to amplify smaller envelope regions (e.g., V1-V5 and V3) from plasma and serum proviral DNA, but attempts were not successful. However it was possible to amplify the human CCR5 gene (data not shown), suggesting that there was DNA in the samples, but proviral DNA was not present or had a very low copy number. Unfortunately, enriched white cells from blood were not available.

For plasma and serum, RT-PCR was used to amplify full length envelopes from viral RNA. However, no envelopes were isolated from either of these samples. As with the proviral DNA samples, subsequent attempts to PCR amplify smaller envelope regions from the plasma and serum were unsuccessful. Plasma and serum samples were analyzed for viral load by the Infectious Disease Laboratory at the Children's Hospital of Chicago using Abbott RealTime HIV-1 RNA PCR. For both samples, viral load was undetectable with <40 copies/ml (Table 2.1). Subject 162 was on HAART (Table 2.1) and appears to have had well controlled viral replication at death.

3.2.2 No mutations were observed that have previously been associated with macrophage tropism or CXCR4 use

Sequences were examined for the presence of mutations associated with changes in coreceptor use or macrophage tropism. For example, the presence of either an arginine or lysine at residues 11 or 25 of the V3 loop is associated with

CXCR4 use, while the loss of an asparagine at N283, the glycan at N386 or an E153G substitution have been associated with changes in macrophage tropism (Peters et al, 2004; Dunfee et al, 2006; Dunfee et al, 2007; Duenas-Decamp et al, 2009; Musich et al, 2012). None of these were observed in any of the 75 sequences. There were some insertions/deletions observed, but they were not so large that they would clearly disrupt function. However many sequences, particularly in *envs* derived from the lung, had numerous premature stop codons. These may render the Env non-functional. All Envs were tested for functionality, discussed in Chapter IV.

There were many other polymorphisms that resulted in amino acid changes. None of these appeared to correlate exclusively with a particular tissue or phenotype, discussed in Chapter IV. For example, when neutralization by PG16 monoclonal antibody was tested, it was discovered that K130E was present in many envelopes that were resistant to neutralization. However there were also a number of envelopes with the K130E mutation that were sensitive to PG16.

3.2.3 Sequences were compartmentalized in brain tissue

Full length envelope gp160 sequences were isolated from frontal lobe, occipital lobe, parietal lobe, colon, lung, and lymph node (Table 3.1). The 53 functional sequences (assessed in Chapter IV) were used to construct a maximum likelihood phylogenetic tree (Figure 3.1) using Molecular Evolutionary Genetics

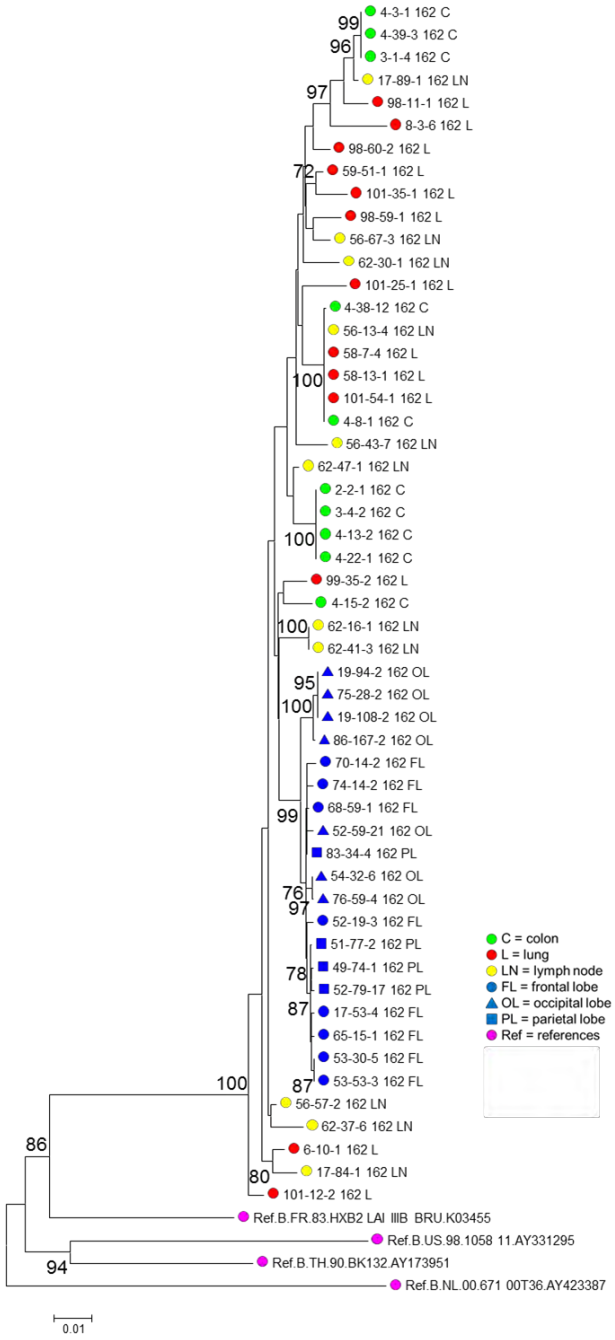

Figure 3.1 Phylogenetic analysis of Subject 162 gp160 sequences Full length HIV-1 *envs* were amplified from three brain regions (frontal lobe, occipital lobe, and parietal lobe), colon, lung, and lymph node. Four unrelated reference sequences were used as an outgroup. A maximum likelihood tree was constructed using MEGA version 5 for functional HIV-1 *envs*. Bootstrap vaues ≥70% are noted at branch points. Sequences from the brain regions are tightly compartmentalized. Compartmentalization was confirmed using the Slatkin-Maddison test with $P < 0.001$. Scale bar shows nucleotide substitutions per site.

Analysis (MEGA) version 5 software (Tamura et al, 2011). The tree was rooted using four unrelated clade B reference sequences. Genetic compartmentalization was observed between envelopes isolated from brain tissues and tissues from the body. Compartmentalization was confirmed using the Slatkin-Maddison test with $P < 0.001$.

Phylogenetic trees were also constructed for regions of the envelope: gp120, gp41, V1-V2, V1-V5, C1, C2, C3, C4, C5, V1, V2, V3, V4, and V5 (Appendix A). MEGA software was used to calculate mean genetic distances for each tree (Figure 3.2). The V1 and V5 regions had the greatest evolutionary divergence, while the C5 region had the least. The V3 loop was also highly conserved among tissues within the brain and in the periphery. This is consistent with previous observations, as it is known that all V regions except for the V3 loop have hypervariable sequences (Los Alamos National Laboratory, 2016).

3.2.4 Length of envelope regions did not differ significantly between different tissue sites

Functional envelopes were compared to determine if envelopes from different tissue compartments differed in the length of V1-V2 or V1-V5 (Figures 3.3 - 3.6). The length of the V1-V2 loops was more variable in peripheral tissues compared to those in brain. However, no significant differences were observed, when values were analyzed by unpaired, two-tailed t tests using GraphPad Prism software.

3.2.5 V1-V2 and V1-V5 net charges had greater variability in tissues from the body than in brain tissues

Net charges of V1-V2 and V1-V5 regions were calculated using the The European Molecular Biology Open Software Suite (EMBOSS) Pepstats program to count charged amino acids (Figures 3.7 - 3.10). Overall charges in V1-V2 and V1-V5 regions were more variable in envelopes derived from colon, lung, and lymph node compared to those in brain tissues. However, only a few envelopes from colon and lung carried a higher positive charge.

Using GraphPad Prism for unpaired, two-tailed t tests, it was determined that overall differences in V1-V2 and V1-V5 charges between envelopes present in brain tissues (frontal lobe, occipital lobe, and parietal lobe) and in tissues of the body (colon, lung, and lymph node) were not significant (Figures 3.8B and 3.10B). Nevertheless, significant differences were noted in V1-V2 charge between the following brain and body tissues, FL:OL, FL:C, FL:LN, OL:PL, PL:LN, as well as between C:L (Figure 3.7B). However, there was no consistent trend of higher charged envelopes in body tissues compared to brain tissues. Differences in the charges of the longer V1-V5 region were statistically significant between FL:OL, FL:LN, OL:PL, and PL:LN (Figure 3.9B). It was observed that there was much more variability in charges of envelope regions outside the brain than in the brain for both V1-V2 and V1-V5 regions, as shown by the means and standard deviations for each compartment (Figures 3.7C and 3.9C).

A

Region	Mean Distance
gp160	0.029
gp120	0.027
gp41	0.024
V1-V2	0.078
V1-V5	0.038
C1	0.028
C2	0.025
C3	0.028
C4	0.032
C5	0.011
V1	0.117
V2	0.059
V3	0.021
V4	0.053
V5	0.110

B

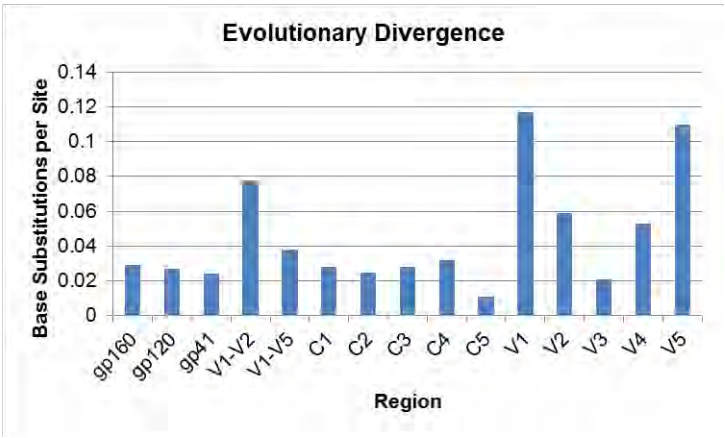

Figure 3.2 Evolutionary divergence of HIV-1 *envs by* region MEGA version 5 software was used to calculate the mean distance (**A**) and evolutionary divergence (**B**) for each *env* region based on the number of base substitutions per site.

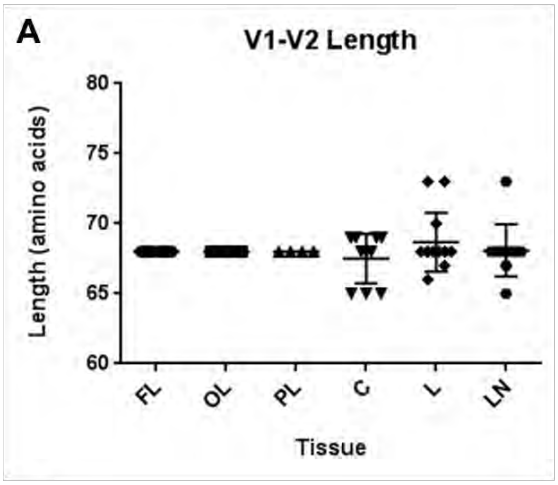

B

Tissues	P value
FL:OL	*
FL:PL	*
FL:C	0.4412
FL:L	0.3668
FL:LN	0.8930
OL:PL	*
OL:C	0.4730
OL:L	0.3998
OL:LN	0.9003
PL:C	0.5935
PL:L	0.5283
PL:LN	0.9258
C:L	0.1643
C:LN	0.4682
L:LN	0.4699

C

Tissue	Mean	Standard Deviation
FL	68.00	0
OL	68.00	0
PL	68.00	0
C	67.50	1.780
L	68.69	2.097
LN	68.09	1.868

Figure 3.3 V1-V2 lengths of HIV-1 *envs* from different tissues A) V1-V2 amino acid sequence lengths were calculated for each *env* and plotted using GraphPad Prism. **B)** An unpaired, two-tailed t test was used to test for statistical difference in the mean between the *env* populations in each tissue compartment. An asterisk denotes that t test could not be performed because the samples in both tissues had the same values. **C)** Mean and standard deviation are given to show the spread of the data range for the *envs* from each tissue compartment.

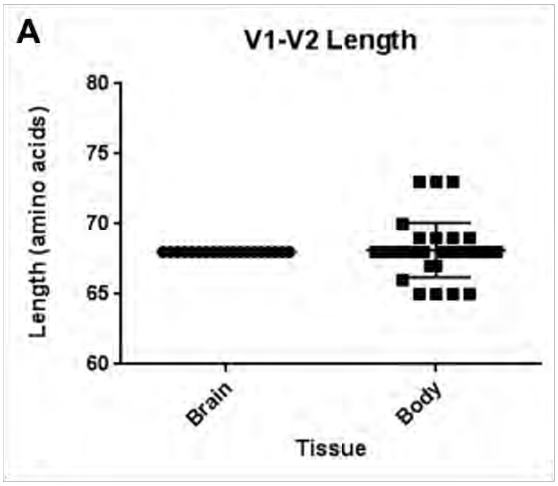

B

Tissues	P value
Brain:Body	0.7436

C

Tissue	Mean	Standard Deviation
Brain	68.00	0
Body	68.15	1.941

Figure 3.4 V1-V2 lengths of HIV-1 *envs* from the brain and body A) V1-V2 amino acid sequence lengths were calculated for each *env* in the brain and body and plotted using GraphPad Prism. **B)** An unpaired, two-tailed t test was used to test for statistical difference in the mean between the *env* populations of the brain and body. **C)** Mean and standard deviation are given to show the spread of the data range for the *envs* from each compartment.

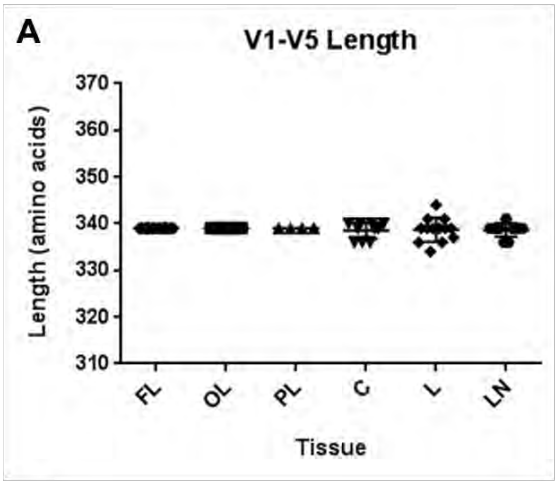

B

Tissues	P value
FL:OL	*
FL:PL	*
FL:C	0.4412
FL:L	0.7403
FL:LN	0.4862
OL:PL	*
OL:C	0.4730
OL:L	0.7573
OL:LN	0.5163
PL:C	0.5935
PL:L	0.8175
PL:LN	0.6286
C:L	0.8416
C:LN	0.8480
L:LN	0.9493

C

Tissue	Mean	Standard Deviation
FL	339.0	0
OL	339.0	0
PL	339.0	0
C	338.5	1.780
L	338.7	2.562
LN	338.6	1.433

Figure 3.5 V1-V5 lengths of HIV-1 *envs* from different tissues A) V1-V5 amino acid sequence lengths were calculated for each *env* and plotted using GraphPad Prism. **B)** An unpaired, two-tailed t test was used to test for statistical difference in the mean between the *env* populations in each tissue compartment. An asterisk denotes that t test could not be performed because the samples in both tissues had the same values. **C)** Mean and standard deviation are given to show the spread of the data range for the *envs* from each tissue compartment.

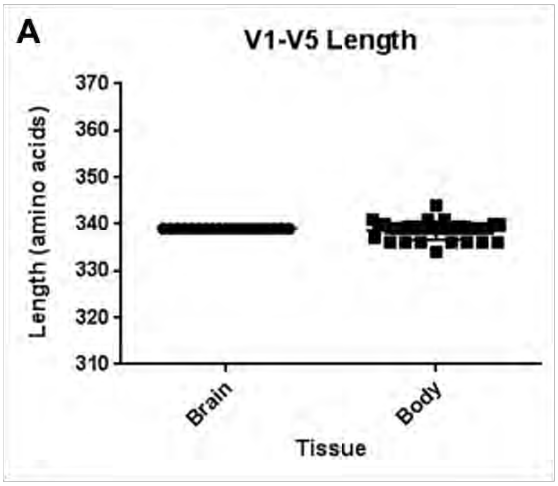

B

Tissues	P value
Brain:Body	0.4034

C

Tissue	Mean	Standard Deviation
Brain	339.0	0
Body	338.6	1.970

Figure 3.6 V1-V5 lengths of HIV-1 *envs* from the brain and body A) V1-V5 amino acid sequence lengths were calculated for each *env* in the brain and body and plotted using GraphPad Prism. **B)** An unpaired, two-tailed t test was used to test for statistical difference in the mean between the *env* populations of the brain and body. **C)** Mean and standard deviation are given to show the spread of the data range for the *envs* from each compartment.

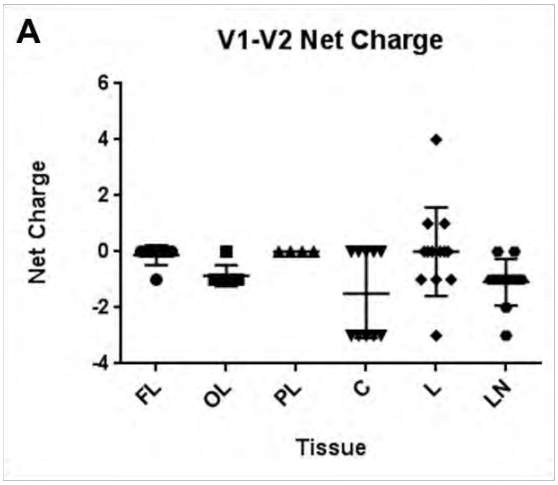

B

Tissues	P value
FL:OL	0.0019
FL:PL	0.5059
FL:C	0.0290
FL:L	0.8296
FL:LN	0.0069
OL:PL	0.0016
OL:C	0.3124
OL:L	0.1796
OL:LN	0.4976
PL:C	0.0888
PL:L	> 0.9999
PL:LN	0.0236
C:L	0.0349
C:LN	0.4609
L:LN	0.0519

C

Tissue	Mean	Standard Deviation
FL	-0.125	0.354
OL	-0.857	0.378
PL	0	0
C	-1.500	1.581
L	0	1.581
LN	-1.091	0.831

Figure 3.7 V1-V2 net charges of HIV-1 *envs* from different tissues A) V1-V2 amino acid net charges were calculated for each *env* and plotted using GraphPad Prism. **B)** An unpaired, two-tailed t test was used to test for statistical difference in the mean between the *env* populations in each tissue compartment. Statistically significant values are shown in red. **C)** Mean and standard deviation are given to show the spread of the data range for the *envs* from each tissue compartment.

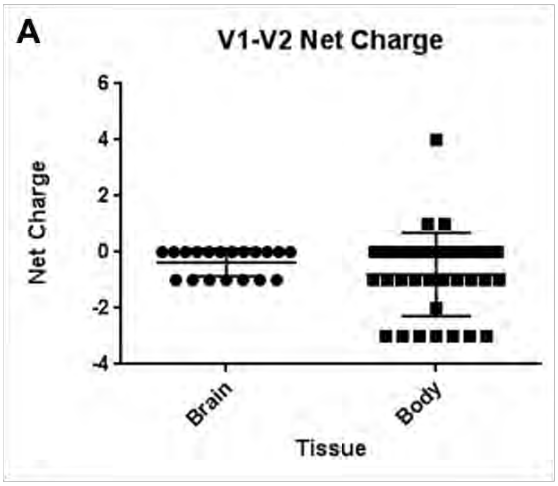

B

Tissues	P value
Brain:Body	0.2349

C

Tissue	Mean	Standard Deviation
Brain	-0.368	0.496
Body	-0.794	1.493

Figure 3.8 V1-V2 net charges of HIV-1 *envs* from the brain and body A) V1-V2 amino acid net charges were calculated for each *env* in the brain and body and plotted using GraphPad Prism. **B)** An unpaired, two-tailed t test was used to test for statistical difference in the mean between the *env* populations of the brain and body. **C)** Mean and standard deviation are given to show the spread of the data range for the *envs* from each compartment.

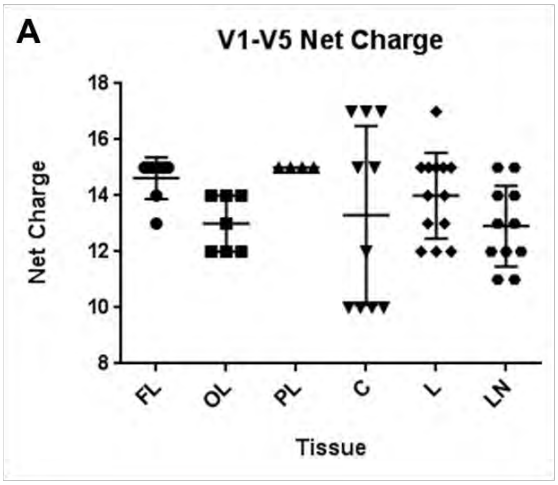

B

Tissues	P value
FL:OL	0.0032
FL:PL	0.3484
FL:C	0.2709
FL:L	0.2963
FL:LN	0.0071
OL:PL	0.0036
OL:C	0.8151
OL:L	0.1381
OL:LN	0.8865
PL:C	0.3201
PL:L	0.2200
PL:LN	0.0144
C:L	0.4941
C:LN	0.7178
L:LN	0.0879

C

Tissue	Mean	Standard Deviation
FL	14.63	0.744
OL	13.00	1.000
PL	15.00	0
C	13.30	3.199
L	14.00	1.528
LN	12.91	1.446

Figure 3.9 V1-V5 net charges of HIV-1 *envs* from different tissues A) V1-V5 amino acid net charges were calculated for each *env* and plotted using GraphPad Prism. **B)** An unpaired, two-tailed t test was used to test for statistical difference in the mean between the *env* populations in each tissue compartment. Statistically significant values are shown in red. **C)** Mean and standard deviation are given to show the spread of the data range for the *envs* from each tissue compartment.

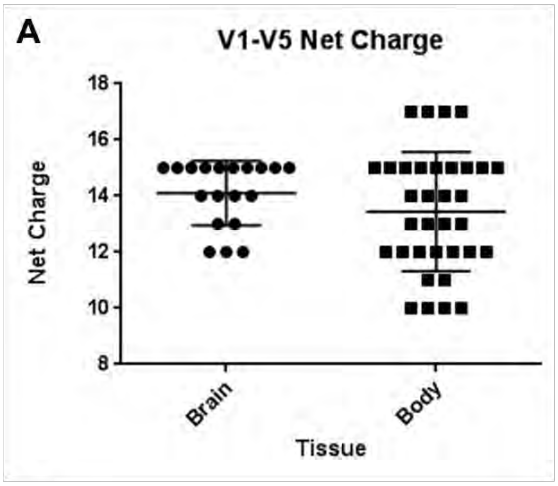

B

Tissues	P value
Brain:Body	0.2127

C

Tissue	Mean	Standard Deviation
Brain	14.11	1.150
Body	13.44	2.120

Figure 3.10 V1-V5 net charges of HIV-1 *envs* from the brain and body A) V1-V5 amino acid net charges were calculated for each *env* in the brain and body and plotted using GraphPad Prism. **B)** An unpaired, two-tailed t test was used to test for statistical difference in the mean between the *env* populations of the brain and body. **C)** Mean and standard deviation are given to show the spread of the data range for the *envs* from each compartment.

3.2.6 Average number of predicted N-linked glycosylation sites was more variable in tissue compartments outside the brain

The low concentration of antibodies present inside the brain compartment may result in the evolution of envelopes with fewer glycans and an altered glycan shield. Potential N-linked glycosylation sites (PNGS) were predicted for functional envelope sequences using the Los Alamos National Laboratory N-Glycosite program for the V1-V5 region (Figures 3.11 and 3.12) and the full length envelope (Figures 3.13 and 3.14). Unpaired, two-tailed t tests were performed using GraphPad Prism. For the V1-V5 region, significant differences were found between FL:OL, OL:PL, and OL:LN (Figure 3.11B). For the envelope, significant differences were observed for FL:OL, FL:L, FL:LN, and OL:PL (Figure 3.13B). While regions outside of the brain had more variability (Figures 3.12C and 3.14C) in the number of PNGS than regions within the brain, these differences were not statistically significant (Figures 3.12B and 3.14B).

3.2.7 The lung compartment had a higher frequency of hypermutated envelopes than other tissues

All 75 envelope sequences were analyzed for hypermutation by Thomas Leitner at Los Alamos National Laboratory using the Hypermut program (Rose and Korber, 2000). A phylogenetic tree was constructed showing 19 envelope sequences in 5 lineages with hypermutation (Figure 3.15). Hypermutated sequences came from occipital lobe, colon, and lung. However the majority, 15 out of 19 envelopes, were from lung tissue. All of the envelopes with hypermutated

sequences were non-functional and unable to mediate infection of HeLa TZM-bl cells, as described in Chapter IV.

3.2.8 Recombination was extensive in all tissue compartments

Sequences were analyzed for potential recombination by Thomas Leitner at Los Alamos National Laboratory using a hierarchical PHI test (Bruen et al, 2006; Immonen and Leitner, 2014). Hypermutated sequences were not assessed for recombination and are removed from the counts below. Out of 56 remaining sequences, 39 were the product of recombination events (Figure 3.15). Of the non-hypermutated sequences, this includes 6 out of 8 frontal lobe sequences, 7 out of 7 occipital lobe sequences, 3 out of 5 parietal lobe sequences, 9 out of 10 colon sequences, 9 out of 14 lung sequences, and 5 out of 12 lymph node sequences. As discussed in Chapter IV, the majority of the recombinant sequences, 37 of the 39, were functional.

3.2.9 PacBio sequencing

A total of 32,152 sequences were generated from the parietal lobe, colon, lung, and lymph node of Subject 162 using PacBio sequencing (Table 3.2). Specifically, 13,791 were from the parietal lobe, 8,263 were from the colon, 66 were from the lung, and 10,032 were from the lymph node. PacBio sequencing was not performed for the frontal lobe or occipital lobe because it was not possible to amplify sufficient amounts of PCR product. For each sequence, the V3 loop was

analyzed to predict coreceptor use using WebPSSM (University of Washington). All of the sequences were predicted to use CCR5 (Table 3.2).

To create phylogenetic trees, 250 random sequences were selected for each tissue. For lung, all 66 were used. A maximum likelihood tree was constructed, showing compartmentalization within the brain, as well as the colon (Figure 3.16). Sequences from the lung and lymph node were mixed.

3.3 Discussion

Subject 162 was an HIV-1 positive patient who died of complications from end stage AIDS. Despite this, it was difficult to amplify proviral DNA from patient tissue samples. Some tissues were more challenging than others, with plasma/serum and tissues of the brain being the most difficult. In the end, no *envs* were isolated from the plasma or serum. After many attempts to amplify viral RNA and proviral DNA, plasma and serum samples were sent out for viral load testing. It was discovered that neither sample had detectable viral loads. This would be expected in a subject that was on antiretroviral treatment with well controlled viremia. However this subject died from end stage AIDS, which is typically characterized by a spike in viral RNA copies in the plasma (Figure 1.2). It is unclear why a subject at this stage of HIV-1 infection would not have detectable viral loads. It is possible that the patient's current drug regimen was effective at reducing the viral load in blood even though severe immune deficiencies led to their death.

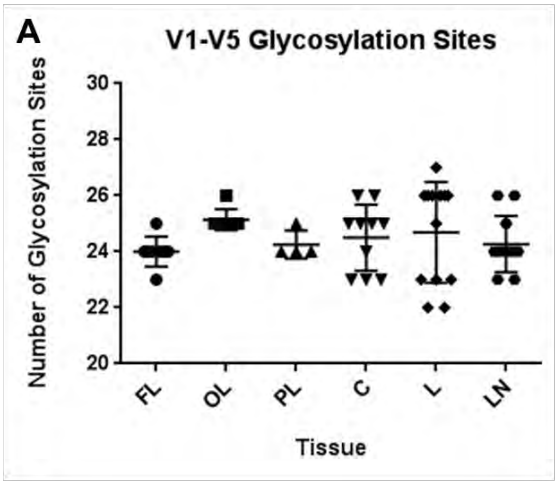

B

Tissues	P value
FL:OL	0.0004
FL:PL	0.4543
FL:C	0.2845
FL:L	0.3061
FL:LN	0.4974
OL:PL	0.0082
OL:C	0.1871
OL:L	0.5253
OL:LN	0.0457
PL:C	0.6946
PL:L	0.6405
PL:LN	0.9668
C:L	0.7727
C:LN	0.6395
L:LN	0.4995

C

Tissue	Mean	Standard Deviation
FL	24.00	0.535
OL	25.14	0.378
PL	24.25	0.500
C	24.50	1.179
L	24.69	1.797
LN	24.27	1.009

Figure 3.11 V1-V5 potential N-linked glycosylation sites (PNGS) of HIV-1 *envs* from different tissues A) V1-V5 PNGS were calculated for each *env* using N-Glycosite (LANL) and plotted using GraphPad Prism. **B)** An unpaired, two-tailed t test was used to test for statistical difference in the mean between the *env* populations in each tissue compartment. Statistically significant values are shown in red. **C)** Mean and standard deviation are given to show the spread of the data range for the *envs* from each tissue compartment.

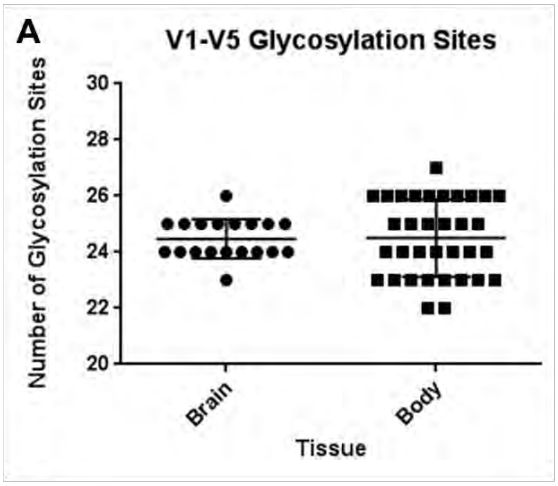

B

Tissues	P value
Brain:Body	0.9383

C

Tissue	Mean	Standard Deviation
Brain	24.47	0.697
Body	24.50	1.376

Figure 3.12 V1-V5 potential N-linked glycosylation sites (PNGS) of HIV-1 *envs* from the brain and body A) V1-V5 PNGS were calculated for each *env* in the brain and body using N-Glycosite (LANL) and plotted using GraphPad Prism. **B)** An unpaired, two-tailed t test was used to test for statistical difference in the mean between the *env* populations of the brain and body. **C)** Mean and standard deviation are given to show the spread of the data range for the *envs* from each compartment.

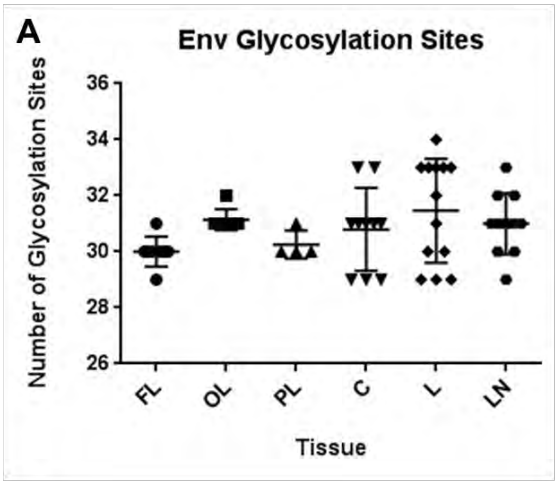

B

Tissues	P value
FL:OL	0.0004
FL:PL	0.4543
FL:C	0.1660
FL:L	0.0441
FL:LN	0.0298
OL:PL	0.0082
OL:C	0.5602
OL:L	0.6619
OL:LN	0.7460
PL:C	0.4889
PL:L	0.2246
PL:LN	0.2172
C:L	0.3659
C:LN	0.7265
L:LN	0.4765

C

Tissue	Mean	Standard Deviation
FL	30.00	0.535
OL	31.14	0.378
PL	30.25	0.500
C	30.80	1.476
L	31.46	1.854
LN	31.00	1.095

Figure 3.13 Env potential N-linked glycosylation sites of HIV-1 *envs* from different tissues A) Env PNGS were calculated for each *env* using N-Glycosite (LANL) and plotted using GraphPad Prism. **B)** An unpaired, two-tailed t test was used to test for statistical difference in the mean between the *env* populations in each tissue compartment. Statistically significant values are shown in red. **C)** Mean and standard deviation are given to show the spread of the data range for the *envs* from each tissue compartment.

A

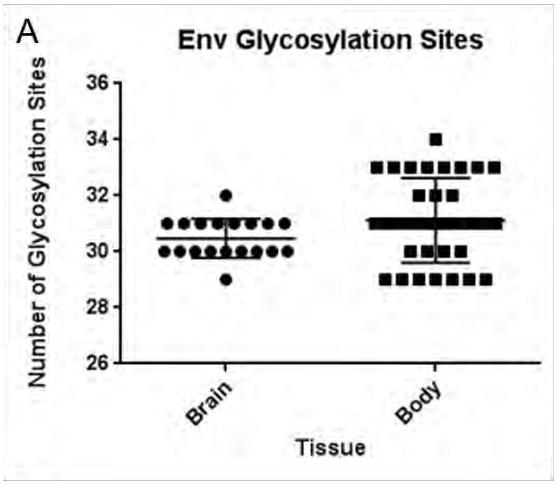

B

Tissues	P value
Brain:Body	0.0863

C

Tissue	Mean	Standard Deviation
Brain	30.47	0.697
Body	31.12	1.513

Figure 3.14 Env potential N-linked glycosylation sites of HIV-1 *envs* from the brain and body A) Env PNGS were calculated for each *env* in the brain and body using N-Glycosite (LANL) and plotted using GraphPad Prism. **B)** An unpaired, two-tailed t test was used to test for statistical difference in the mean between the *env* populations of the brain and body. **C)** Mean and standard deviation are given to show the spread of the data range for the *envs* from each compartment.

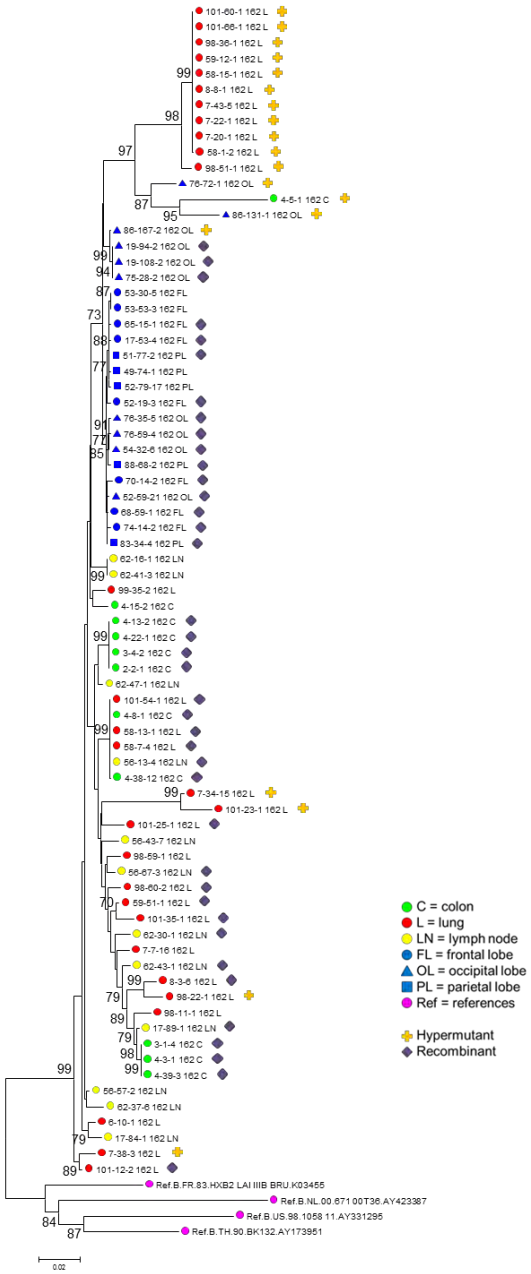

Figure 3.15 Hypermutation and recombination of gp160 sequences Full length HIV-1 *envs* were amplified from three brain regions (frontal lobe, occipital lobe, and parietal lobe), colon, lung, and lymph node. Four unrelated reference sequences were used as an outgroup. A maximum likelihood tree was constructed using MEGA version 5 for all 75 HIV-1 *envs*. Bootstrap values ≥70% are noted at branch points. Hypermutation was assessed using the LANL Hypermut program and is shown by orange crosses (Rose and Korber, 2000). Sequences were analyzed for potential recombination using a hierarchical PHI test (Bruen et al, 2006; Immonen and Leitner, 2014). Recombinants are shown by purple diamonds. Scale bar shows nucleotide substitutions per site.

Tissue	Total Sequences	CCR5-using		CXCR4-using	
		Number	Percent	Number	Percent
Parietal Lobe	13,791	13,791	100	0	0
Colon	8,263	8,263	100	0	0
Lung	66	66	100	0	0
Lymph Node	10,032	10,032	100	0	0
Total	32,152	32,152	100	0	0

Table 3.2 Subject 162 PacBio sequencing results The V3 loop nucleic acid sequences for all sequences in each data set were isolated using Geneious software version 9 (Kearse et al, 2012). Gene Cutter (Los Alamos National Laboratory) was used to codon align and translate sequences. The sequencing approach resulted in some gapped positions, so any V3 amino acid sequence containing an ambiguous position was removed from the alignment. Tropism prediction was performed using WebPSSM (Jensen et al, 2003) and the x4r5 matrix.

Figure 3.16 Phylogenetic analysis of Subject 162 PacBio sequences A python script was generated to randomly select 250 sequences from each tissue. Due to the small number of sequences generated, all lung sequences were used. Maximum likelihood phylogenies were generated with phyML (Guindon et al, 2010) using the HKY85 substitution model, the NNI tree improvement method, and the approximate likelihood ratio test (Anisimova and Gascuel, 2006). Tree was graphed and colored according to tissue type using FigTree software (http://tree.bio.ed.ac.uk/software/figtree/). Tree was midpoint rooted. Branch support is shown on the scale to the left, with red indicating branches with very high support.

Alternatively, plasma and serum samples may not have been handled optimally during tissue harvesting or shipment and RNA could have been degraded.

While it was also difficult to isolate *envs* from brain tissue, this was not surprising. It has previously been reported that viral loads are low in the brain tissues of neurologically normal subjects (Bell et al, 1993; Donaldson et al, 1994; McCrossan et al, 2006). Subject 162 did not have a diagnosis of any neurological disorders and therefore was considered neurologically normal. Regardless, 24 *envs* were isolated from brain tissues, along with 51 from other tissues (Table 3.1).

Tissues from the brain harbored *envs* that were compartmentalized from those in colon, lung, and lymph node. However, *envs* from these latter tissue sites were not. This compartmentalization was observed in full length *env* sequences, but not in all individual *env* regions (e.g., V3 loop). Evolutionary diversity was greatest in the V1 and V5 *env* regions (Figure 3.2), while other regions were more homogeneous. This is an important observation considering that many previous studies looked at only specific regions the of *env* sequences and in some cases concluded that there was no evidence of compartmentalization (Ince et al, 2009; Imamichi et al, 2011). For Subject 162, specific *env* regions including the V3 loop were nearly identical inside and outside the brain. This highlights the importance of examining full length *env* for studies of compartmentalization and viral diversity.

Sequence analysis revealed many mutations in *env* sequences, though none have been previously attributed to changes in macrophage tropism. An asparagine at position 283 and loss of an N-linked glycosylation site at 386 have

been shown to be associated with macrophage tropic brain variants in subjects with HIV-Associated Dementia (HAD) (Dunfee et al, 2006; Dunfee et al, 2007). An E153G mutation has also been shown to be a determinant of macrophage tropism in a pediatric subject with neurological complications (Musich et al, 2012). However none of the sequences had any of these mutations.

Few statistically significant differences were observed for the means of *env* length, charge, or number of PNGS, as determined using unpaired, two-tailed t tests. However, there was a clear difference in the variation of the range of values for *env* length, charge, and number of PNGS. In all cases, values for brain regions (frontal lobe, occipital lobe, and parietal lobe) were limited to a very narrow set of values. Interestingly, OL *envs* had a PNGS that was not present in FL or PL *envs*, as well as a lower net charge.

In contrast, *env* length, charge, and number of PNGS from colon, lung, and lymph node were much more varied. Several studies on V1-V2 length and PNGS have suggested that shorter V1-V2 regions and fewer PNGS are characteristic of transmitted variants and early infection (Pollakis et al, 2001; Derdeyn et al, 2004; Chohan et al, 2005; Sagar et al, 2006; Liu et al, 2008; Curlin et al, 2010; Huang et al, 2012; Wang et al, 2012; Pollakis et al, 2015). One hypothesis is that this could be due to fewer immune pressures early in infection, and thus less need for variation and protection by PNGS. However this does not explain how these variants would be present in an individual later during the course of infection such that they could be transmitted to others. In addition, brain *envs* did appear to be

slightly shorter and have fewer PNGS, though this was not statistically significant. This is consistent with previous findings, as it is likely brain *envs* would also not be subjected to as severe immune pressures as *envs* in tissues of the body would.

Recombination was widespread in all tissues types and did not affect the function of the Envs, as discussed in Chapter IV (Figure 3.15). On the other hand, predicted rates of hypermutation were varied between different tissue types (Figure 3.15). It was noted during sequence analysis that many of the sequences contained premature stop codons. Upon further inspection, it was discovered that these were almost entirely G to A mutations, a signature of APOBEC activity (reviewed in Refsland and Harris, 2013). When these sequences were analyzed using the Hypermut program, it was confirmed that these mutations were consistent with APOBEC activity. Three tissues had hypermutation: the occipital lobe, colon, and lung. The majority, 15 out of 19 hypermutated sequences, were from lung. Interestingly, studies have shown that the lung has high levels of APOBEC expression (Koning et al, 2009; Refsland et al, 2010; Fourati et al, 2014). However other sites, including immune tissues, have also been shown to express APOBEC but did not have a high level of hypermutation in this study.

PacBio sequencing data provided a first look at a large number of *env* sequences from multiple tissue sites. However, this data is preliminary and thus limited conclusions can be drawn from it. A major obstacle of this study was that no established protocol for data analysis existed prior to beginning this work.

Collaborators continue to develop a pipeline for analysis and this project remains in progress.

Based on preliminary data, the phylogenetic tree from PacBio sequences showed similar compartmentalization as was observed using PCR amplified clones (Figures 3.1 and 3.16). One difference was that colon sequences appeared much more compartmentalized on the tree of PacBio sequences. It is not clear why this would be, but may be the result of low proviral load in the tissues sampled. Thus only a small number of variants were sampled for PacBio seqeuncing, resulting in many of the same sequences. It is also possible that the there were just too few PCR clones to see compartmentalization in the colon. Several small groups of colon sequences did cluster together on the PCR clone tree, but only 11 *envs* were examined, in comparison to 250 on the PacBio sequence tree. Compartmentalization may have become more clear if additional PCR clone sequences were added to the tree. It is not known why so few sequences were generated from the lung tissue. PacBio sequencing may be repeated for this tissue.

In summary, it is clear that *envs* outside of the brain are much more diverse than *envs* inside the brain. Though *envs* from the body were not genetically compartmentalized from one another, they did have differences in length, charge, number of PNGS, and rates of hypermutation. This may indicate that different tissue microenvironments result in unique viral variants, which could be explored further in future studies.

Envelopes from within the brain tissues were in an immune privileged site, with fewer permissive cell types. Accordingly, *envs* in the brain faced fewer and less diverse evolutionary pressures, resulting in more constrained sequences. In Chapter IV these Envs were tested for phenotypes to determine if they were similarly influenced by evolution in distinct tissue compartments.

CHAPTER IV: FUNCTIONAL CHARACTERIZATION OF HIV-1 ENVELOPES FROM TISSUES OF AN HIV-1 INFECTED SUBJECT

4.1 Introduction

In the first part of this study, discussed in Chapter III, 75 full length *envs* were amplified from six different tissue compartments and compared for genotypic variation. In this second part, these Envs were expressed on pseudoviruses and subjected to functional assays to compare phenotypic variation. Similar to previous genotypic studies, phenotypic studies have been limited to few tissue types and thus do not adequately address quasispecies variation within an infected individual. Here, Envs were characterized by their functionality, cell tropism, coreceptor use, and susceptibility to neutralization by inhibitors and monoclonal antibodies.

Coreceptor use and tropism have been previously studied in some tissues, such as the brain, immune tissues, and plasma, as reviewed in Chapter I. These studies have shown that T cell tropic R5-using variants are typically transmitted, but may evolve to use X4 or infect macrophages as disease progresses (Keele et al, 2008; Salazar-Gonzalez et al, 2009; Wilen et al, 2011; Ochsenbauer et al, 2012). Previous studies have also shown that Envs from the brain were macrophage tropic and those outside the brain were predominantly, but not always, non-macrophage tropic (Gorry et al, 2001; Peters et al, 2004; Gonzalez-Perez et al, 2012).

To further characterize envelope phenotypes and gain insight into possible structural differences between envelopes from different tissues, pseudoviruses were subjected to inhibition assays using sCD4 and maraviroc, and neutralization assays with monoclonal antibodies b12, PG16, 17b, and 447-52D. These reagents were selected to provide information on whether the trimer was closed or open, the V3 loop was exposed or occluded, and to further probe the extent that the CD4 binding site was exposed.

These functional studies provide new insight into phenotypic differences in quasispecies from various tissue compartments. The results of this study will aid in the understanding of how viral variants may evolve differently due to distinct tissue specific pressures.

4.2 Results

4.2.1 Most envelopes were able to infect HeLa TZM-bl cells

All envelopes isolated were tested for functionality based on the ability of Env+ pseudoviruses to infect HeLa TZM-bl cells (Figures 4.1 – 4.4). Infectivity was evaluated by titrating Env+ pseudoviruses and counting FFUs. Infectivity titers of $>10^3$ FFU/ml were considered sufficiently functional for further study, explained further in Chapter II. For brain, 100% of frontal lobe envelopes (8/8), 70% of occipital lobe envelopes (7/10), and 80% of parietal lobe envelopes (4/5) were functional. Outside brain, 91% of colon envelopes (10/11), 45% of lung envelopes (13/29), and 92% of lymph node envelopes (11/12) were also functional.

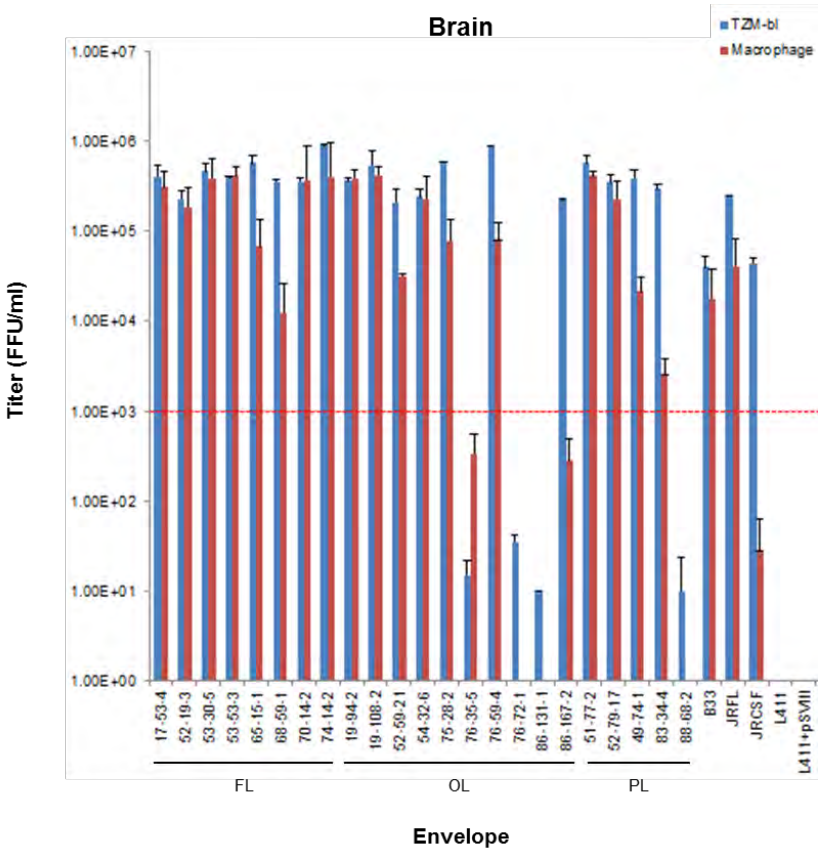

Figure 4.1 TZM-bl and macrophage titers of Envs from the brain Envs derived from the brain tissues (frontal lobe, occipital lobe, and parietal lobe) of Subject 162 were made into pseudoviruses and tested for their ability to infect TZM-bl cells and macrophages. Laboratory strains B33, JRFL, and JRCSF were used as controls. B33 and JRFL were functional and macrophage tropic controls. JRCSF was a functional and non-macrophage tropic control. The L411 *env*- plasmid and L411 *env*- plasmid + pSVIII plasmid were used as negative controls. The red line shows the cut off titer value for an Env to be considered functional on TZM-bl cells or macrophage tropic.

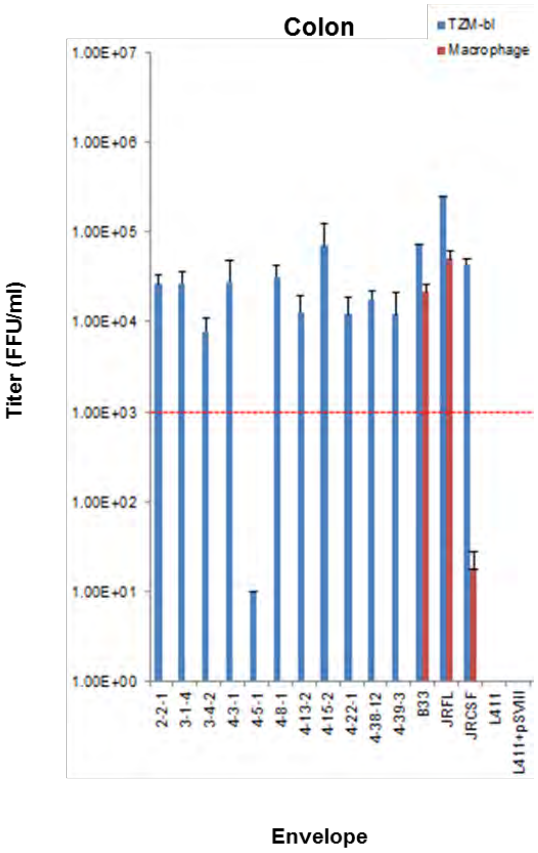

Figure 4.2 TZM-bl and macrophage titers of Envs from the colon Envs derived from the colon tissue of Subject 162 were made into pseudoviruses and tested for their ability to infect TZM-bl cells and macrophages. Laboratory strains B33, JRFL, and JRCSF were used as controls. B33 and JRFL were functional and macrophage tropic controls. JRCSF was a functional and non-macrophage tropic control. The L411 *env*- plasmid and L411 *env*- plasmid + pSVIII plasmid were used as negative controls. The red line shows the cut off titer value for an Env to be considered functional on TZM-bl cells or macrophage tropic.

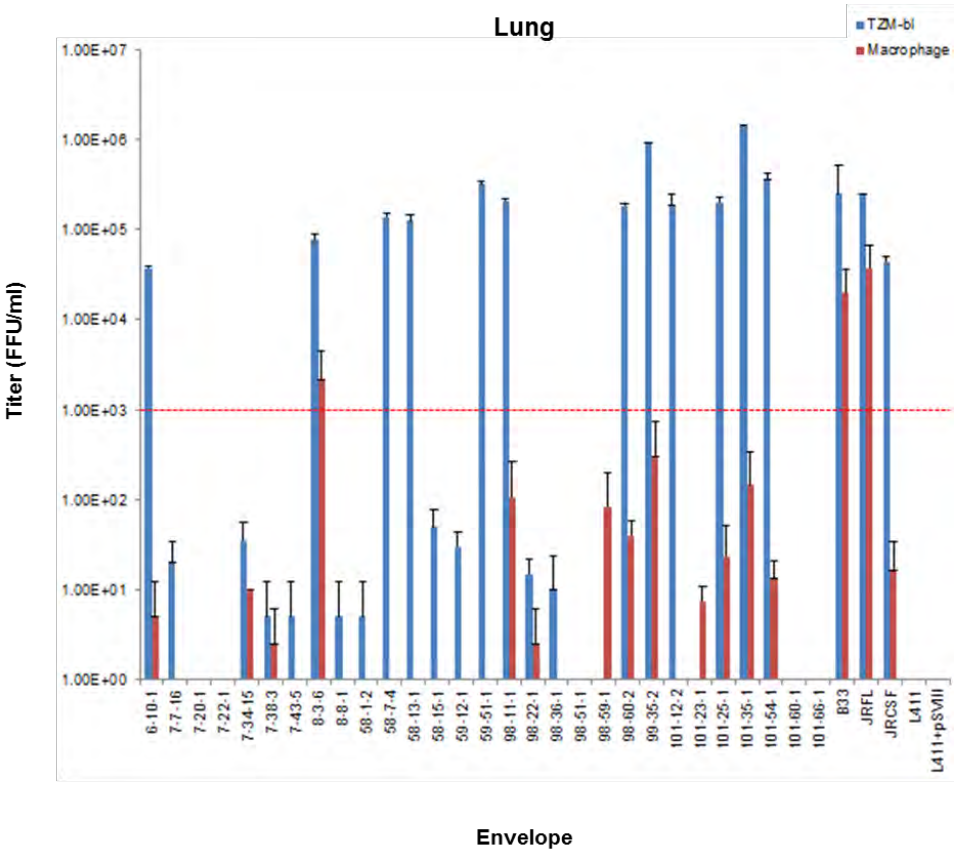

Figure 4.3 TZM-bl and macrophage titers of Envs from the lung Envs derived from the lung tissue of Subject 162 were made into pseudoviruses and tested for their ability to infect TZM-bl cells and macrophages. Laboratory strains B33, JRFL, and JRCSF were used as controls. B33 and JRFL were functional and macrophage tropic controls. JRCSF was a functional and non-macrophage tropic control. The L411 *env*- plasmid and L411 *env*- plasmid + pSVIII plasmid were used as negative controls. The red line shows the cut off titer value for an Env to be considered functional on TZM-bl cells or macrophage tropic.

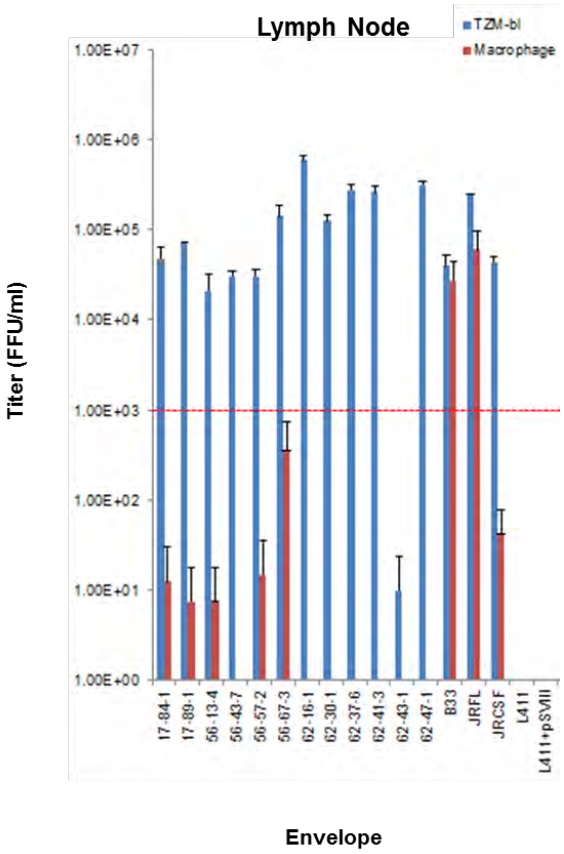

Figure 4.4 TZM-bl and macrophage titers of Envs from the lymph node Envs derived from the lymph node tissue of Subject 162 were made into pseudoviruses and tested for their ability to infect TZM-bl cells and macrophages. Laboratory strains B33, JRFL, and JRCSF were used as controls. B33 and JRFL were functional and macrophage tropic controls. JRCSF was a functional and non-macrophage tropic control. The L411 *env*- plasmid and L411 *env*- plasmid + pSVIII plasmid were used as negative controls. The red line shows the cut off titer value for an Env to be considered functional on TZM-bl cells or macrophage tropic.

4.2.2 All envelopes amplified used CCR5 and could not use CXCR4

Coreceptor use was predicted for all envelopes using the WebPSSM program (University of Washington). This program utilizes an algorithm that predicts coreceptor use from V3 loop sequences (Jensen et al, 2003). All envelopes were predicted to use CCR5 as a coreceptor. All shared similar charges and carried amino acids S and A at positions 11 and 25, respectively.

Functional pseudoviruses were able to infect HeLa TZM-bl cells, which express both CCR5 and CXCR4 coreceptors (Figures 4.1 – 4.4). However none of the functional pseudoviruses were able to infect HeLa HIJ cells which express CD4 and CXCR4 but not CCR5 (not shown). This is consistent with the WebPSSM prediction that all envelopes use CCR5 as a coreceptor and rules out the possibility that they could have been dual-tropic.

4.2.3 Brain derived envelopes were macrophage tropic while envelopes from tissues from the body were not

All pseudoviruses were tested for macrophage tropism on donor macrophages (Figures 4.1 – 4.4). All pseudoviruses constructed with envelopes derived from brain tissues were able to infect macrophages, with the exception of one occipital lobe envelope: 86-167-2. Conversely, only one pseudovirus with an envelope from tissue outside of the brain, 8-3-6 from the lung, was able to infect macrophages. All other envelopes from colon, lung, and lymph node were non-macrophage tropic.

4.2.4 Sensitivity to entry inhibitors and neutralizing monoclonal antibodies

sCD4

Consistent with previous studies, pseudoviruses prepared from envelopes from all three regions of the brain were inhibited at very low concentrations of sCD4 (Figures 4.5 and 4.6). In contrast, Envs from colon, lung, and lymph node varied in their sensitivity to sCD4, with colon Envs significantly more sensitive compared to those from lung and lymph node.

The difference in sensitivity to sCD4 between tissues from the brain (frontal lobe, occipital lobe, and parietal lobe) and the body (colon, lung, and lymph node) was also found to be highly significant ($P < 0.0001$) (Figure 4.6B). Highly significant differences were also noted for sCD4 sensitivity between FL:C, FL:L, FL:LN, OL:C, OL:L, OL:LN, PL:L, PL:LN, C:L, and C:LN (Figure 4.5B). Together these data are consistent with distinct selective pressures in brain and colon compared to lung and lymph node that influence the exposure of the CD4bs or the capacity of Envs to respond to CD4 binding.

Maraviroc

Maraviroc is an entry inhibitor that acts as a CCR5 antagonist and strongly inhibits entry of CCR5-using viral variants (Dorr et al, 2005; Wood and Armour, 2005). Maraviroc strongly inhibited most of the pseudoviruses (Figures 4.7 and 4.8). Envs from the lymph node were inhibited with IC50s ranging from 3.81-50.00 ng/ml. One colon Env, 4-38-12, was highly resistant with an IC50 >100 ng/ml. All other pseudoviruses were inhibited at low concentrations of maraviroc, with IC50s

between 2.35 and 21.88 ng/ml. These results do not indicate dramatic tissue dependent variation in CCR5 use. A significant difference was observed only between L:LN using an unpaired, two-tailed t test (Figure 4.7B).

b12

The b12 monoclonal antibody epitope maps to a region overlapping the CD4 binding site on gp120 (Burton et al, 1991; Barbas et al, 1992; Burton et al, 1994; Roben et al, 1994). Previous studies have shown that the majority of clade B macrophage tropic CCR5-using envelopes are sensitive to b12, while only a fraction of non-macrophage tropic envelopes are (Peters et al. 2008; Dunfee et al, 2009; O'Connell et al, 2013). For many of these latter envelopes, the b12 epitope is occluded within the trimer. Here, most Env+ pseudoviruses with envelopes from brain and other tissues were resistant or had IC50s in a narrow range of b12 concentrations of 35 - 50 μg/ml (Figures 4.9 and 4.10). However, several envelopes from lung and lymph node, and one from frontal lobe, were highly sensitive. Using an unpaired, two-tailed t test, a significant difference was observed between C:LN, but not with any other tissues or between the brain and body (Figures 4.9B and 4.10B). These data are not consistent with previous studies that mainly used Envs derived from subjects with dementia (Peters et al, 2008; Dunfee et al, 2009; Gonzalez-Perez et al, 2012).

PG16

The PG16 antibody recognizes a glycosylation and trimer dependent conformational epitope at the apex of the trimer association domain (Walker et al,

2009; Doores and Burton, 2010). PG16 neutralized all pseudoviruses with brain envelopes at low concentrations (~0.01 μg/ml). Pseudoviruses with envelopes from other tissues were either strongly neutralized or strongly resistant (Figures 4.11 and 4.12). The resistance of these latter envelopes was not due to the absence of either of the critical N-linked glycosylation sites at N156 and N160 (McLellan et al, 2011; Julien et al, 2013; Wang et al, 2013).

A statistically significant difference was observed between IC50s of tissues from the brain (frontal lobe, occipital lobe, and parietal lobe) and tissues from the body (colon, lung, and lymph node) using an unpaired two-tailed t test in GraphPad Prism (Figure 4.12B). Specific tissues were also compared and it was found that only frontal lobe and colon had a statistically significant difference (Figure 4.11B). However, differences between other tissues had P values that approached significance (~0.05).

17b

The 17b antibody recognizes a CD4-induced epitope that overlaps the coreceptor binding site (Thali et al, 1993; Wyatt et al, 1995; Trkola et al, 1996; Kwong et al, 1998; Sullivan et al, 1998; Wyatt et al, 1998). 17b neutralizes several T cell line adapted laboratory isolates but does not usually neutralize primary HIV-1 strains. Almost all pseudoviruses were resistant to 17b neutralization with IC50s >50 μg/ml, the highest concentration used in this experiment (Figure 4.13 and 4.14). Only 58-13-1 from the lung and 62-30-1 from the lymph node showed some sensitivity, but with high IC50s at 33.17 μg/ml and 38.14 μg/ml, respectively.

447-52D

The 447-52D antibody recognizes the KSIHIGPGRAF epitope of the V3 region of the HIV-1 envelope with the GPGR motif especially critical (Gorny et al, 1992; Gorny et al, 1993; Conley et al, 1994; Zolla-Pazner et al, 1995; Gorny et al, 1997; Binley et al, 2004; Stanfield et al, 2004; Krachmarov et al, 2006; Burke et al, 2009; Hioe et al, 2010). Sequence analysis showed that all *envs* had the 447-52D epitope. Despite this, only one pseudovirus was inhibited: 8-3-6 from the lung. All other pseudoviruses were strongly resistant to neutralization by 447-52D, even at the highest concentration of 50 μg/ml (Figures 4.15 and 4.16). There was no difference between envelopes from different tissue compartments. These data indicate that the V3 loop crown was occluded within the trimer association domain for all envelopes except 8-3-6 from lung.

4.3 Discussion

In this second part of the study, HIV-1 *envs* that were isolated and genotypically characterized in Chapter III were prepared as Env+ pseudoviruses to test their phenotypes. Once pseudoviruses were made, they were first tested on TZM-bl cells to determine whether or not they were functional. Due to the high rate of mutation in HIV-1, some *envs* acquire mutations that render the Env glycoprotein non-infectious. TZM-bl cells are a permissive cell line that expresses

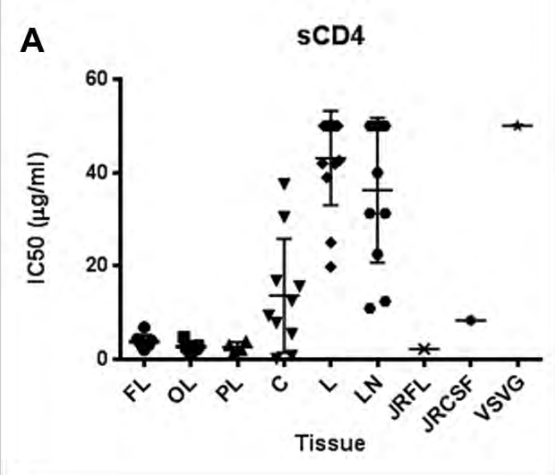

B

Tissues	P value
FL:OL	0.1280
FL:PL	0.1971
FL:C	0.0376
FL:L	< 0.0001
FL:LN	< 0.0001
OL:PL	0.9015
OL:C	0.0330
OL:L	< 0.0001
OL:LN	< 0.0001
PL:C	0.1030
PL:L	< 0.0001
PL:LN	0.0010
C:L	< 0.0001
C:LN	0.0016
L:LN	0.2045

C

Tissue	Mean	Standard Deviation
FL	3.78	1.456
OL	2.71	1.011
PL	2.62	1.111
C	13.65	12.180
L	43.10	10.090
LN	36.22	15.510

Figure 4.5 sCD4 inhibition of HIV-1 Envs from different tissues A) Each Env was tested for sensitivity to inhibition by sCD4. IC50s were calculated and plotted using GraphPad Prism. Laboratory strains JRFL and JRCSF were used as sCD4 sensitive controls. Vesicular Stomatitis Virus G protein (VSVG) was used as a sCD4 resistant control. **B)** An unpaired, two-tailed t test was used to test for statistical difference in the mean between the Env populations in each tissue compartment. Statistically significant values are shown in red. **C)** Mean and standard deviation are given to show the spread of the data range for the Envs from each tissue compartment.

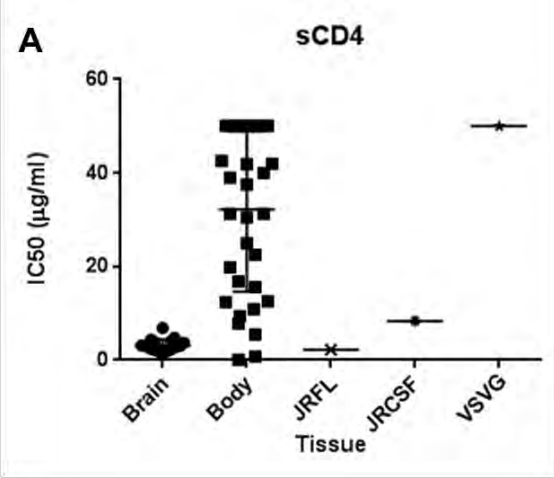

B

Tissues	P value
Brain:Body	< 0.0001

C

Tissue	Mean	Standard Deviation
Brain	3.14	1.287
Body	32.21	17.520

Figure 4.6 sCD4 inhibition of HIV-1 Envs from the brain and body A) Each Env in the brain and body was tested for sensitivity to inhibition by sCD4. IC50s were calculated and plotted using GraphPad Prism. Laboratory strains JRFL and JRCSF were used as sCD4 sensitive controls. Vesicular Stomatitis Virus G protein (VSVG) was used as a sCD4 resistant control. **B)** An unpaired, two-tailed t test was used to test for statistical difference in the mean between the Env populations of the brain and body. Statistically significant values are shown in red. **C)** Mean and standard deviation are given to show the spread of the data range for the Envs from each compartment.

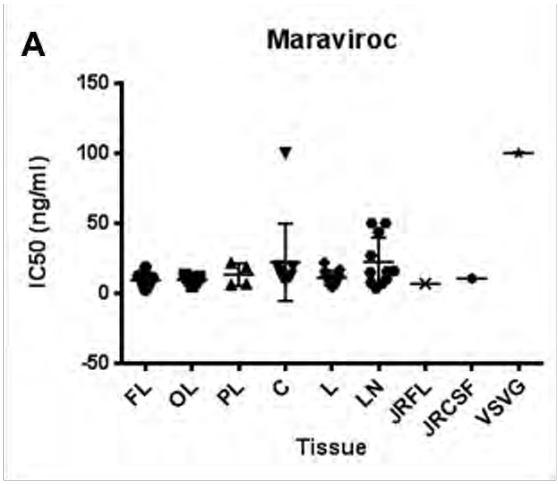

B

Tissues	P value
FL:OL	0.9038
FL:PL	0.3136
FL:C	0.2198
FL:L	0.5125
FL:LN	0.0621
OL:PL	0.2824
OL:C	0.2578
OL:L	0.5548
OL:LN	0.0811
PL:C	0.5542
PL:L	0.4703
PL:LN	0.3548
C:L	0.1649
C:LN	0.9845
L:LN	0.0363

C

Tissue	Mean	Standard Deviation
FL	9.49	5.070
OL	9.75	2.803
PL	13.46	8.023
C	22.16	27.550
L	11.01	5.069
LN	22.36	17.580

Figure 4.7 Maraviroc inhibition of HIV-1 Envs from different tissues A) Each Env was tested for sensitivity to inhibition by maraviroc. IC50s were calculated and plotted using GraphPad Prism. Laboratory strains JRFL and JRCSF were used as maraviroc sensitive controls. Vesicular Stomatitis Virus G protein (VSVG) was used as a maraviroc resistant control. **B)** An unpaired, two-tailed t test was used to test for statistical difference in the mean between the Env populations in each tissue compartment. Statistically significant values are shown in red. **C)** Mean and standard deviation are given to show the spread of the data range for the Envs from each tissue compartment.

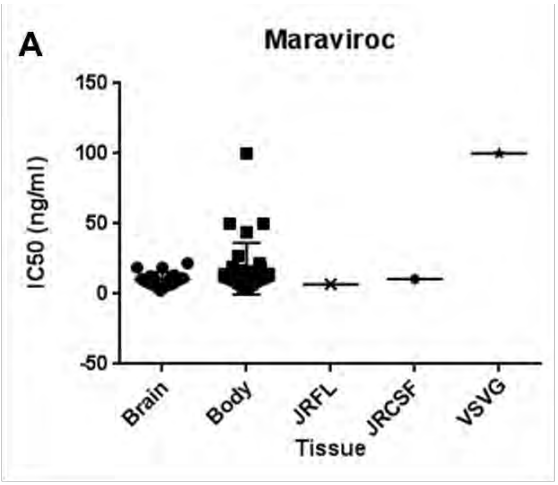

B

Tissues	P value
Brain:Body	0.0884

C

Tissue	Mean	Standard Deviation
Brain	10.42	5.094
Body	17.96	18.460

Figure 4.8 Maraviroc inhibition of HIV-1 Envs from the brain and body A) Each Env in the brain and body was tested for sensitivity to inhibition by maraviroc. IC50s were calculated and plotted using GraphPad Prism. Laboratory strains JRFL and JRCSF were used as maraviroc sensitive controls. Vesicular Stomatitis Virus G protein (VSVG) was used as a maraviroc resistant control. **B)** An unpaired, two-tailed t test was used to test for statistical difference in the mean between the Env populations of the brain and body. **C)** Mean and standard deviation are given to show the spread of the data range for the Envs from each compartment.

A

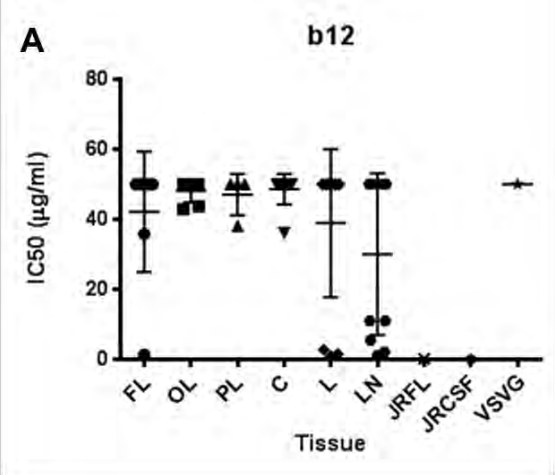

B

Tissues	P value
FL:OL	0.3865
FL:PL	0.6000
FL:C	0.2665
FL:L	0.7165
FL:LN	0.2295
OL:PL	0.7075
OL:C	0.7923
OL:L	0.2723
OL:LN	0.0593
PL:C	0.5895
PL:L	0.4659
PL:LN	0.1786
C:L	0.1684
C:LN	0.0220
L:LN	0.3400

C

Tissue	Mean	Standard Deviation
FL	42.15	17.210
OL	48.09	3.264
PL	47.04	5.915
C	48.62	4.370
L	38.87	21.150
LN	30.05	23.110

Figure 4.9 b12 neutralization of HIV-1 Envs from different tissues A) Each Env was tested for sensitivity to neutralization by b12. IC50s were calculated and plotted using GraphPad Prism. Laboratory strains JRFL and JRCSF were used as b12 sensitive controls. Vesicular Stomatitis Virus G protein (VSVG) was used as a b12 resistant control. **B)** An unpaired, two-tailed t test was used to test for statistical difference in the mean between the Env populations in each tissue compartment. Statistically significant values are shown in red. **C)** Mean and standard deviation are given to show the spread of the data range for the Envs from each tissue compartment.

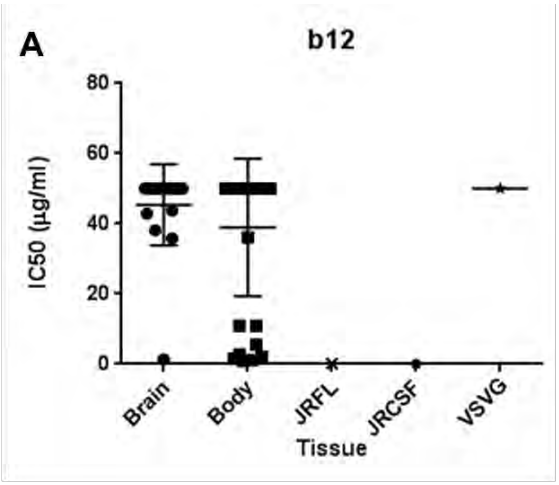

B

Tissues	P value
Brain:Body	0.1938

C

Tissue	Mean	Standard Deviation
Brain	45.37	11.520
Body	38.88	19.610

Figure 4.10 b12 neutralization of HIV-1 Envs from the brain and body A) Each Env in the brain and body was tested for sensitivity to neutralization by b12. IC50s were calculated and plotted using GraphPad Prism. Laboratory strains JRFL and JRCSF were used as b12 sensitive controls. Vesicular Stomatitis Virus G protein (VSVG) was used as a b12 resistant control. **B)** An unpaired, two-tailed t test was used to test for statistical difference in the mean between the Env populations of the brain and body. **C)** Mean and standard deviation are given to show the spread of the data range for the Envs from each compartment.

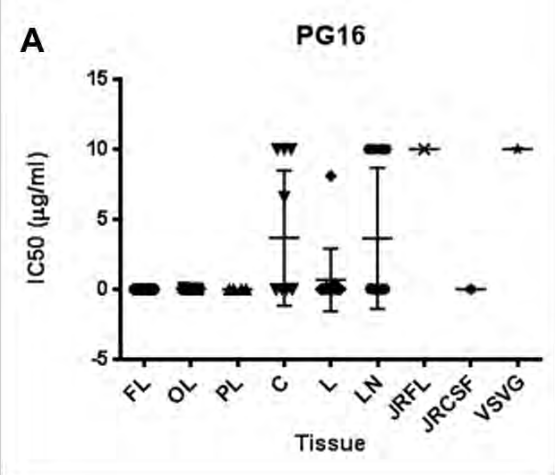

B

Tissues	P value
FL:OL	0.1686
FL:PL	*
FL:C	0.0488
FL:L	0.4152
FL:LN	0.0588
OL:PL	0.3426
OL:C	0.0666
OL:L	0.4596
OL:LN	0.0786
PL:C	0.1644
PL:L	0.5694
PL:LN	0.1821
C:L	0.0602
C:LN	0.9925
L:LN	0.0679

C

Tissue	Mean	Standard Deviation
FL	0.01	0
OL	0.03	0.036
PL	0.01	0
C	3.67	4.820
L	0.68	2.238
LN	3.65	5.037

Figure 4.11 PG16 neutralization of HIV-1 Envs from different tissues A) Each Env was tested for sensitivity to neutralization by PG16. IC50s were calculated and plotted using GraphPad Prism. Laboratory strain JRCSF was used as a PG16 sensitive control. Laboratory strain JRFL and Vesicular Stomatitis Virus G protein (VSVG) were used as PG16 resistant controls. **B)** An unpaired, two-tailed t test was used to test for statistical difference in the mean between the Env populations in each tissue compartment. Statistically significant values are shown in red. An asterisk denotes that t test could not be performed because the samples in both tissues had the same values. **C)** Mean and standard deviation are given to show the spread of the data range for the Envs from each tissue compartment.

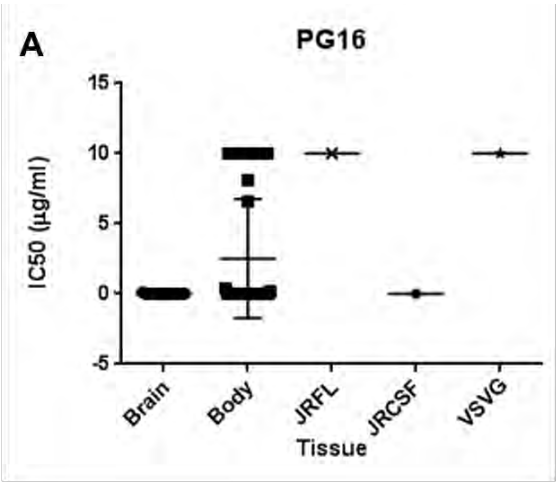

B

Tissues	P value
Brain:Body	0.0136

C

Tissue	Mean	Standard Deviation
Brain	0.02	0.023
Body	2.52	4.243

Figure 4.12 PG16 neutralization of HIV-1 Envs from the brain and body A) Each Env in the brain and body was tested for sensitivity to neutralization by PG16. IC50s were calculated and plotted using GraphPad Prism. Laboratory strain JRCSF was used as a PG16 sensitive control. Laboratory strain JRFL and Vesicular Stomatitis Virus G protein (VSVG) were used as PG16 resistant controls. **B)** An unpaired, two-tailed t test was used to test for statistical difference in the mean between the Env populations of the brain and body. Statistically significant values are shown in red. **C)** Mean and standard deviation are given to show the spread of the data range for the Envs from each compartment.

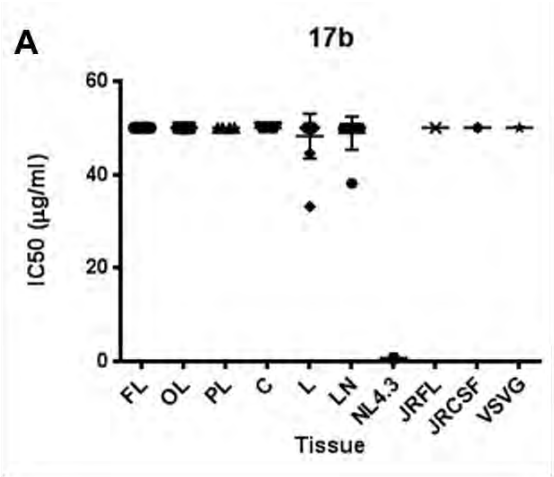

B

Tissues	P value
FL:OL	*
FL:PL	*
FL:C	*
FL:L	0.3187
FL:LN	0.4093
OL:PL	*
OL:C	*
OL:L	0.3520
OL:LN	0.4418
PL:C	*
PL:L	0.4855
PL:LN	0.5661
C:L	0.2630
C:LN	0.3535
L:LN	0.7064

C

Tissue	Mean	Standard Deviation
FL	50.00	0
OL	50.00	0
PL	50.00	0
C	50.00	0
L	48.25	4.775
LN	48.92	3.576

Figure 4.13 17b neutralization of HIV-1 Envs from different tissues A) Each Env was tested for sensitivity to neutralization by 17b. IC50s were calculated and plotted using GraphPad Prism. Laboratory strain NL4.3 was used as a 17b sensitive control. Laboratory strains JRFL and JRCSF and Vesicular Stomatitis Virus G protein (VSVG) were used as 17b resistant controls. **B)** An unpaired, two-tailed t test was used to test for statistical difference in the mean between the Env populations in each tissue compartment. An asterisk denotes that t test could not be performed because the samples in both tissues had the same values. **C)** Mean and standard deviation are given to show the spread of the data range for the Envs from each tissue compartment.

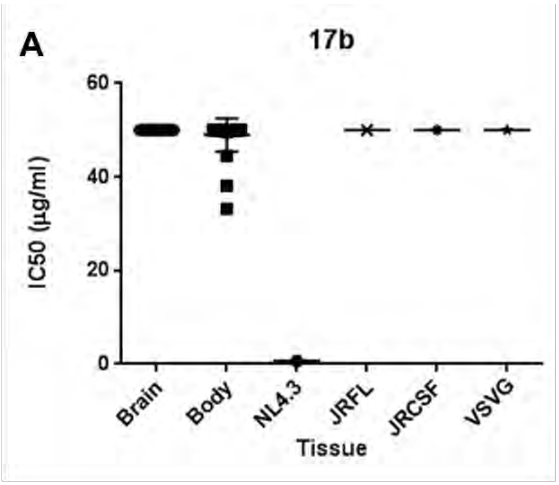

B

Tissues	P value
Brain:Body	0.2212

C

Tissue	Mean	Standard Deviation
Brain	50.00	0
Body	48.98	3.562

Figure 4.14 17b neutralization of HIV-1 Envs from the brain and body A) Each Env in the brain and body was tested for sensitivity to neutralization by 17b. IC50s were calculated and plotted using GraphPad Prism. Laboratory strain NL4.3 was used as a 17b sensitive control. Laboratory strains JRFL and JRCSF and Vesicular Stomatitis Virus G protein (VSVG) were used as 17b resistant controls. **B)** An unpaired, two-tailed t test was used to test for statistical difference in the mean between the Env populations of the brain and body. **C)** Mean and standard deviation are given to show the spread of the data range for the Envs from each compartment.

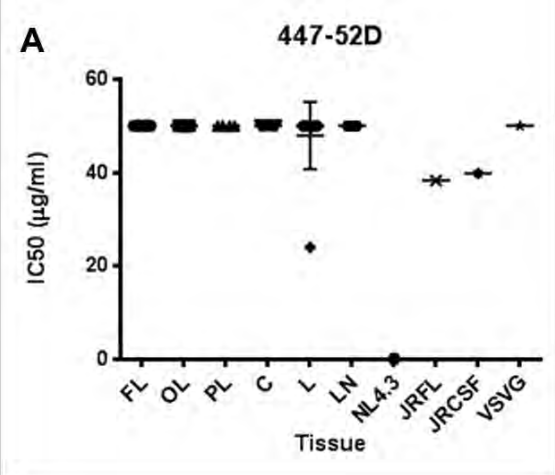

B

Tissues	P value
FL:OL	*
FL:PL	*
FL:C	*
FL:L	0.4408
FL:LN	*
OL:PL	*
OL:C	*
OL:L	0.4721
OL:LN	*
PL:C	*
PL:L	0.5906
PL:LN	*
C:L	0.3866
C:LN	*
L:LN	0.3629

C

Tissue	Mean	Standard Deviation
FL	50.00	0
OL	50.00	0
PL	50.00	0
C	50.00	0
L	47.98	7.199
LN	50.00	0

Figure 4.15 447-52D neutralization of HIV-1 Envs from different tissues A) Each Env was tested for sensitivity to neutralization by 447-52D. IC50s were calculated and plotted using GraphPad Prism. Laboratory strain NL4.3 was used as a 447-52D sensitive control. Laboratory strains JRFL and JRCSF and Vesicular Stomatitis Virus G protein (VSVG) were used as 447-52D resistant controls. **B)** An unpaired, two-tailed t test was used to test for statistical difference in the mean between the Env populations in each tissue compartment. An asterisk denotes that t test could not be performed because the samples in both tissues had the same values. **C)** Mean and standard deviation are given to show the spread of the data range for the Envs from each tissue compartment.

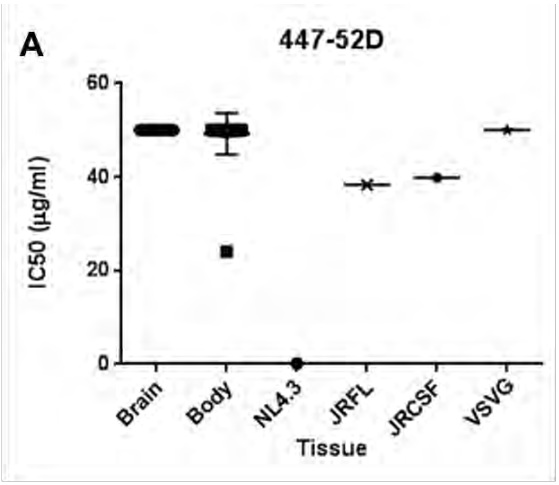

B

Tissues	P value
Brain:Body	0.4543

C

Tissue	Mean	Standard Deviation
Brain	50.00	0
Body	49.23	4.454

Figure 4.16 447-52D neutralization of HIV-1 Envs from the brain and body **A)** Each Env in the brain and body was tested for sensitivity to neutralization by 447-52D. IC50s were calculated and plotted using GraphPad Prism. Laboratory strain NL4.3 was used as a 447-52D sensitive control. Laboratory strains JRFL and JRCSF and Vesicular Stomatitis Virus G protein (VSVG) were used as 447-52D resistant controls. **B)** An unpaired, two-tailed t test was used to test for statistical difference in the mean between the Env populations of the brain and body. **C)** Mean and standard deviation are given to show the spread of the data range for the Envs from each compartment.

the CD4 receptor, as well as both the CCR5 and CXCR4 coreceptors, so pseudoviruses with functional Envs should be able to infect them. Most of the Envs were functional, as assessed by their ability to infect TZM-bl cells (Figures 4.1 - 4.4). However 22 out of 75 were non-functional, with a disproportionate number coming from the lung. A total of 29 envelopes were amplified from the lung and 16, or 55%, were non-functional. Only 6 of the non-functional Envs were from other tissues. When lung *env* sequences were examined, as described in Chapter III, it was clear why they were non-functional. The *envs* derived from lung tissue had far higher rates of hypermutation than *envs* from other tissues. In fact, all but one of the non-functional envelopes from lung were the result of hypermutation, probably due to APOBEC activity. The remaining non-functional envelopes were non-functional due to hypermutation along with premature stop codons.

Of the functional Envs, all of them used CCR5 as a coreceptor. This was not surprising since this was predicted based on sequence using the WebPSSM program (Jensen et al, 2003). Envs from brain tissues were able to infect macrophages, consistent with previous findings (Gorry et al, 2001; Peters et al, 2004; Gonzalez-Perez et al, 2012). This was not due to the presence of known determinants, such as N283, loss of an N-linked glycosylation site at 386, or E153G. Only one Env from the colon, lung, or lymph node was macrophage tropic, 8-3-6 from the lung, although several others also conferred low level infection. Previous studies have described macrophage tropic HIV-1 variants in the lung and suggested that the lung may serve as a reservoir (Clarke et al, 1990; Jambo et al,

2014). The 8-3-6 *env* did not have the same mutations observed in brain derived macrophage tropic *envs* and did not cluster with these sequences on the phylogenetic tree (Figure 3.1). It is therefore likely that macrophage tropism evolved independently in the brain and in the lung compartments.

The functional Envs were also tested for their sensitivity to sCD4 and maraviroc inhibitors, as well as a panel of monoclonal antibodies. It has been shown previously that sCD4 inhibition is correlated with macrophage tropism and suggests a trimer conformation with increased exposure of the CD4bs, although an enhanced interaction with CD4 is also possible (Peters et al, 2008; Gonzalez-Perez et al, 2012; O'Connell et al, 2013). Subject 162 macrophage tropic Envs were sensitive to sCD4 inhibition, consistent with these findings. However, there were also a number of non-macrophage tropic Envs from the colon, lung, and lymph node that were also sensitive to sCD4. In these tissues a range of IC50 values were observed, whereas with Envs from brain regions, inhibition occurred at a very low concentration of sCD4 for all Envs. An enhanced Env:CD4 interaction for Env trimers is presumably required for infection of resident macrophages of the brain, which express lower levels of CD4 compared to T cells (Lee et al, 1999; Bannert et al, 2000; Mori et al, 2000). In addition, Envs would also not need to be as tightly closed to protect from neutralizing antibodies as those outside brain, since the concentration of antibodies in the brain tissues is low (Triguero et al, 1989; Kuang et al, 2004). It's not known why a range of resistant and sensitive phenotypes were present in the colon, lung, and lymph node tissues. Env trimers

in these tissues are more susceptible to immune pressures, so it is logical that they would remain in a more closed conformation to protect the CD4bs. It is possible that in this end stage AIDS subject, the immune system was failing and the resulting reduced immune pressure allowed for more open trimers to emerge and possibly the appearance of macrophage tropic variants. Macrophage tropic variants often do arise late in disease progression (Li et al, 1999; Tuttle et al, 2002; Gray et al, 2005; Thomas et al, 2007). Perhaps these more open, but not macrophage tropic, variants represent an intermediate phenotype in these tissue compartments, as recently suggested by work from the Swanstrom Lab (Arrildt et al, 2015).

Almost all Envs were inhibited by maraviroc, which is a strong inhibitor of R5-using HIV-1 variants. All of the Envs from this subject were shown to use the R5 coreceptor. Only one Env, 4-38-12 from the colon, was highly resistant. However, several from lymph node were modestly resistant, consistent with an enhanced Env:CCR5 interaction late in disease (Gorry et al, 2002; Reeves et al, 2002; Karlsson et al, 2004; Reeves et al, 2004; Gray et al, 2005; Repits et al, 2005; Repits et al, 2008; Etemad et al, 2009). Envs that can use the X4 coreceptor are resistant to maraviroc. However 4-38-12 was shown to use R5 both based on envelope sequence predictions and its inability to infect HeLa HIJ cells via CXCR4. It is possible that this Env can use an alternative coreceptor for entry that was not tested. Alternatively, some CCR5-using Envs are resistant to maraviroc. This may be due to enhanced affinity for CCR5 or the ability to use maraviroc-occupied

CCR5 (Westby et al, 2007; Agrawal-Gamse et al, 2009; Pfaff et al, 2010; Tilton et al, 2010).

The b12 antibody overlaps the CD4 binding site and sensitivity has been associated with R5 macrophage tropism (Peters et al, 2008; Dunfee et al, 2009; O'Connell et al, 2013). In Subject 162, this was not the case. The majority of Envs were resistant to neutralization by b12 regardless of whether or not they were macrophage tropic. A few highly sensitive Envs were observed from the frontal lobe, lung, and lymph node. Neutralization by PG16 is dependent on Env glycosylation and conformation. PNGS at N156 and N160 have been shown to play a role in PG16 recognition (McLellan et al, 2011; Julien et al, 2013; Wang et al, 2013). All Envs had these PNGS and most were highly sensitive to PG16 neutralization. The frontal lobe, occipital lobe, and parietal lobe Envs were all neutralized at very low PG16 concentrations. Envs from the colon, lung, and lymph node compartments were either very resistant or very sensitive to neutralization, without any intermediate phenotypes. While no known mutations associated with PG16 resistance were observed, resistant envelopes had a K130E mutation. However several envelopes that were sensitive to PG16 also had this mutation, so this alone cannot be sufficient to confer resistance.

Using the final two antibodies, 17b and 447-52D, no differences were observed between different tissues compartments. All Envs were resistant to neutralization with 17b, which recognizes a CD4-induced epitope. Similarly, all Envs were resistant to neutralization by 447-52D, which recognizes a

KSIHIGPGRAF epitope of the V3 loop. While all envelopes had this sequence, none of them were sensitive, indicating that the epitope was occluded within the structure. Only one Env, 8-3-6 from the lung, showed moderate sensitivity to neutralization by 447-52D. Interestingly, this Env is also macrophage tropic and sensitive to inhibition with sCD4. This suggests that this Env trimer has a more open conformation where the V3 loop and CD4bs are more exposed, thus helping to explain its ability to use low levels of CD4 to infect macrophages as well as its susceptibility to sCD4.

Chapter III investigated the genotypic differences in *envs* derived from different tissues of an HIV-1 positive individual. It was observed that *envs* from tissues within the brain were very similar in their sequences and properties, while *envs* from other regions of the body had much more varied characteristics. Here, these same Envs were examined for their phenotypes and a similar outcome was observed. Envs from regions of the brain behaved almost identically in all functional tests, while those from tissues of the body had a wide range of phenotypes. This again highlights the differences in these tissues and the evolutionary pressures that contribute to Env evolution. Envs in the brain must adapt to use low CD4 on the resident macrophages of the brain. However, they may be under less pressure from interaction with antibodies. Conversely, Envs in the body must evolve to avoid antibody neutralization but have access to several permissive cell types, allowing for more diversity in phenotypes. Studying these

different functional characteristics will aid in the understanding of viral quasispecies populations.

CHAPTER V: GENERAL DISCUSSION

5.1 Summary

In this study, full length HIV-1 envelopes were characterized in three different ways: by genotypic properties, through functional phenotypes, and using next generation sequencing. These *envs* were derived from the frontal lobe, occipital lobe, parietal lobe, colon, lung, and lymph node of an HIV-1 infected subject who died from end stage AIDS. This is the first study in which envelopes from an individual patient have been so extensively characterized. In addition, this is the first study to use Pacific Biosciences next generation sequencing to study full length proviral HIV-1 *envs*.

The first part of this study, discussed in Chapter III, used limiting dilution nested PCR to amplify full length HIV-1 *envs* from each tissue. These *envs* were examined for mutations known to affect tropism, length, charge, PNGS, hypermutation, and recombination. The *env* sequences were assembled into a phylogenetic tree and assessed for compartmentalization. The *envs* isolated from brain tissues (frontal lobe, occipital lobe, and parietal lobe) were very homogeneous in all areas. However, *envs* from tissues of the body (colon, lung, and lymph node) were very diverse in their genotypes.

The same outcome was observed in the second part of this study, discussed in Chapter IV. The Envs from each tissue were incorporated into pseudoviruses to examine functionality, coreceptor use, macrophage tropism, and

sensitivity to sCD4 and maraviroc inhibitors and neutralization by b12, PG16, 17b, and 447-52D monoclonal antibodies. Envs derived from tissues of the brain were similar in all phenotypes tested, while Envs from tissues of the body were more varied in their phenotypes.

5.2 Future Studies

The results of this study provide the first picture of how HIV-1 variants may evolve differently at various tissue sites within an infected individual. Additional studies could further elucidate the variation observed in different tissue compartments and help decipher the role this plays in disease progression.

Structural differences could explain changes in tropism or sensitivity to inhibitors and antibodies. Modeling programs could be used to predict structural changes of Envs based on sequences or structures could be examined using X-ray crystallography or Cryo-EM. Structural studies may reveal that some Envs are more open, such as those from the brain or 8-3-6 from the lung, allowing them to infect macrophages and be inhibited by sCD4. This could be supported by experiments to test envelope affinity for receptors, inhibitors, and antibodies.

None of the mutations known to change tropism (e.g., N283, loss of an N-linked glycosylation site at 386, and E153G) were observed. However there were other mutations throughout the *env* sequence, some of which were more frequent in a specific tissue compartment. In the case of the brain, it is possible that these mutations could be involved in macrophage tropism. To test this possibility, an

extensive mutagenesis study could be conducted in which all of the mutations that were specific to the brain tissues were introduced to *envs* from peripheral tissues with closely related sequences to see if they confer macrophage tropism. Likewise, it may be possible to determine what mutations are responsible for the differences observed in the inhibition and neutralization assays.

PacBio studies are ongoing and will be used to further examine *env* sequences in each tissue and will investigate whether tissue specific signature sequences and characteristics exist. In addition, time rooted phylogenetic trees will be constructed to determine which tissues may have been infected first and the migration patterns of viral variants throughout the body.

Finally, it would be useful to conduct further studies in additional subjects. A major limitation of this study is that it only examines one subject. It would be useful to determine if the observations are specific to Subject 162 or if they are common to all HIV-1 infected subjects. If possible, it would be helpful to work with a cohort where more information was available on the subject and their history. If a cohort could be established, additional questions could be asked as well. For example, how do these genotypes and phenotypes change over time? This is difficult to study in humans, as it is challenging or impossible to take longitudinal samples from some tissue sites. Thus previous longitudinal studies have been limited to few tissues compartments (Churchill et al, 2004; Schnell et al, 2010; Bull et al, 2013; Sturdevant et al, 2015; Vazquez-Santiago et al, 2015). It would be useful to know how quasispecies populations change over time within an

individual. The studies presented here could be expanded by modifying sampling methods to include biopsy where appropriate (e.g., colon and lymph node), bronchial lavage for lungs, and cerebrospinal fluid for brain.

5.3 Conclusions

This study added to the understanding of HIV-1 quasispecies populations by characterizing envelopes from multiple tissues within a single HIV-1 infected subject by both genotype and phenotype, which had not been done in any previous study. This is the most comprehensive study of HIV-1 envelope characteristics to date. It is clear in this subject that HIV-1 envelopes within the frontal lobe, occipital lobe, and parietal lobe of the brain have very low diversity. Envelopes from colon, lung, and lymph node peripheral tissues are much more diverse in both their genotypes and phenotypes. This diversity varied across the *env* sequence, highlighting the importance of studying full length *env*. Better understanding of viral quasispecies populations may aid in developing vaccines by defining new targets as well as promote discovery of curative treatments by describing populations in potential HIV-1 reservoir sites.

APPENDIX A: PHYLOGENETIC TREES FOR CHAPTER III

The following appendix contains phylogenetic trees for different *env* regions for Subject 162. Methods were followed as described in Chapter II to construct trees for gp120, gp41, V1-V2, V1-V5, C1, C2, C3, C4, C5, V1, V2, V3, V4, and V5. These phylogenetic trees were discussed in Chapter III and used to calculate evolutionary divergence (Figure 3.2).

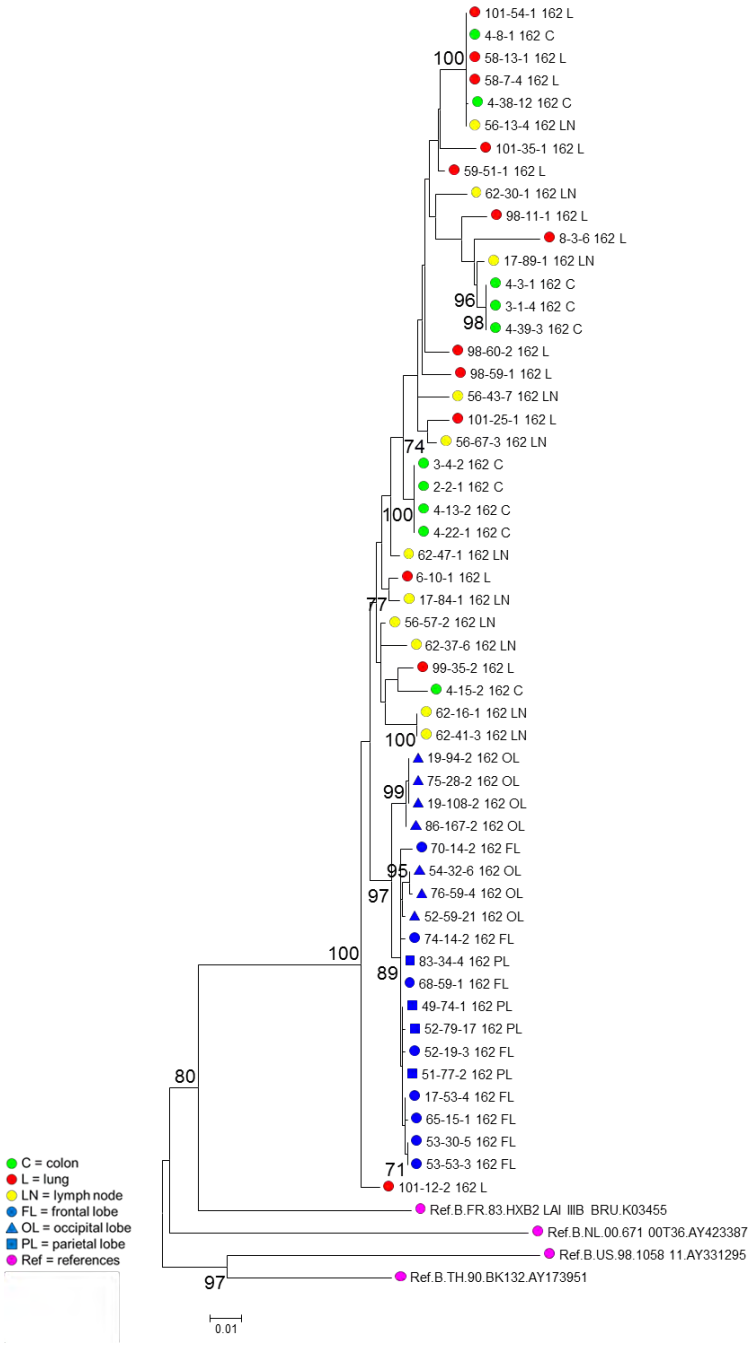

Figure A.1 Phylogenetic analysis of Subject 162 gp120 sequences Full length HIV-1 *envs* were amplified from three brain regions (frontal lobe, occipital lobe, and parietal lobe), colon, lung, and lymph node. Four unrelated reference sequences were used as an outgroup. A maximum likelihood tree was constructed using MEGA version 5 for functional HIV-1 *env* gp120 regions. Bootstrap vaues ≥70% are noted at branch points. Scale bar shows nucleotide substitutions per site.

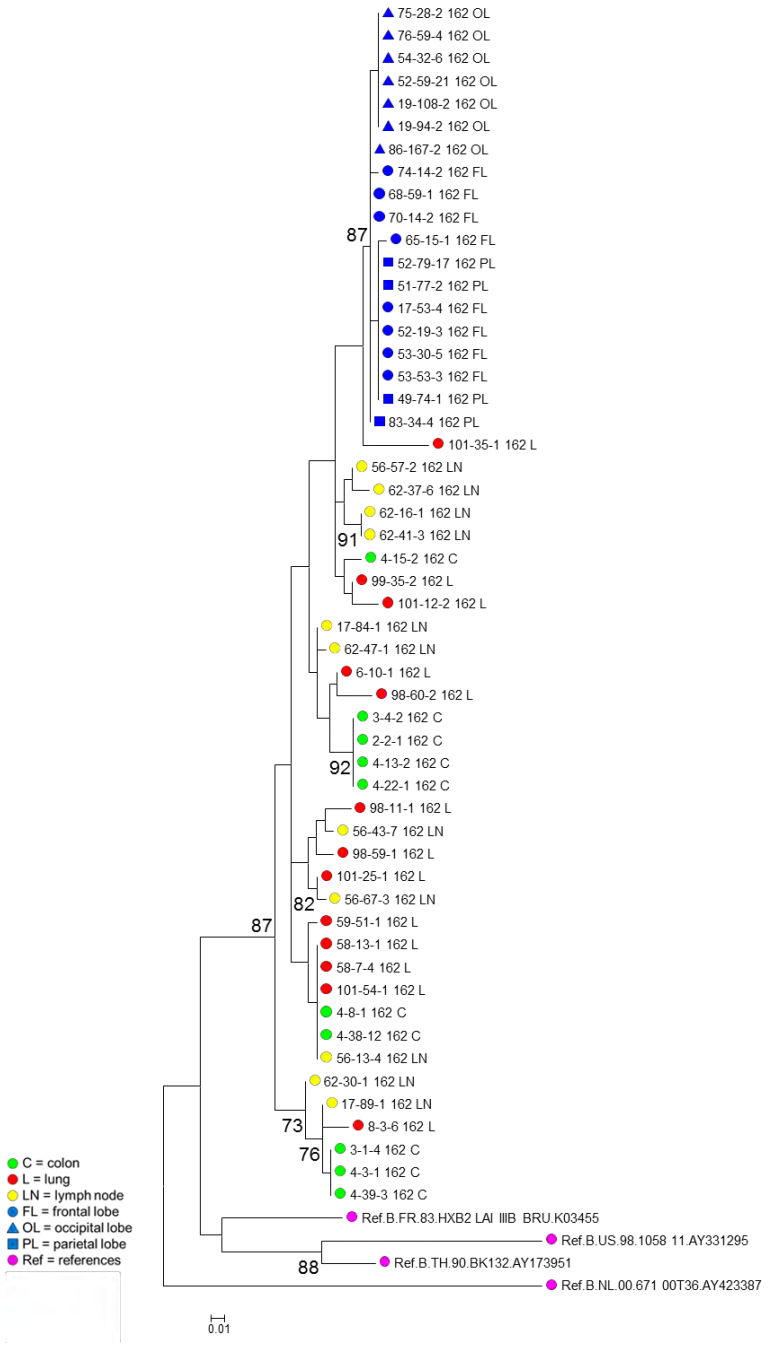

Figure A.2 Phylogenetic analysis of Subject 162 gp41 sequences Full length HIV-1 *envs* were amplified from three brain regions (frontal lobe, occipital lobe, and parietal lobe), colon, lung, and lymph node. Four unrelated reference sequences were used as an outgroup. A maximum likelihood tree was constructed using MEGA version 5 for functional HIV-1 *env* gp41 regions. Bootstrap vaues ≥70% are noted at branch points. Scale bar shows nucleotide substitutions per site.

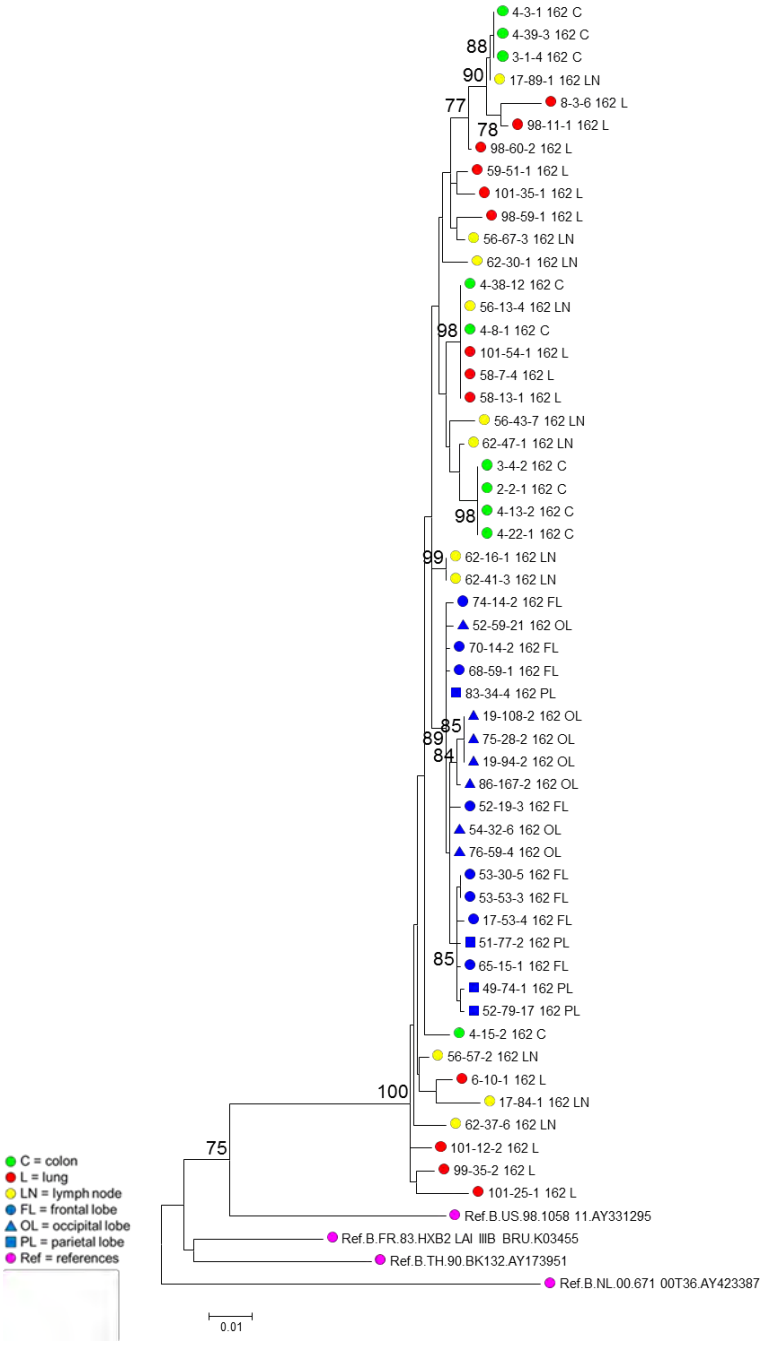

Figure A.3 Phylogenetic analysis of Subject 162 V1-V2 sequences Full length HIV-1 *envs* were amplified from three brain regions (frontal lobe, occipital lobe, and parietal lobe), colon, lung, and lymph node. Four unrelated reference sequences were used as an outgroup. A maximum likelihood tree was constructed using MEGA version 5 for functional HIV-1 *env* V1-V2 regions. Bootstrap vaues ≥70% are noted at branch points. Scale bar shows nucleotide substitutions per site.

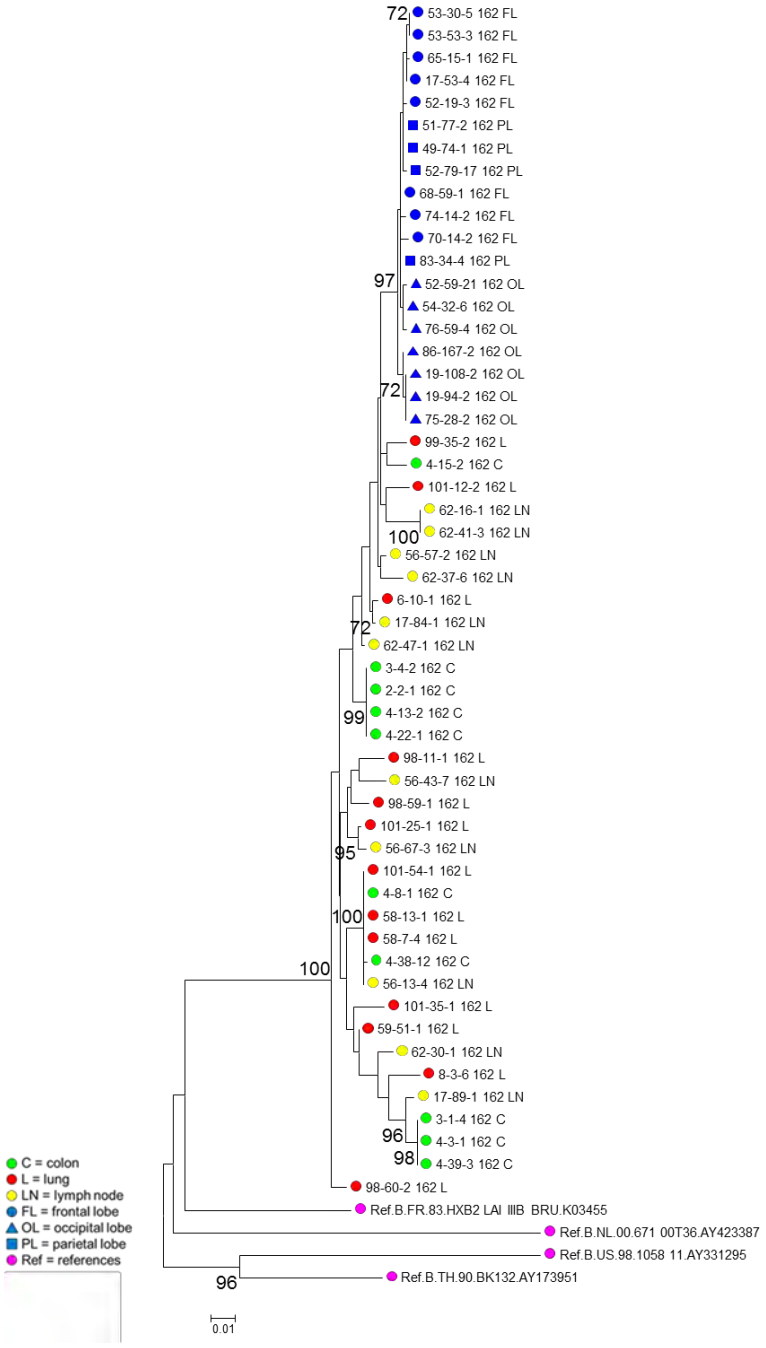

Figure A.4 Phylogenetic analysis of Subject 162 V1-V5 sequences Full length HIV-1 *envs* were amplified from three brain regions (frontal lobe, occipital lobe, and parietal lobe), colon, lung, and lymph node. Four unrelated reference sequences were used as an outgroup. A maximum likelihood tree was constructed using MEGA version 5 for functional HIV-1 *env* V1-V5 regions. Bootstrap vaues ≥70% are noted at branch points. Scale bar shows nucleotide substitutions per site.

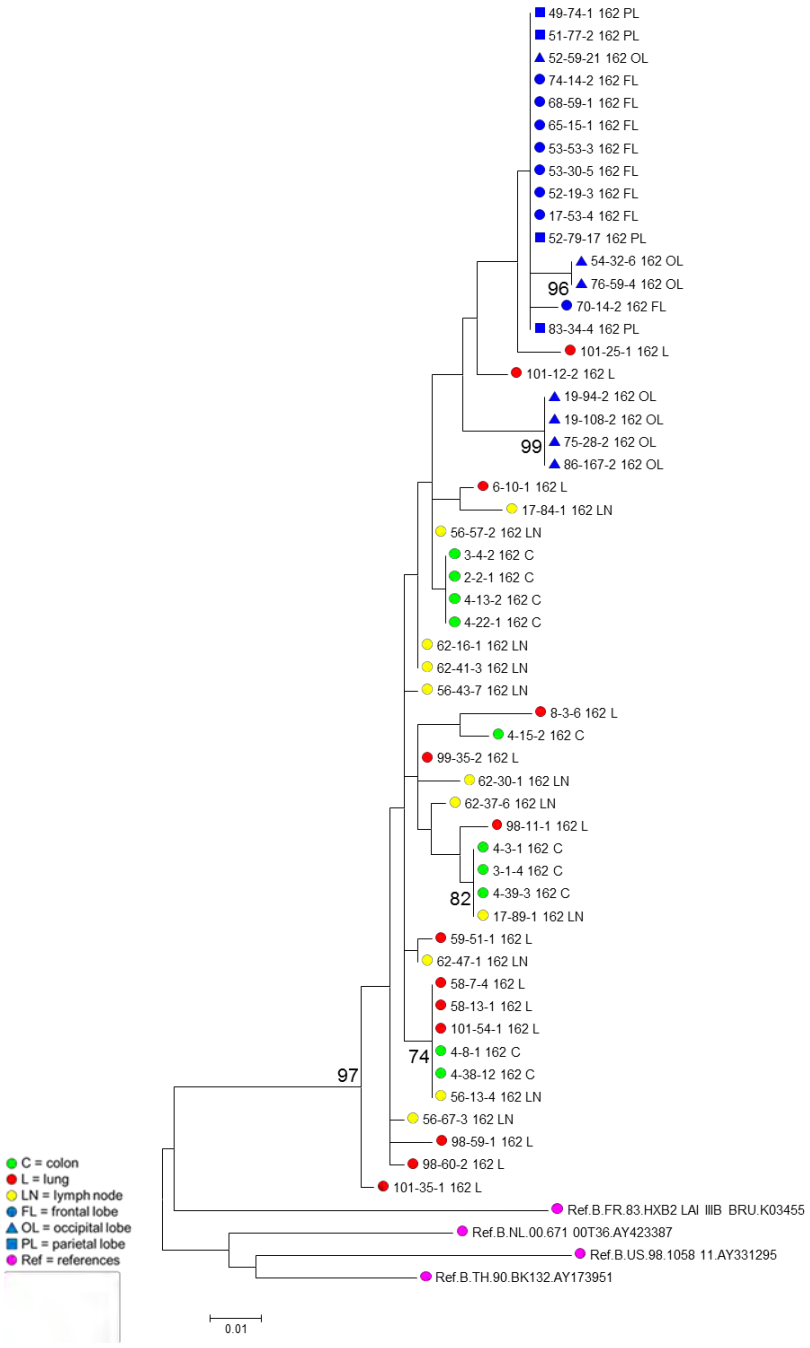

Figure A.5 Phylogenetic analysis of Subject 162 C1 sequences Full length HIV-1 *envs* were amplified from three brain regions (frontal lobe, occipital lobe, and parietal lobe), colon, lung, and lymph node. Four unrelated reference sequences were used as an outgroup. A maximum likelihood tree was constructed using MEGA version 5 for functional HIV-1 *env* C1 regions. Bootstrap vaues ≥70% are noted at branch points. Scale bar shows nucleotide substitutions per site.

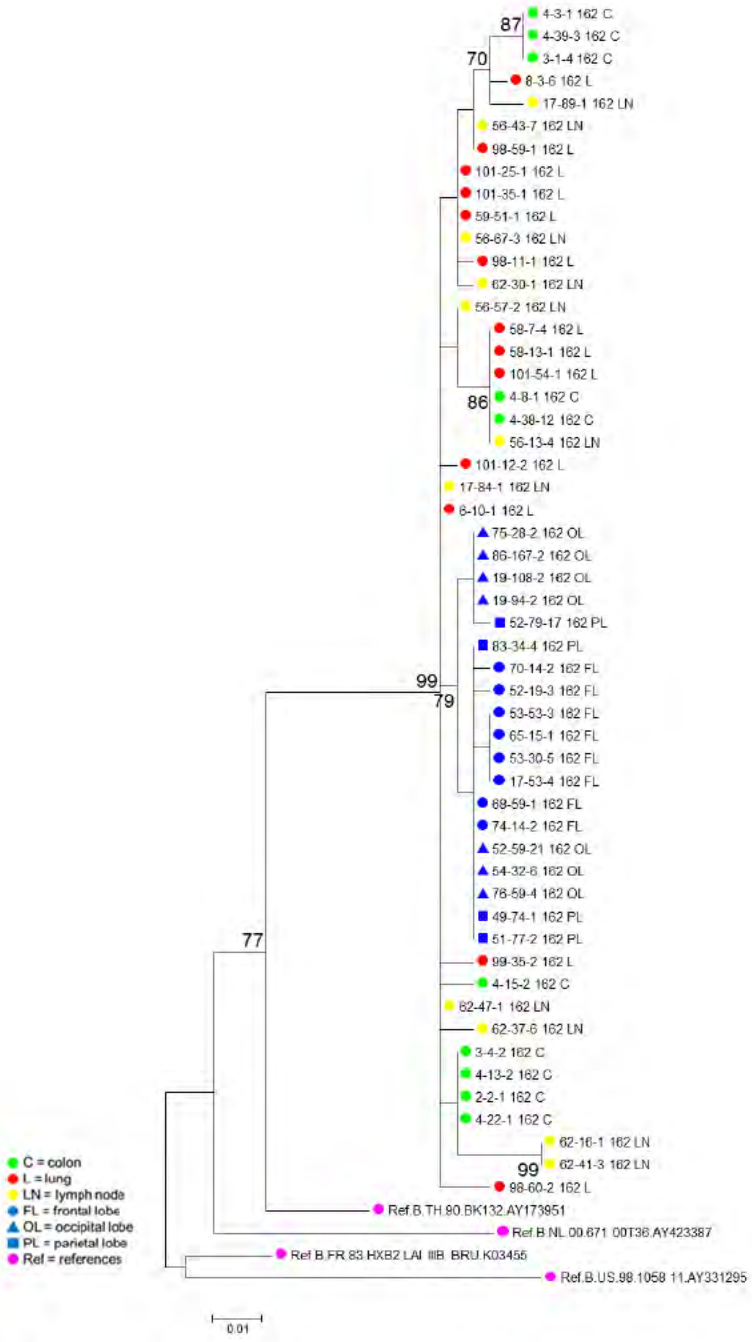

Figure A.6 Phylogenetic analysis of Subject 162 C2 sequences Full length HIV-1 *envs* were amplified from three brain regions (frontal lobe, occipital lobe, and parietal lobe), colon, lung, and lymph node. Four unrelated reference sequences were used as an outgroup. A maximum likelihood tree was constructed using MEGA version 5 for functional HIV-1 *env* C2 regions. Bootstrap vaues ≥70% are noted at branch points. Scale bar shows nucleotide substitutions per site.

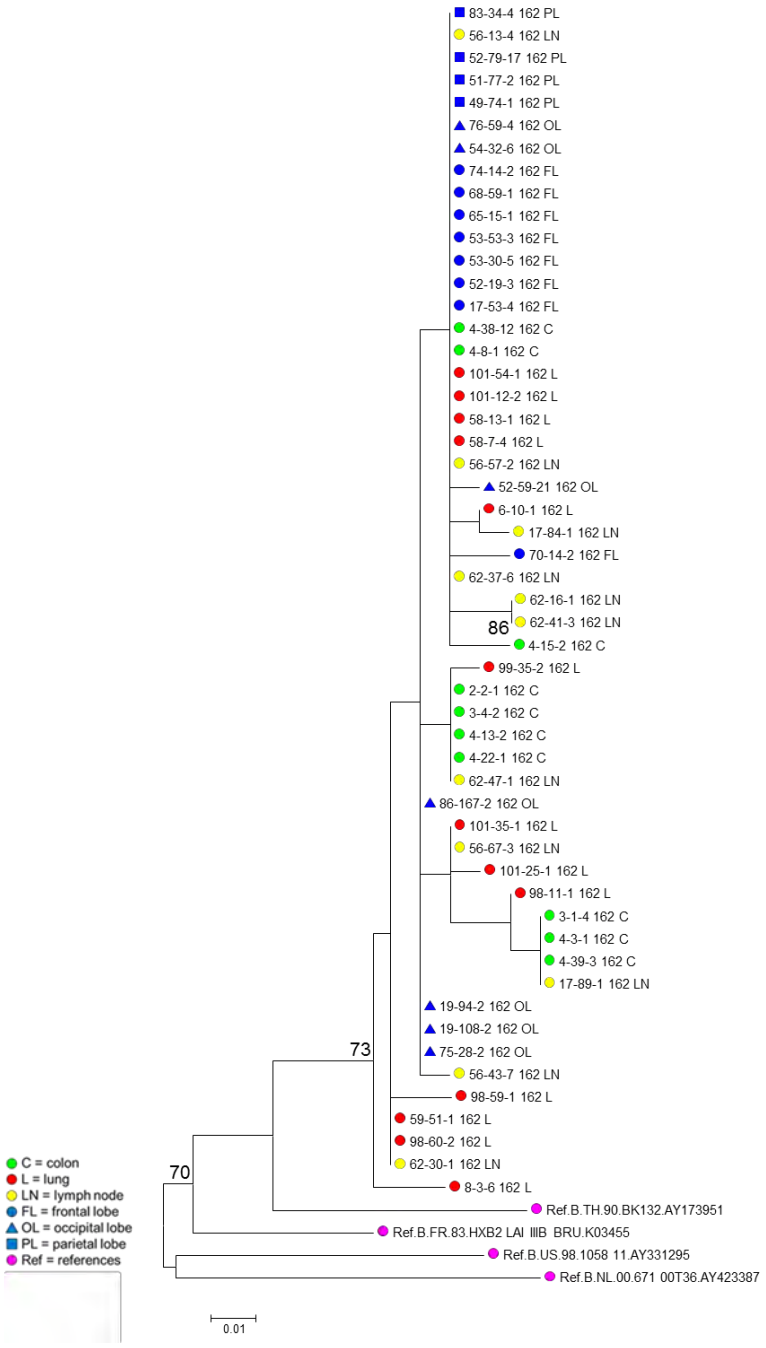

Figure A.7 Phylogenetic analysis of Subject 162 C3 sequences Full length HIV-1 *envs* were amplified from three brain regions (frontal lobe, occipital lobe, and parietal lobe), colon, lung, and lymph node. Four unrelated reference sequences were used as an outgroup. A maximum likelihood tree was constructed using MEGA version 5 for functional HIV-1 *env* C3 regions. Bootstrap vaues ≥70% are noted at branch points. Scale bar shows nucleotide substitutions per site.

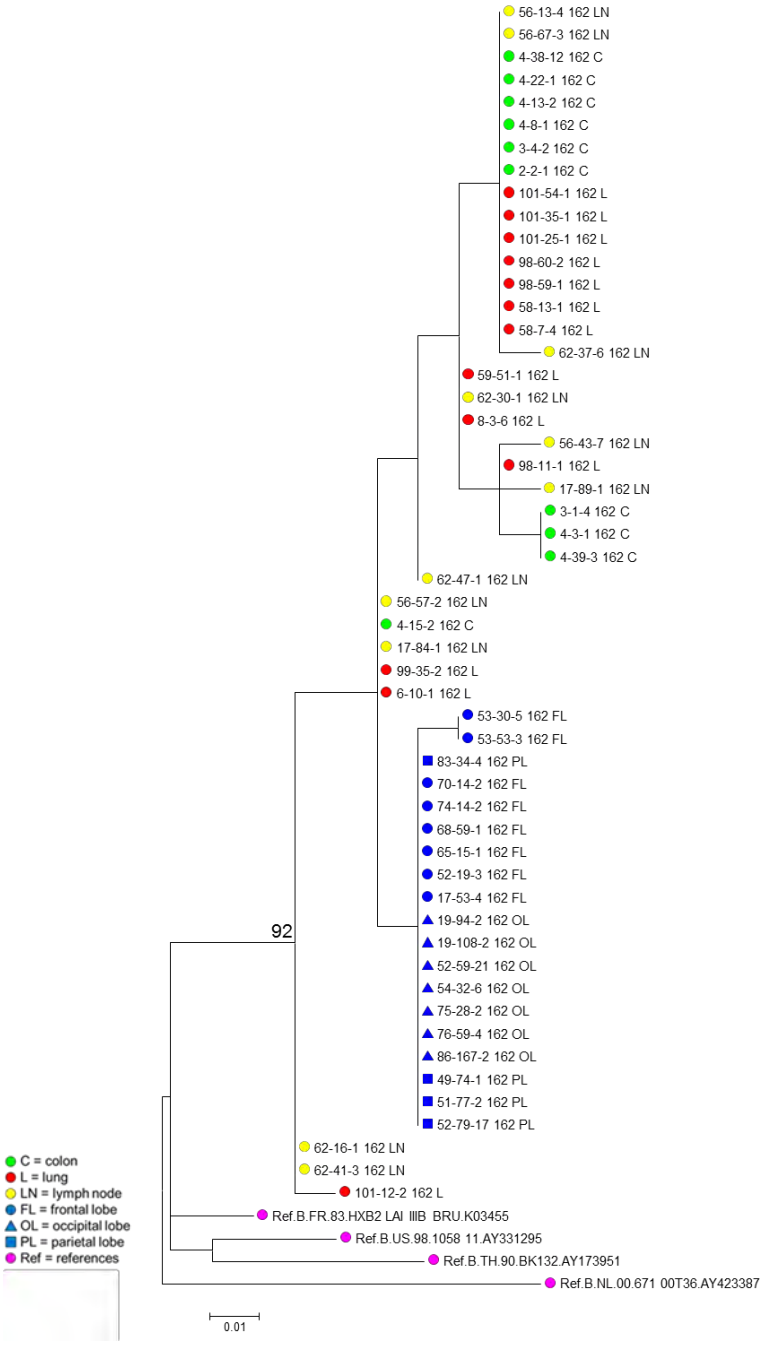

Figure A.8 Phylogenetic analysis of Subject 162 C4 sequences Full length HIV-1 *envs* were amplified from three brain regions (frontal lobe, occipital lobe, and parietal lobe), colon, lung, and lymph node. Four unrelated reference sequences were used as an outgroup. A maximum likelihood tree was constructed using MEGA version 5 for functional HIV-1 *env* C4 regions. Bootstrap vaues ≥70% are noted at branch points. Scale bar shows nucleotide substitutions per site.

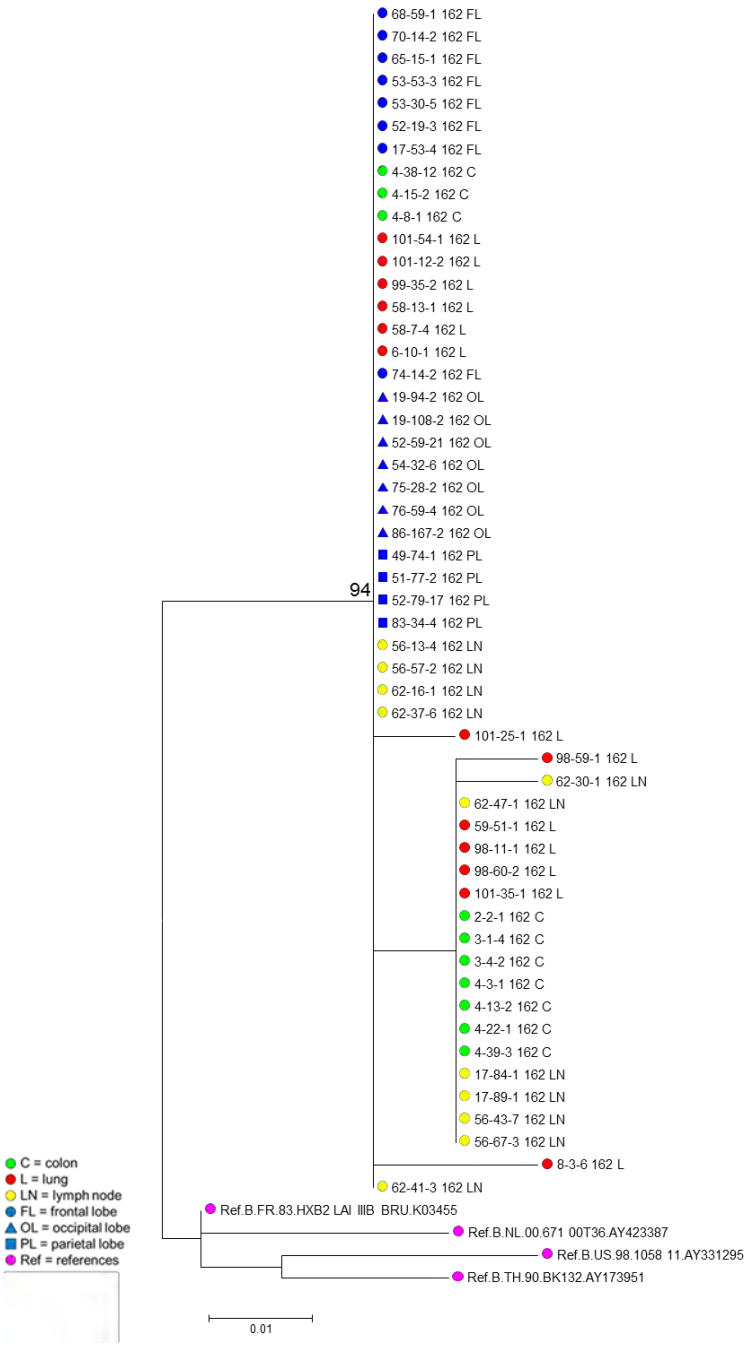

Figure A.9 Phylogenetic analysis of Subject 162 C5 sequences Full length HIV-1 *envs* were amplified from three brain regions (frontal lobe, occipital lobe, and parietal lobe), colon, lung, and lymph node. Four unrelated reference sequences were used as an outgroup. A maximum likelihood tree was constructed using MEGA version 5 for functional HIV-1 *env* C5 regions. Bootstrap vaues ≥70% are noted at branch points. Scale bar shows nucleotide substitutions per site.

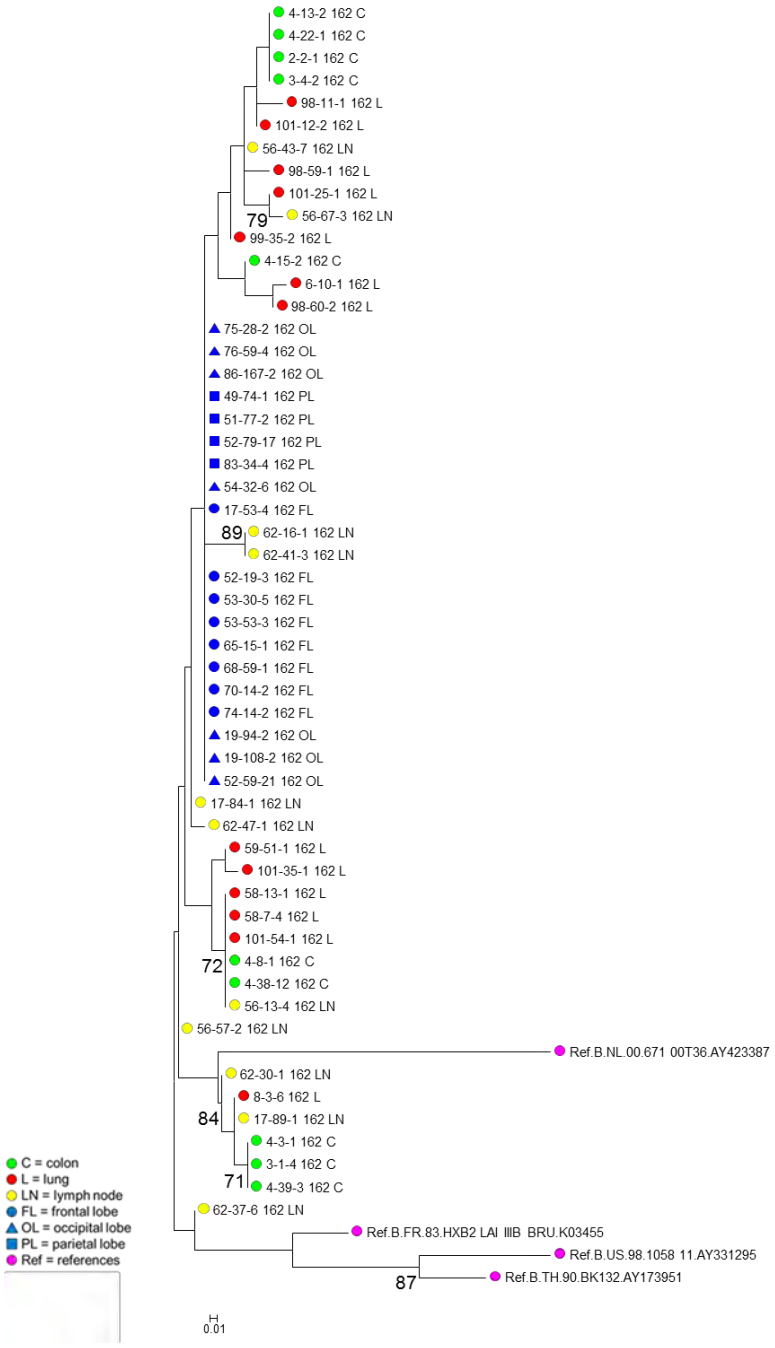

Figure A.10 Phylogenetic analysis of Subject 162 V1 sequences Full length HIV-1 *envs* were amplified from three brain regions (frontal lobe, occipital lobe, and parietal lobe), colon, lung, and lymph node. Four unrelated reference sequences were used as an outgroup. A maximum likelihood tree was constructed using MEGA version 5 for functional HIV-1 *env* V1 regions. Bootstrap vaues ≥70% are noted at branch points. Scale bar shows nucleotide substitutions per site.

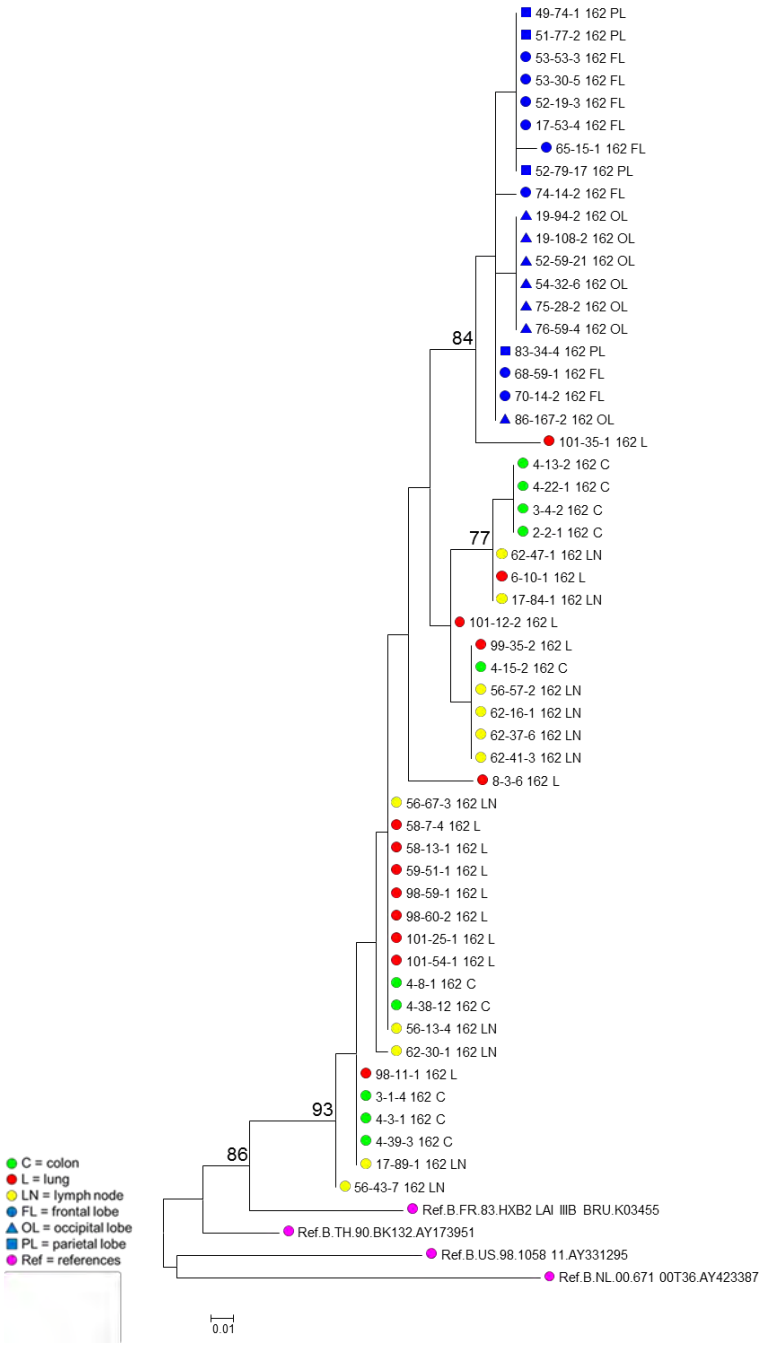

Figure A.11 Phylogenetic analysis of Subject 162 V2 sequences Full length HIV-1 *envs* were amplified from three brain regions (frontal lobe, occipital lobe, and parietal lobe), colon, lung, and lymph node. Four unrelated reference sequences were used as an outgroup. A maximum likelihood tree was constructed using MEGA version 5 for functional HIV-1 *env* V2 regions. Bootstrap vaues ≥70% are noted at branch points. Scale bar shows nucleotide substitutions per site.

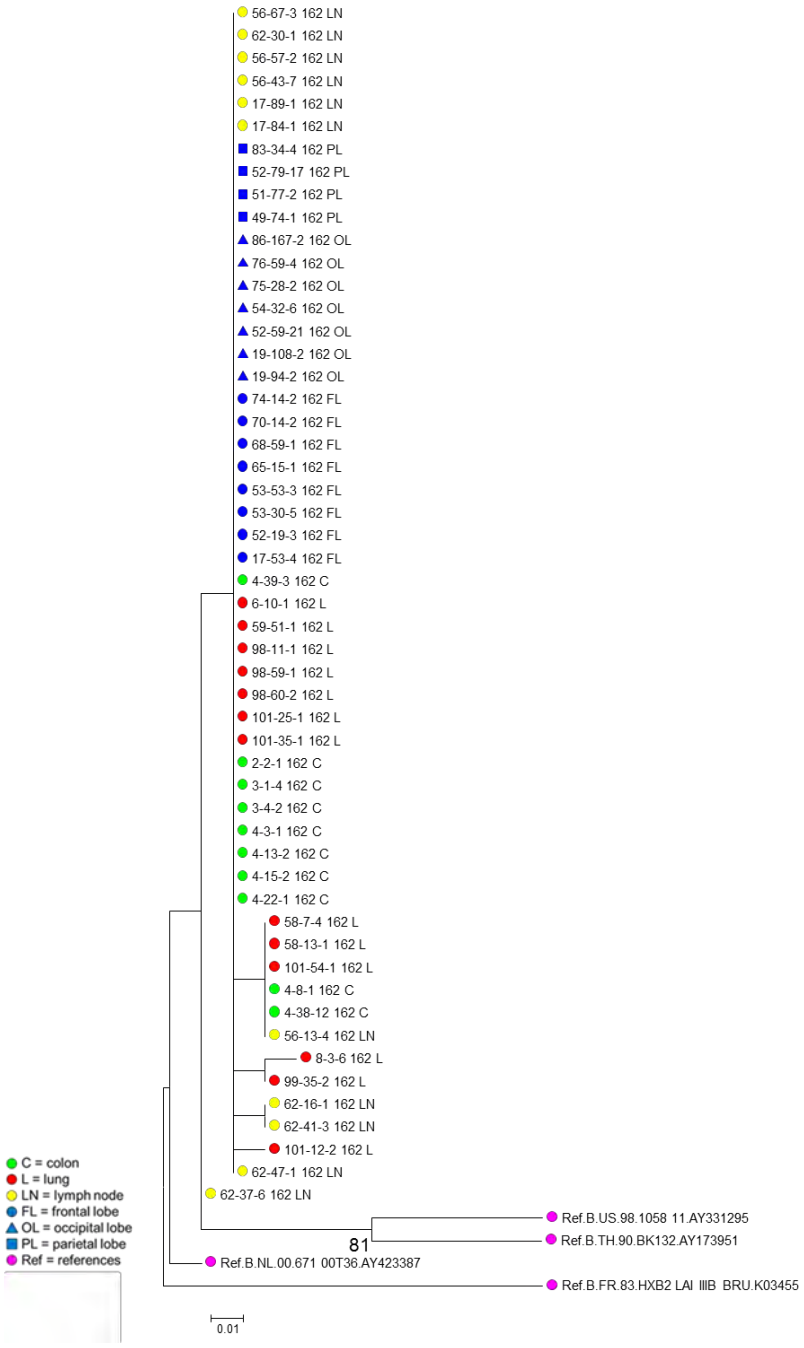

Figure A.12 Phylogenetic analysis of Subject 162 V3 sequences Full length HIV-1 *envs* were amplified from three brain regions (frontal lobe, occipital lobe, and parietal lobe), colon, lung, and lymph node. Four unrelated reference sequences were used as an outgroup. A maximum likelihood tree was constructed using MEGA version 5 for functional HIV-1 *env* V3 regions. Bootstrap vaues ≥70% are noted at branch points. Scale bar shows nucleotide substitutions per site.

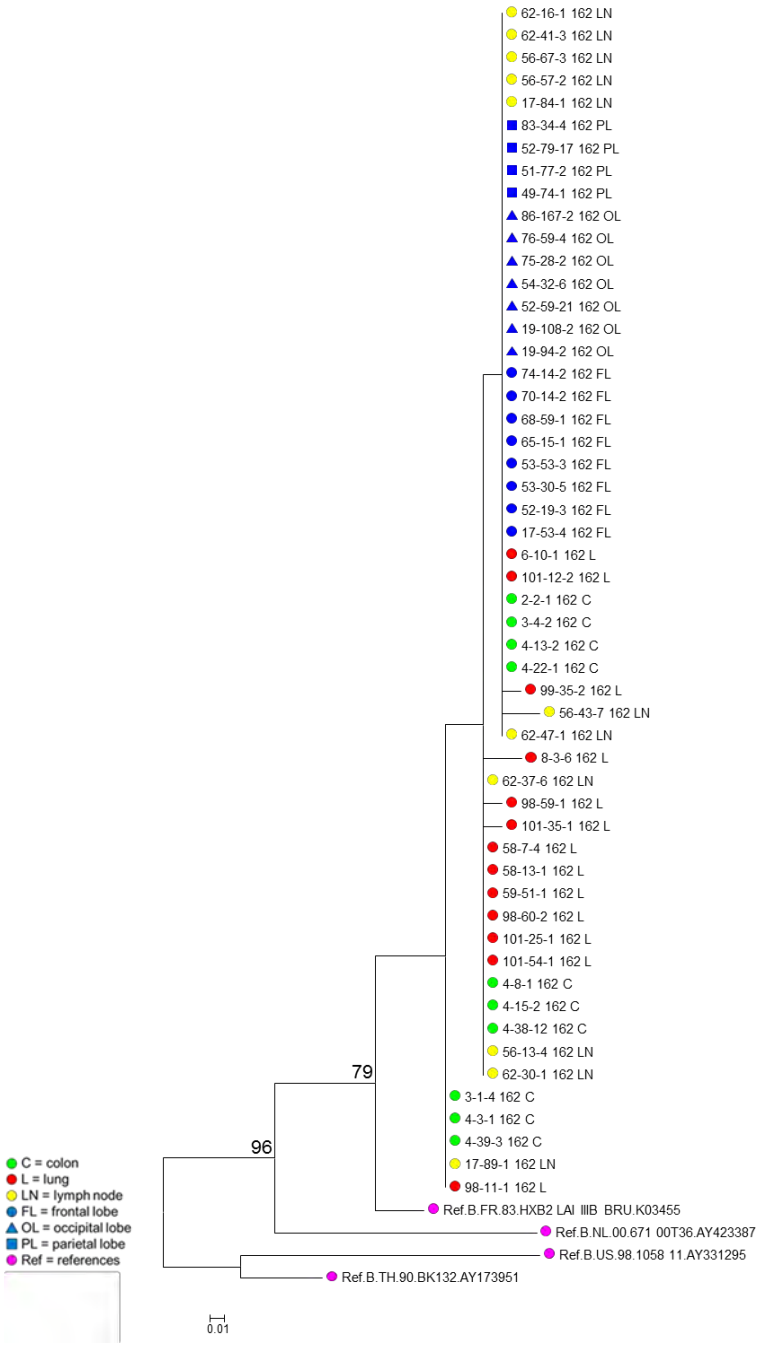

Figure A.13 Phylogenetic analysis of Subject 162 V4 sequences Full length HIV-1 *envs* were amplified from three brain regions (frontal lobe, occipital lobe, and parietal lobe), colon, lung, and lymph node. Four unrelated reference sequences were used as an outgroup. A maximum likelihood tree was constructed using MEGA version 5 for functional HIV-1 *env* V4 regions. Bootstrap vaues ≥70% are noted at branch points. Scale bar shows nucleotide substitutions per site.

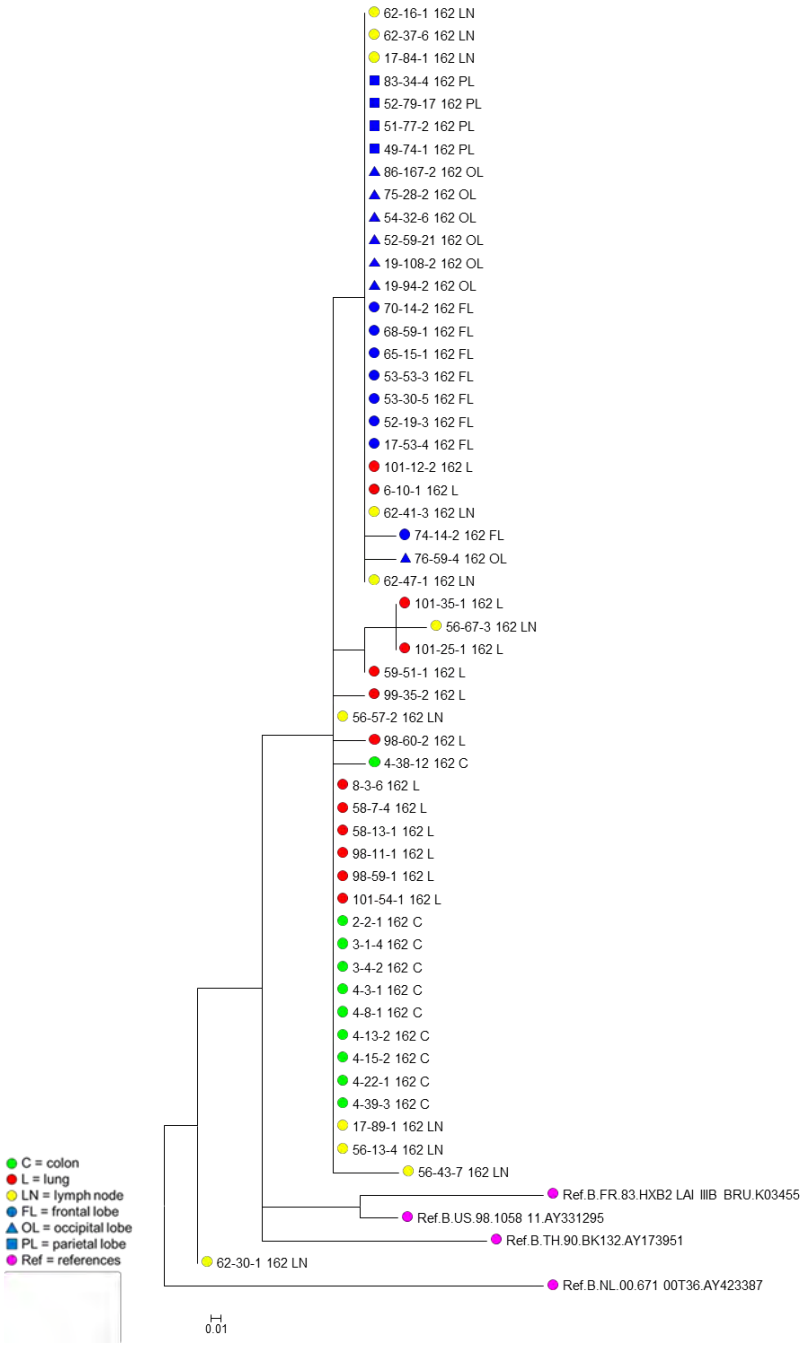

Figure A.14 Phylogenetic analysis of Subject 162 V5 sequences Full length HIV-1 *envs* were amplified from three brain regions (frontal lobe, occipital lobe, and parietal lobe), colon, lung, and lymph node. Four unrelated reference sequences were used as an outgroup. A maximum likelihood tree was constructed using MEGA version 5 for functional HIV-1 *env* V5 regions. Bootstrap vaues ≥70% are noted at branch points. Scale bar shows nucleotide substitutions per site.

APPENDIX B: ANALYSIS OF AN HIV-1 INFECTED SUBJECT WITH TWO DISTINCT VIRAL POPULATIONS

Introduction

Previous chapters describe the characterization of HIV-1 envelopes derived from multiple tissues of Subject 162, an HIV-1 infected subject who died from end stage AIDS and was neurologically normal. Initial study plans included an additional subject, Subject 123, who also died of end stage AIDS, but had HIV-Associated Dementia (HAD). However preliminary sequence analyses revealed distinct, seemingly unrelated viral populations. These populations could not be directly compared for tissue specific genotypic and phenotypic changes because they may not have originated from the same viral variant. These populations were characterized to determine if they were the result of contamination or if Subject 123 was infected with two viral variants.

Methods

All methods were followed as described in Chapter II with additional methods described below.

Subject 123

HIV-1 positive tissue was obtained from the National Disease Research Interchange (NDRI; Philadelphia, PA). Tissue was harvested postmortem and stored at -80°C until use. Seven tissues were examined from Subject 123 (Table

A.1). These included three brain lobes (frontal lobe (FL), occipital lobe (OL), and parietal lobe (PL)), blood cells (BC), colon (C), lung (L), and lymph node (LN). Subject 123 died of end stage AIDS.

Short Tandem Repeat Analysis

Short Tandem Repeat (STR) Analysis (reviewed in Gettings et al, 2015) was performed by Jonathan Ball's laboratory at the University of Nottingham (Nottingham, UK). STR Analysis examines the number of repeats at specific loci in the human genome known to have varying numbers of repeats in different individuals. By examining several different STR loci, it can be determined with high probability whether or not different DNA samples came from the same person. The lab was sent ten coded DNA samples from the tissues of three different subjects. The number of subjects and tissues was not disclosed to the lab. The TH01, vWA, and D21S11 loci were examined using STR Analysis and then each DNA sample was assigned to a profile based on which DNA samples were believed to have come from the same subject.

Next Generation Sequencing

Methods for Pacific Biosciences (PacBio) sequencing were followed as described in Chapter II. The only change made for Subject 123 was that nested PCR was performed with a first PCR of 12 cycles, followed by a second PCR of 35 cycles.

Results

Envelopes were isolated from all tissues of Subject 123

Envelopes were isolated from Subject 123 frontal lobe, occipital lobe, parietal lobe, blood cells, colon, lung, and lymph node using limiting dilution PCR (Table A.2). In total, 31 *envs* were amplified: 14 from the frontal lobe, 1 from the occipital lobe, 1 from the parietal lobe, 1 from blood cells, 3 from colon, 9 from lung, and 2 from lymph node.

Subject 123 *envs* were compartmentalized in brain and body tissues

All 31 full length *env* sequences were used to construct a maximum likelihood phylogenetic tree using Molecular Evolutionary Genetics Analysis (MEGA) 5 software (Tamura et al, 2011). Compartmentalization was observed between tissues of the brain and tissues of the body (Figure A.15).

Sequences from brain and body *envs* were very different

Sequence alignments revealed that *env* sequences from the brain and body were substantially different and possibly not related. Alignment of the V3 loop region shows the extreme variability between the viral populations derived from tissues of the brain and tissues of the body (Figure A.16).

Subject	A/R/S	Tissues	Plasma Viral Load	CD4 Count	HIV Treatment
123	43/C/M	Brain - Frontal Lobe Brain - Occipital Lobe Brain - Parietal Lobe Colon Lung Lymph Node Blood Cells	<75 copies/ml (7 months prior to death)	not available	Viread Norvir Ziagen Aptivis Isentress Intelence

Table A.1 Subject 123 data Tissue was obtained from the National Disease Research Interchange (NDRI; Philadelphia, PA). A/R/S = age/race/sex.

Tissue	Envelope
Brain - Frontal Lobe (FL)	
14 envelopes	33-2-2
	33-10-5
	33-25-3
	35-11-3
	35-15-4
	35-20-1
	35-21-2
	35-22-1
	35-28-4
	35-31-2
	35-35-1
	35-47-1
	35-49-1
	35-79-1
Brain - Occipital Lobe (OL)	
1 envelope	19-26
Brain - Parietal Lobe (PL)	
1 envelope	20-32-1

Tissue	Envelope
Blood Cells (BC)	
1 envelope	103-5-1
Colon (C)	
3 envelopes	26-5-3
	26-4-1
	23-69-1
Lung (L)	
9 envelopes	10-22-2
	10-23-1
	10-27-3
	10-29-2
	10-32-1
	10-40-4
	10-45-5
	12-39-17
	12-44-10
Lymph Node (LN)	
2 envelopes	16-38-2
	34-26-4

Table A.2 Subject 123 HIV-1 envelopes isolated from different tissues HIV-1 *envs* were isolated from three brain regions (frontal lobe, occipital lobe, and parietal lobe), blood cells, colon, lung, and lymph node using nested PCR and DNA at limiting dilution.

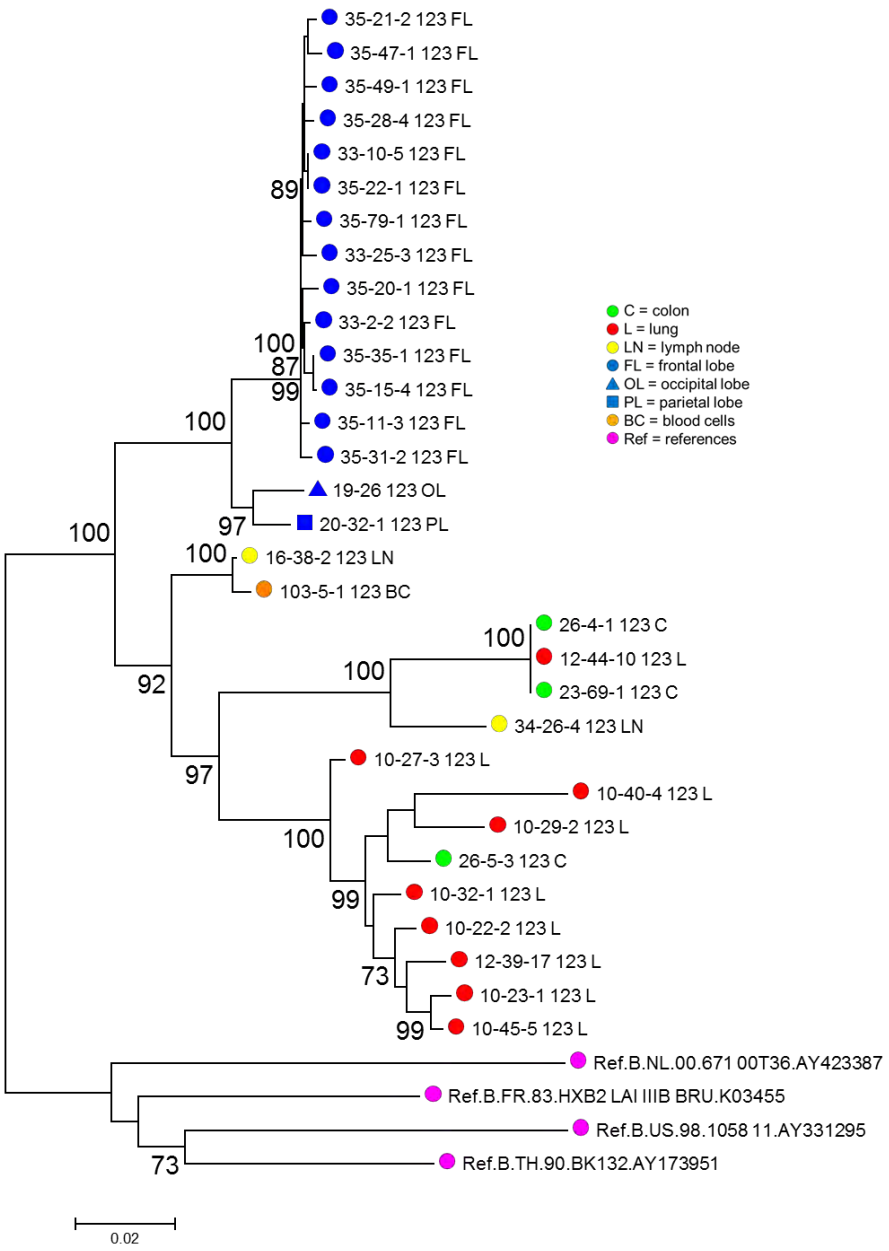

Figure A.15 Phylogenetic analysis of Subject 123 gp160 sequences Full length HIV-1 *envs* were amplified from three brain regions (frontal lobe, occipital lobe, and parietal lobe), blood cells, colon, lung, and lymph node. Four unrelated reference sequences were used as an outgroup. A maximum likelihood tree was constructed using MEGA version 5 for functional HIV-1 *envs*. Bootstrap vaues ≥70% are noted at branch points. Scale bar shows nucleotide substitutions per site.

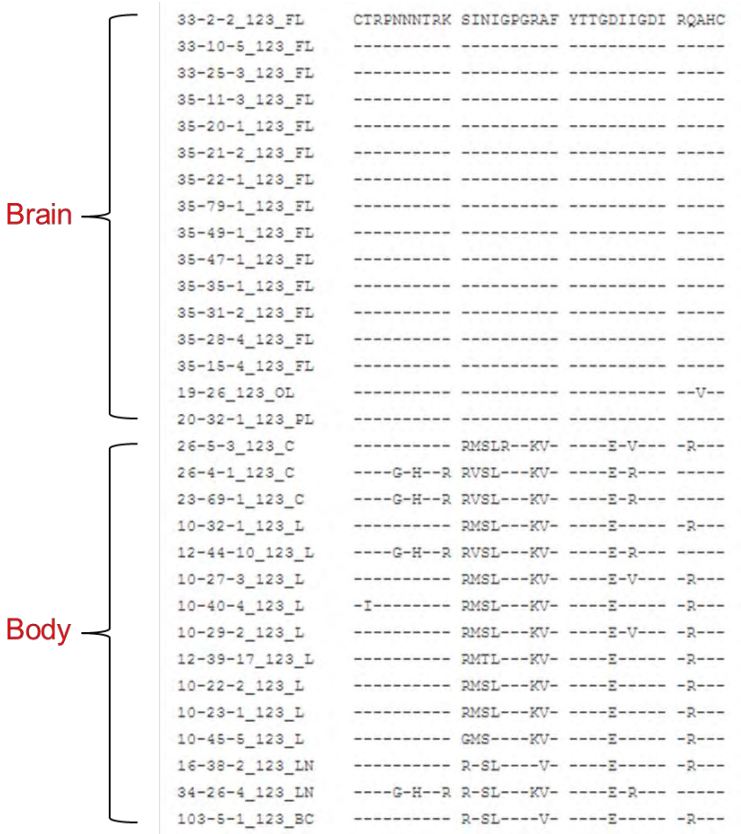

Figure A.16 Alignment of Subject 123 V3 loop sequences V3 loop sequences were aligned using GeneDoc (Pittsburgh Supercomputing Center). Sequences from the brain (frontal lobe, occipital lobe, and parietal lobe) were compared to sequences from the body (blood cells, colon, lung, and lymph node).

Envs from the brain were predicted to use CCR5 and Envs from the body were predicted to use CXCR4

V3 loop sequences were used to predict coreceptor use using the WebPSSM program (University of Washington; Jensen et al, 2003) based on V3 net charge and amino acids at postions 11 and 25, which are known to play a role in coreceptor use (Table A.3). An increased net charge or an arginine or lysine at position 11 or 25 have been correlated with a switch to use the CXCR4 coreceptor. The WebPSSM program also compares *envs* to known and functional tested CCR5-using and CXCR4-using variants. All envelopes from brain tissues were predicted to use CCR5, while all envelopes from tissues of the body were predicted to use CXCR4 (Table A.3). Envelopes from the brain had a lower net charge around 4 and S and D at amino acid positions 11 and 25, respectively. However envelopes from the tissues of the body had a net charge around 6 with R at amino acid position 11 and E at amino acid position 25.

Different *env* populations in the brain and body tissues were from the same subject

To rule out the possibility of laboratory contamination or accidentally switching tissues with another subject, Subject 123 tissues were examined using STR Analysis to determine if they came from the same person. STR Analysis confirmed that tissues from Subject 123 had the same STR profile and therefore were from the same subject (Table A.4).

Tissue	Genotype 11/25	Average Net Charge	Predicted Coreceptor
Frontal Lobe	SD	4	CCR5
Occipital Lobe	SD	4	CCR5
Parietal Lobe	SD	4	CCR5
Blood Cells	RE	6	CXCR4
Colon	RE	6	CXCR4
Lung	RE	6	CXCR4
Lymph Node	RE	6	CXCR4

Table A.3 Predicted coreceptor use for Subject 123 Envs WebPSSM (University of Washington) was used to determine amino acid genotype at positions 11 and 25 of the V3 loop, calculate the net charge, and predict coreceptor use.

Pacific Biosciences sequencing revealed low levels of mixing between CCR5- and CXCR4-using variants

Pacific Biosciences (PacBio) next generation sequencing was used to examine several thousand sequences from Subject 123 (Table A.5). In total, 44,630 full length *env* sequnces were generated: 3,702 from the frontal lobe, 12,625 from the occipital lobe, 12,834 from the parietal lobe, 4,474 from the blood cells, 202 from the colon, 7,099 from the lung, and 3,694 from the lymph node.

Phylogenetic trees were assembled from 250 randomly selected sequences from each tissue (Figure A.17). Trees showed tight compartmentalization of *envs* from tissues of the brain (frontal lobe, occipital lobe, and parietal lobe) and from tissues of the body (blood cells, colon, lung, and lymph node). The majority of brain derived envelopes were predicted to use CCR5 as a coreceptor, while most of the body derived envelopes were predicted to use CXCR4 as a coreceptor (Table A.5). However interestingly, a small number of CXCR4-using variants were detected in the brain and CCR5-using variants were detected in each of the body tissues (Table A.5; Figure A.17).

Discussion

Subject 123 had two distinct viral populations that did not appear to be related. This was observed in the complete segregation of populations from the brain and body on the phylogenetic tree (Figure A.15), as well as by comparing sequence alignments of the V3 loop (Figure A.16). STR Analysis was used to

Subject	Tissue	Profile
123	Frontal Lobe	A
123	Occipital Lobe	A
123	Parietal Lobe	A
123	Lymph Node	A
123	Lung	A
162	Frontal Lobe	B
162	Lung	B
162	Colon	B
124	Frontal Lobe	C
124	Lung	C

Table A.4 Short Tandem Repeat (STR) Analysis STR Analysis was performed on ten DNA samples from three subjects for three different loci. It was determined that the DNA samples could be categorized into three profiles, A, B, and C, and that these corresponded to the DNA samples from the three different subjects.

Tissue	Total Sequences	CCR5-using		CXCR4-using	
		Number	Percent	Number	Percent
Frontal Lobe	3,702	3,702	100	0	0
Occipital Lobe	12,625	12,625	100	0	0
Parietal Lobe	12,834	12,831	99.98	3	0.02
Blood Cells	4,474	104	2.32	4,370	97.68
Colon	202	68	33.66	134	66.33
Lung	7,099	14	0.20	7,085	99.80
Lymph Node	3,694	101	2.73	3,593	97.27
Total	44,630	29,445	65.98	15,185	34.02

Table A.5 Subject 123 PacBio sequencing results The V3 loop nucleic acid sequences for all sequences in each data set were isolated using Geneious software version 9 (Kearse et al, 2012). Gene Cutter (Los Alamos National Laboratory) was used to codon align and translate sequences. The sequencing approach resulted in some gapped positions, so any V3 amino acid sequence containing an ambiguous position was removed from the alignment. Tropism prediction was performed using WebPSSM (Jensen et al, 2003) and the x4r5 matrix.

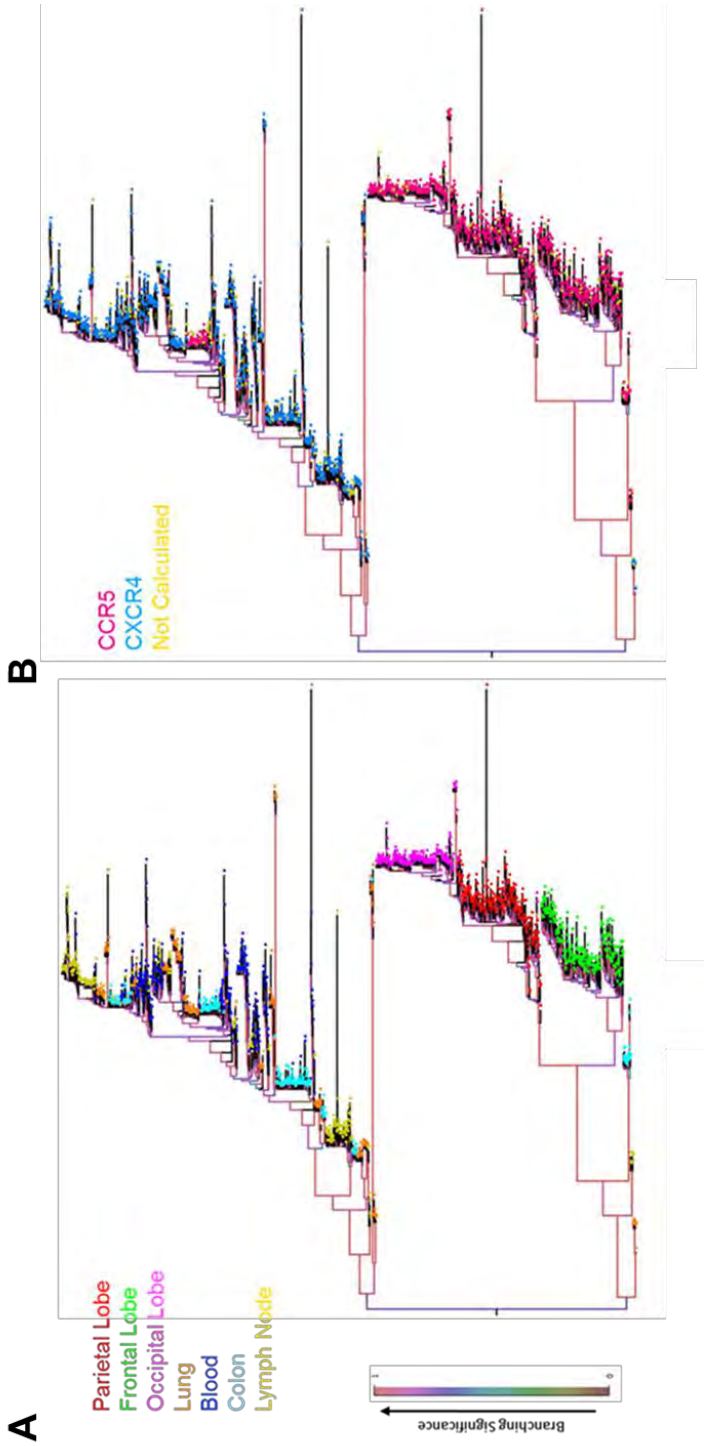
A
Parietal Lobe
Frontal Lobe
Occipital Lobe
Lung
Blood
Colon
Lymph Node
Branching Significance
B
CCR5
CXCR4
Not Calculated

Figure A.17 Phylogenetic analysis of Subject 123 PacBio sequences A python script was generated to randomly select 250 sequences from each tissue. Due to the small number of sequences generated, all colon sequences were used. Maximum likelihood phylogenies were generated with phyML (Guindon et al, 2010) using the HKY85 substitution model, the NNI tree improvement method, and the approximate likelihood ratio test (Anisimova and Gascuel, 2006). Trees were graphed and colored according to tissue type (**A**) and predicted coreceptor usage (**B**) using FigTree software (http://tree.bio.ed.ac.uk/software/figtree/). Trees were midpoint rooted. Branch support is shown on the scale to the left, with red indicating branches with very high support.

confirm that all tissue samples did actually come from the same subject (Table A.4). It was therefore possible that Subject 123 had dual infection. This may arise as a result of coinfection or superinfection. Coinfection occurs when a subject is infected with more than one viral variant at the same time and both variants establish infection. Alternatively, Subject 123 may have been superinfected with a second variant after an initial infection event, with both variants establishing viral populations. It is also possible that the two populations originated from a single viral variant that acquired many mutations and became highly compartmentalized due to different selection pressures in the tissues of the brain and the body. Previous studies have shown that this level of diversity can be possible (Lin et al, 2012).

Though sequences from the tissues of the brain and the body were tightly compartmentalized, preliminary results from PacBio sequencing data showed low levels of CXCR4-using variants in the brain and CCR5-using variants in the body. PacBio studies are ongoing, as a pipeline for analysis had to be developed for this project. Future studies will examine whether recombination occurred between CXCR4-using and CCR5-using variants and will include additional phylogenetic analyses, such as constructing time rooted trees to investigate which tissues became infected first and how viral variants may have trafficked throughout the body. In addition, future studies will include phenotypic analyses to look at tropism (coreceptor use and macrophage tropism).

APPENDIX C: FUNDING SOURCES

Support for this research was provided by NIH grants AI089334, NS084910, and AI097265.

REFERENCES

Agrawal-Gamse, C., Lee, F. H., Haggarty, B., Jordan, A. P., Yi, Y., Lee, B., Collman, R. G., Hoxie, J. A., Doms, R. W., and Laakso, M. M. 2009. Adaptive mutations in a human immunodeficiency virus type 1 envelope protein with a truncated V3 loop restore function by improving interactions with CD4. J Virol, 83(21), 11005-11015.

Aiken, C., Konner, J., Landau, N. R., Lenburg, M. E., and Trono, D. 1994. Nef induces CD4 endocytosis: requirement for a critical dileucine motif in the membrane-proximal CD4 cytoplasmic domain. Cell, 76(5), 853-864.

Althaus, C. L., Joos, B., Perelson, A. S., and Gunthard, H. F. 2014. Quantifying the turnover of transcriptional subclasses of HIV-1-infected cells. PLoS Comput Biol, 10(10).

amfAR. 2016. Statistics: Worldwide. Retrieved from: http://www.amfar.org/worldwide-aids-stats/.

An, P., and Winkler, C. A. 2010. Host genes associated with HIV/AIDS: advances in gene discovery. Trends Genet, 26(3), 119-131.

An, W., and Telesnitsky, A. 2002. HIV-1 genetic recombination: experimental approaches and observations. AIDS Rev, 4(4), 195-212.

Anisimova, M., and Gascuel, O. 2006. Approximate likelihood-ratio test for branches: A fast, accurate, and powerful alternative. Syst Biol, 55(4), 539-552.

AVERT. 2016. Global HIV and AIDS statistics. Retrieved from: http://www.avert.org/professionals/hiv-around-world/global-statistics.

Baltimore, D. 1970. RNA-dependent DNA polymerase in virions of RNA tumour viruses. Nature, 226(5252), 1209-1211.

Bannert, N., Schenten, D., Craig, S., and Sodroski, J. 2000. The level of CD4 expression limits infection of primary rhesus monkey macrophages by a T-tropic simian immunodeficiency virus and macrophagetropic human immunodeficiency viruses. J Virol, 74(23), 10984-10993.

Barbas, C. F., 3rd, Bjorling, E., Chiodi, F., Dunlop, N., Cababa, D., Jones, T. M., Zebedee, S. L., Persson, M. A., Nara, P. L., Norrby, E., and Burton, D. R. 1992.

Recombinant human Fab fragments neutralize human type 1 immunodeficiency virus in vitro. Proc Natl Acad Sci U S A, 89(19), 9339-9343.

Barre-Sinoussi, F., Chermann, J. C., Rey, F., Nugeyre, M. T., Chamaret, S., Gruest, J., Dauguet, C., Axler-Blin, C., Vezinet-Brun, F., Rouzioux, C., Rozenbaum, W., and Montagnier, L. 1983. Isolation of a T-lymphotropic retrovirus from a patient at risk for acquired immune deficiency syndrome (AIDS). Science, 220(4599), 868-871.

Bartel, D. P., Zapp, M. L., Green, M. R., and Szostak, J. W. 1991. HIV-1 Rev regulation involves recognition of non-Watson-Crick base pairs in viral RNA. Cell, 67(3), 529-536.

Bell, J. E., Busuttil, A., Ironside, J. W., Rebus, S., Donaldson, Y. K., Simmonds, P., and Peutherer, J. F. 1993. Human immunodeficiency virus and the brain: investigation of virus load and neuropathologic changes in pre-AIDS subjects. J Infect Dis, 168(4), 818-824.

Berger, E. A., Doms, R. W., Fenyo, E. M., Korber, B. T., Littman, D. R., Moore, J. P., Sattentau, Q. J., Schuitemaker, H., Sodroski, J., and Weiss, R. A. 1998. A new classification for HIV-1. Nature, 391(6664), 240.

Berkowitz, R. D., Beckerman, K. P., Schall, T. J., and McCune, J. M. 1998. CXCR4 and CCR5 expression delineates targets for HIV-1 disruption of T cell differentiation. J Immunol, 161(7), 3702-3710.

Berman, P. W., Nunes, W. M., and Haffar, O. K. 1988. Expression of membrane-associated and secreted variants of gp160 of human immunodeficiency virus type 1 in vitro and in continuous cell lines. J Virol, 62(9), 3135-3142.

Bernstein, H. B., Tucker, S. P., Hunter, E., Schutzbach, J. S., and Compans, R. W. 1994. Human immunodeficiency virus type 1 envelope glycoprotein is modified by O-linked oligosaccharides. J Virol, 68(1), 463-468.

Bhattacharya, J., Peters, P. J., and Clapham, P. R. 2004. Human immunodeficiency virus type 1 envelope glycoproteins that lack cytoplasmic domain cysteines: impact on association with membrane lipid rafts and incorporation onto budding virus particles. J Virol, 78(10), 5500-5506.

Binley, J. M., Wrin, T., Korber, B., Zwick, M. B., Wang, M., Chappey, C., Stiegler, G., Kunert, R., Zolla-Pazner, S., Katinger, H., Petropoulos, C. J., and Burton, D. R. 2004. Comprehensive cross-clade neutralization analysis of a panel of anti-human immunodeficiency virus type 1 monoclonal antibodies. J Virol, 78(23), 13232-13252.

Blaak, H., van't Wout, A. B., Brouwer, M., Hooibrink, B., Hovenkamp, E., and Schuitemaker, H. 2000. In vivo HIV-1 infection of CD45RA(+)CD4(+) T cells is established primarily by syncytium-inducing variants and correlates with the rate of CD4(+) T cell decline. Proc Natl Acad Sci U S A, 97(3), 1269-1274.

Blackard, J. T. 2012. HIV compartmentalization: a review on a clinically important phenomenon. Curr HIV Res, 10(2), 133-142.

Bleul, C. C., Wu, L., Hoxie, J. A., Springer, T. A., and Mackay, C. R. 1997. The HIV coreceptors CXCR4 and CCR5 are differentially expressed and regulated on human T lymphocytes. Proc Natl Acad Sci U S A, 94(5), 1925-1930.

Bosch, M. L., Earl, P. L., Fargnoli, K., Picciafuoco, S., Giombini, F., Wong-Staal, F., and Franchini, G. 1989. Identification of the fusion peptide of primate immunodeficiency viruses. Science, 244(4905), 694-697.

Bowerman, B., Brown, P. O., Bishop, J. M., and Varmus, H. E. 1989. A nucleoprotein complex mediates the integration of retroviral DNA. Genes Dev, 3(4), 469-478.

Brenchley, J. M., Schacker, T. W., Ruff, L. E., Price, D. A., Taylor, J. H., Beilman, G. J., Nguyen, P. L., Khoruts, A., Larson, M., Haase, A. T., and Douek, D. C. 2004. CD4+ T cell depletion during all stages of HIV disease occurs predominantly in the gastrointestinal tract. J Exp Med, 200(6), 749-759.

Brown, P. O., Bowerman, B., Varmus, H. E., and Bishop, J. M. 1987. Correct integration of retroviral DNA in vitro. Cell, 49(3), 347-356.

Brown, P. O., Bowerman, B., Varmus, H. E., and Bishop, J. M. 1989. Retroviral integration: structure of the initial covalent product and its precursor, and a role for the viral IN protein. Proc Natl Acad Sci U S A, 86(8), 2525-2529.

Brown, R. J., Peters, P. J., Caron, C., Gonzalez-Perez, M. P., Stones, L., Ankghuambom, C., Pondei, K., McClure, C. P., Alemnji, G., Taylor, S., Sharp, P. M., Clapham, P. R., and Ball, J. K. 2011. Intercompartmental recombination of HIV-1 contributes to env intrahost diversity and modulates viral tropism and sensitivity to entry inhibitors. J Virol, 85(12), 6024-6037.

Bruen, T. C., Philippe, H., and Bryant, D. 2006. A simple and robust statistical test for detecting the presence of recombination. Genetics, 172(4), 2665-2681.

Bull, M. E., Heath, L. M., McKernan-Mullin, J. L., Kraft, K. M., Acevedo, L., Hitti, J. E., Cohn, S. E., Tapia, K. A., Holte, S. E., Dragavon, J. A., Coombs, R. W., Mullins, J. I., and Frenkel, L. M. 2013. Human immunodeficiency viruses appear

compartmentalized to the female genital tract in cross-sectional analyses but genital lineages do not persist over time. J Infect Dis, 207(8), 1206-1215.

Bunnik, E. M., Quakkelaar, E. D., van Nuenen, A. C., Boeser-Nunnink, B., and Schuitemaker, H. 2007. Increased neutralization sensitivity of recently emerged CXCR4-using human immunodeficiency virus type 1 strains compared to coexisting CCR5-using variants from the same patient. J Virol, 81(2), 525-531.

Burke, V., Williams, C., Sukumaran, M., Kim, S. S., Li, H., Wang, X. H., Gorny, M. K., Zolla-Pazner, S., and Kong, X. P. 2009. Structural basis of the cross-reactivity of genetically related human anti-HIV-1 mAbs: implications for design of V3-based immunogens. Structure, 17(11), 1538-1546.

Burton, D. R., Barbas, C. F., 3rd, Persson, M. A., Koenig, S., Chanock, R. M., and Lerner, R. A. 1991. A large array of human monoclonal antibodies to type 1 human immunodeficiency virus from combinatorial libraries of asymptomatic seropositive individuals. Proc Natl Acad Sci U S A, 88(22), 10134-10137.

Burton, D. R., Desrosiers, R. C., Doms, R. W., Koff, W. C., Kwong, P. D., Moore, J. P., Nabel, G. J., Sodroski, J., Wilson, I. A., and Wyatt, R. T. 2004. HIV vaccine design and the neutralizing antibody problem. Nat Immunol, 5(3), 233-236.

Burton, D. R., Pyati, J., Koduri, R., Sharp, S. J., Thornton, G. B., Parren, P. W., Sawyer, L. S., Hendry, R. M., Dunlop, N., Nara, P. L., Lamacchia, M., Garratty, E., Stiehm, E. R., Bryson, Y. J., Cao, Y., Moore, J. P., Ho, D. D., and Barbas, C. F., 3rd. 1994. Efficient neutralization of primary isolates of HIV-1 by a recombinant human monoclonal antibody. Science, 266(5187), 1024-1027.

Bushman, F. D., Fujiwara, T., and Craigie, R. 1990. Retroviral DNA integration directed by HIV integration protein in vitro. Science, 249(4976), 1555-1558.

Cann, A. J., Churcher, M. J., Boyd, M., O'Brien, W., Zhao, J. Q., Zack, J., and Chen, I. S. 1992. The region of the envelope gene of human immunodeficiency virus type 1 responsible for determination of cell tropism. J Virol, 66(1), 305-309.

Caragounis, E. C., Gisslen, M., Lindh, M., Nordborg, C., Westergren, S., Hagberg, L., and Svennerholm, B. 2008. Comparison of HIV-1 pol and env sequences of blood, CSF, brain and spleen isolates collected ante-mortem and post-mortem. Acta Neurol Scand, 117(2), 108-116.

CDC. 1981. Pneumocystis pneumonia. MMWR. 30(21); 1-3.

CDC 1982a. Kaposi’s sarcoma and opportunistic infections in previously healthy persons. MMWR. 31(22); 294, 300-301.

CDC. 1982b. Opportunistic infections and Kaposi's sarcoma among Haitians in the United States. MMWR. 31(26); 353-354, 360-361.

CDC 1982c. Pneumocystis carinii pneumonia among persons with hemophilia A. MMWR. 31(27); 365-367.

CDC. 1982d. Unexplained immunodeficiency and opportunistic infections in infants. MMWR. 31(49); 665-667.

CDC 1982e. Current trends update on Acquired Immune Deficiency Syndrome (AIDS). MMWR. 31(37); 507-508, 513-514.

CDC. 1983. Immunodeficiency among female sexual partners of males with Acquired Immune Deficiency Syndrome (AIDS). MMWR. 31(52); 697-698.

CDC. 2016. HIV among gay and bisexual men. Retrieved from: http://www.cdc.gov/hiv/group/msm/.

Chan, D. C., Fass, D., Berger, J. M., and Kim, P. S. 1997. Core structure of gp41 from the HIV envelope glycoprotein. Cell, 89(2), 263-273.

Charpentier, C., Nora, T., Tenaillon, O., Clavel, F., and Hance, A. J. 2006. Extensive recombination among human immunodeficiency virus type 1 quasispecies makes an important contribution to viral diversity in individual patients. J Virol, 80(5), 2472-2482.

Chen, B., Vogan, E. M., Gong, H., Skehel, J. J., Wiley, D. C., and Harrison, S. C. 2005. Structure of an unliganded simian immunodeficiency virus gp120 core. Nature, 433(7028), 834-841.

Chen, J., Powell, D., and Hu, W. S. 2006. High frequency of genetic recombination is a common feature of primate lentivirus replication. J Virol, 80(19), 9651-9658.

Chohan, B., Lang, D., Sagar, M., Korber, B., Lavreys, L., Richardson, B., and Overbaugh, J. 2005. Selection for human immunodeficiency virus type 1 envelope glycosylation variants with shorter V1-V2 loop sequences occurs during transmission of certain genetic subtypes and may impact viral RNA levels. J Virol, 79(10), 6528-6531.

Churchill, M., Sterjovski, J., Gray, L., Cowley, D., Chatfield, C., Learmont, J., Sullivan, J. S., Crowe, S. M., Mills, J., Brew, B. J., Wesselingh, S. L., McPhee, D. A., and Gorry, P. R. 2004. Longitudinal analysis of nef/long terminal repeat-

deleted HIV-1 in blood and cerebrospinal fluid of a long-term survivor who developed HIV-associated dementia. J Infect Dis, 190(12), 2181-2186.

Clarke, J. R., Krishnan, V., Bennett, J., Mitchell, D., and Jeffries, D. J. 1990. Detection of HIV-1 in human lung macrophages using the polymerase chain reaction. AIDS, 4(11), 1133-1136.

Cocchi, F., DeVico, A. L., Garzino-Demo, A., Arya, S. K., Gallo, R. C., and Lusso, P. 1995. Identification of RANTES, MIP-1 alpha, and MIP-1 beta as the major HIV-suppressive factors produced by CD8+ T cells. Science, 270(5243), 1811-1815.

Coffin, J., Haase, A., Levy, J. A., Montagnier, L., Oroszlan, S., Teich, N., Temin, H., Toyoshima, K., Varmus, H., Vogt, P., and Weiss, R. 1986a. Human immunodeficiency viruses. Science, 232(4751), 697.

Coffin, J., Haase, A., Levy, J. A., Montagnier, L., Oroszlan, S., Teich, N., Temin, H., Toyoshima, K., Varmus, H., Vogt, P., and Weiss, R. 1986. What to call the AIDS virus? Nature, 321(6065), 10.

Coffin, J. M. 1995. HIV population dynamics in vivo: implications for genetic variation, pathogenesis, and therapy. Science, 267(5197), 483-489.

Cohen, E. A., Subbramanian, R. A., and Gottlinger, H. G. 1996. Role of auxiliary proteins in retroviral morphogenesis. Curr Top Microbiol Immunol, 214, 219-235.

Cohen, E. A., Terwilliger, E. F., Jalinoos, Y., Proulx, J., Sodroski, J. G., and Haseltine, W. A. 1990. Identification of HIV-1 vpr product and function. J Acquir Immune Defic Syndr, 3(1), 11-18.

Cohen, E. A., Terwilliger, E. F., Sodroski, J. G., and Haseltine, W. A. 1988. Identification of a protein encoded by the vpu gene of HIV-1. Nature, 334(6182), 532-534.

Collier, A. C., Coombs, R. W., Schoenfeld, D. A., Bassett, R. L., Timpone, J., Baruch, A., Jones, M., Facey, K., Whitacre, C., McAuliffe, V. J., Friedman, H. M., Merigan, T. C., Reichman, R. C., Hooper, C., and Corey, L. 1996. Treatment of human immunodeficiency virus infection with saquinavir, zidovudine, and zalcitabine. AIDS Clinical Trials Group. N Engl J Med, 334(16), 1011-1017.

Conley, A. J., Gorny, M. K., Kessler, J. A., 2nd, Boots, L. J., Ossorio-Castro, M., Koenig, S., Lineberger, D. W., Emini, E. A., Williams, C., and Zolla-Pazner, S. 1994. Neutralization of primary human immunodeficiency virus type 1 isolates by

the broadly reactive anti-V3 monoclonal antibody, 447-52D. J Virol, 68(11), 6994-7000.

Connor, R. I., Sheridan, K. E., Ceradini, D., Choe, S., and Landau, N. R. 1997. Change in coreceptor use correlates with disease progression in HIV-1--infected individuals. J Exp Med, 185(4), 621-628.

Corbet, S., Muller-Trutwin, M. C., Versmisse, P., Delarue, S., Ayouba, A., Lewis, J., Brunak, S., Martin, P., Brun-Vezinet, F., Simon, F., Barre-Sinoussi, F., and Mauclere, P. 2000. env sequences of simian immunodeficiency viruses from chimpanzees in Cameroon are strongly related to those of human immunodeficiency virus group N from the same geographic area. J Virol, 74(1), 529-534.

Curlin, M. E., Zioni, R., Hawes, S. E., Liu, Y., Deng, W., Gottlieb, G. S., Zhu, T., and Mullins, J. I. 2010. HIV-1 envelope subregion length variation during disease progression. PLoS Pathog, 6(12).

D'Aquila, R. T., Hughes, M. D., Johnson, V. A., Fischl, M. A., Sommadossi, J. P., Liou, S. H., Timpone, J., Myers, M., Basgoz, N., Niu, M., and Hirsch, M. S. 1996. Nevirapine, zidovudine, and didanosine compared with zidovudine and didanosine in patients with HIV-1 infection. A randomized, double-blind, placebo-controlled trial. National Institute of Allergy and Infectious Diseases AIDS Clinical Trials Group Protocol 241 Investigators. Ann Intern Med, 124(12), 1019-1030.

D'Arc, M., Ayouba, A., Esteban, A., Learn, G. H., Boue, V., Liegeois, F., Etienne, L., Tagg, N., Leendertz, F. H., Boesch, C., Madinda, N. F., Robbins, M. M., Gray, M., Cournil, A., Ooms, M., Letko, M., Simon, V. A., Sharp, P. M., Hahn, B. H., Delaporte, E., Mpoudi Ngole, E., and Peeters, M. 2015. Origin of the HIV-1 group O epidemic in western lowland gorillas. Proc Natl Acad Sci U S A, 112(11), E1343-1352.

Davenport, T. M., Guttman, M., Guo, W., Cleveland, B., Kahn, M., Hu, S. L., and Lee, K. K. 2013. Isolate-specific differences in the conformational dynamics and antigenicity of HIV-1 gp120. J Virol, 87(19), 10855-10873.

Dayton, A. I., Sodroski, J. G., Rosen, C. A., Goh, W. C., and Haseltine, W. A. 1986. The trans-activator gene of the human T cell lymphotropic virus type III is required for replication. Cell, 44(6), 941-947.

De Leys, R., Vanderborght, B., Vanden Haesevelde, M., Heyndrickx, L., van Geel, A., Wauters, C., Bernaerts, R., Saman, E., Nijs, P., Willems, B., Taelman, H., van der Groen, G., Piot, P., Tersmette, T., Huisman, J.G., and van Heuverswyn, H. 1990. Isolation and partial characterization of an unusual human

immunodeficiency retrovirus from two persons of west-central African origin. J Virol, 64(3), 1207-1216.

de Roda Husman, A. M., Blaak, H., Brouwer, M., and Schuitemaker, H. 1999. CC chemokine receptor 5 cell-surface expression in relation to CC chemokine receptor 5 genotype and the clinical course of HIV-1 infection. J Immunol, 163(8), 4597-4603.

Deng, H., Liu, R., Ellmeier, W., Choe, S., Unutmaz, D., Burkhart, M., Di Marzio, P., Marmon, S., Sutton, R. E., Hill, C. M., Davis, C. B., Peiper, S. C., Schall, T. J., Littman, D. R., and Landau, N. R. 1996. Identification of a major co-receptor for primary isolates of HIV-1. Nature, 381(6584), 661-666.

Derdeyn, C. A., Decker, J. M., Bibollet-Ruche, F., Mokili, J. L., Muldoon, M., Denham, S. A., Heil, M. L., Kasolo, F., Musonda, R., Hahn, B. H., Shaw, G. M., Korber, B. T., Allen, S., and Hunter, E. 2004. Envelope-constrained neutralization-sensitive HIV-1 after heterosexual transmission. Science, 303(5666), 2019-2022.

Derdeyn, C. A., Decker, J. M., Sfakianos, J. N., Wu, X., O'Brien, W. A., Ratner, L., Kappes, J. C., Shaw, G. M., and Hunter, E. 2000. Sensitivity of human immunodeficiency virus type 1 to the fusion inhibitor T-20 is modulated by coreceptor specificity defined by the V3 loop of gp120. J Virol, 74(18), 8358-8367.

Donaldson, Y. K., Bell, J. E., Ironside, J. W., Brettle, R. P., Robertson, J. R., Busuttil, A., and Simmonds, P. 1994. Redistribution of HIV outside the lymphoid system with onset of AIDS. Lancet, 343(8894), 383-385.

Doores, K. J., and Burton, D. R. 2010. Variable loop glycan dependency of the broad and potent HIV-1-neutralizing antibodies PG9 and PG16. J Virol, 84(20), 10510-10521.

Dorfman, T., Mammano, F., Haseltine, W. A., and Gottlinger, H. G. 1994a. Role of the matrix protein in the virion association of the human immunodeficiency virus type 1 envelope glycoprotein. J Virol, 68(3), 1689-1696.

Dorfman, T., Bukovsky, A., Ohagen, A., Hoglund, S., and Gottlinger, H. G. 1994b. Functional domains of the capsid protein of human immunodeficiency virus type 1. J Virol, 68(12), 8180-8187.

Dorr, P., Westby, M., Dobbs, S., Griffin, P., Irvine, B., Macartney, M., Mori, J., Rickett, G., Smith-Burchnell, C., Napier, C., Webster, R., Armour, D., Price, D., Stammen, B., Wood, A., and Perros, M. 2005. Maraviroc (UK-427,857), a potent,

orally bioavailable, and selective small-molecule inhibitor of chemokine receptor CCR5 with broad-spectrum anti-human immunodeficiency virus type 1 activity. Antimicrob Agents Chemother, 49(11), 4721-4732.

Douek, D. C., Picker, L. J., and Koup, R. A. 2003. T cell dynamics in HIV-1 infection. Annu Rev Immunol, 21, 265-304.

DuBridge, R. B., Tang, P., Hsia, H. C., Leong, P. M., Miller, J. H., and Calos, M. P. 1987. Analysis of mutation in human cells by using an Epstein-Barr virus shuttle system. Mol Cell Biol, 7(1), 379-387.

Duenas-Decamp, M. J., Peters, P. J., Burton, D., and Clapham, P. R. 2009. Determinants flanking the CD4 binding loop modulate macrophage tropism of human immunodeficiency virus type 1 R5 envelopes. J Virol, 83(6), 2575-2583.

Dunfee, R. L., Thomas, E. R., and Gabuzda, D. 2009. Enhanced macrophage tropism of HIV in brain and lymphoid tissues is associated with sensitivity to the broadly neutralizing CD4 binding site antibody b12. Retrovirology, 6, 69.

Dunfee, R. L., Thomas, E. R., Gorry, P. R., Wang, J., Taylor, J., Kunstman, K., Wolinsky, S. M., and Gabuzda, D. 2006. The HIV Env variant N283 enhances macrophage tropism and is associated with brain infection and dementia. Proc Natl Acad Sci U S A, 103(41), 15160-15165.

Dunfee, R. L., Thomas, E. R., Wang, J., Kunstman, K., Wolinsky, S. M., and Gabuzda, D. 2007. Loss of the N-linked glycosylation site at position 386 in the HIV envelope V4 region enhances macrophage tropism and is associated with dementia. Virology, 367(1), 222-234.

Etemad, B., Fellows, A., Kwambana, B., Kamat, A., Feng, Y., Lee, S., and Sagar, M. 2009. Human immunodeficiency virus type 1 V1-to-V5 envelope variants from the chronic phase of infection use CCR5 and fuse more efficiently than those from early after infection. J Virol, 83(19), 9694-9708.

Etemad, B., Ghulam-Smith, M., Gonzalez, O., White, L. F., and Sagar, M. 2015. Single genome amplification and standard bulk PCR yield HIV-1 envelope products with similar genotypic and phenotypic characteristics. J Virol Methods, 214, 46-53.

FDA. 2016a. HIV/AIDS historical time line 1981-1990. Retrieved from: http://www.fda.gov/ForPatients/Illness/HIVAIDS/History/ucm151074.htm

FDA. 2016b. Antiretroviral drugs used in the treatment of HIV infection. Retrieved from: http://www.fda.gov/ForPatients/Illness/HIVAIDS/Treatment/ucm118915.htm.

Feinberg, M. B., Baltimore, D., and Frankel, A. D. 1991. The role of Tat in the human immunodeficiency virus life cycle indicates a primary effect on transcriptional elongation. Proc Natl Acad Sci U S A, 88(9), 4045-4049.

Felber, B. K., Hadzopoulou-Cladaras, M., Cladaras, C., Copeland, T., and Pavlakis, G. N. 1989. rev protein of human immunodeficiency virus type 1 affects the stability and transport of the viral mRNA. Proc Natl Acad Sci U S A, 86(5), 1495-1499.

Feng, S., and Holland, E. C. 1988. HIV-1 tat trans-activation requires the loop sequence within tar. Nature, 334(6178), 165-167.

Feng, Y., Broder, C. C., Kennedy, P. E., and Berger, E. A. 1996. HIV-1 entry cofactor: functional cDNA cloning of a seven-transmembrane, G protein-coupled receptor. Science, 272(5263), 872-877.

Fisher, A. G., Feinberg, M. B., Josephs, S. F., Harper, M. E., Marselle, L. M., Reyes, G., Gonda, M. A., Aldovini, A., Debouk, C., Gallo, R. C., and Wong-Staal, F. 1986. The trans-activator gene of HTLV-III is essential for virus replication. Nature, 320(6060), 367-371.

Fletcher, C. V., Staskus, K., Wietgrefe, S. W., Rothenberger, M., Reilly, C., Chipman, J. G., Beilman, G. J., Khoruts, A., Thorkelson, A., Schmidt, T. E., Anderson, J., Perkey, K., Stevenson, M., Perelson, A. S., Douek, D. C., Haase, A. T., and Schacker, T. W. 2014. Persistent HIV-1 replication is associated with lower antiretroviral drug concentrations in lymphatic tissues. Proc Natl Acad Sci U S A, 111(6), 2307-2312.

Forte, S. E., Byron, K. S., Sullivan, J. L., and Somasundaran, M. 1994. Non-syncytium-inducing HIV type 1 isolated from infected individuals replicates in MT-2 cells. AIDS Res Hum Retroviruses, 10(12), 1613-1618.

Fouchier, R. A., Groenink, M., Kootstra, N. A., Tersmette, M., Huisman, H. G., Miedema, F., and Schuitemaker, H. 1992. Phenotype-associated sequence variation in the third variable domain of the human immunodeficiency virus type 1 gp120 molecule. J Virol, 66(5), 3183-3187.

Fourati, S., Lambert-Niclot, S., Soulie, C., Wirden, M., Malet, I., Valantin, M. A., Tubiana, R., Simon, A., Katlama, C., Carcelain, G., Calvez, V., and Marcelin, A.

G. 2014. Differential impact of APOBEC3-driven mutagenesis on HIV evolution in diverse anatomical compartments. AIDS, 28(4), 487-491.

Franke, E. K., Yuan, H. E., and Luban, J. 1994. Specific incorporation of cyclophilin A into HIV-1 virions. Nature, 372(6504), 359-362.

Frankel, A. D., and Young, J. A. 1998. HIV-1: fifteen proteins and an RNA. Annu Rev Biochem, 67, 1-25.

Freed, E. O. 1998. HIV-1 gag proteins: diverse functions in the virus life cycle. Virology, 251(1), 1-15.

Freed, E. O., and Martin, M. A. 1995a. The role of human immunodeficiency virus type 1 envelope glycoproteins in virus infection. J Biol Chem, 270(41), 23883-23886.

Freed, E. O., and Martin, M. A. 1995b. Virion incorporation of envelope glycoproteins with long but not short cytoplasmic tails is blocked by specific, single amino acid substitutions in the human immunodeficiency virus type 1 matrix. J Virol, 69(3), 1984-1989.

Freed, E. O., Myers, D. J., and Risser, R. 1989. Mutational analysis of the cleavage sequence of the human immunodeficiency virus type 1 envelope glycoprotein precursor gp160. J Virol, 63(11), 4670-4675.

Freed, E. O., Myers, D. J., and Risser, R. 1990. Characterization of the fusion domain of the human immunodeficiency virus type 1 envelope glycoprotein gp41. Proc Natl Acad Sci U S A, 87(12), 4650-4654.

Frost, S. D., and McLean, A. R. 1994. Quasispecies dynamics and the emergence of drug resistance during zidovudine therapy of HIV infection. AIDS, 8(3), 323-332.

Fujiwara, T., and Mizuuchi, K. 1988. Retroviral DNA integration: structure of an integration intermediate. Cell, 54(4), 497-504.

Gabuzda, D. H., Lawrence, K., Langhoff, E., Terwilliger, E., Dorfman, T., Haseltine, W. A., and Sodroski, J. 1992. Role of vif in replication of human immunodeficiency virus type 1 in CD4+ T lymphocytes. J Virol, 66(11), 6489-6495.

Gallo, R. C., Salahuddin, S. Z., Popovic, M., Shearer, G. M., Kaplan, M., Haynes, B. F., Palker, T. J., Redfield, R., Oleske, J., Safai, B., White, G., Foster, P., and Markham, P. D. 1984. Frequent detection and isolation of cytopathic retroviruses

(HTLV-III) from patients with AIDS and at risk for AIDS. Science, 224(4648), 500-503.

Gamble, T. R., Vajdos, F. F., Yoo, S., Worthylake, D. K., Houseweart, M., Sundquist, W. I., and Hill, C. P. 1996. Crystal structure of human cyclophilin A bound to the amino-terminal domain of HIV-1 capsid. Cell, 87(7), 1285-1294.

Gamble, T. R., Yoo, S., Vajdos, F. F., von Schwedler, U. K., Worthylake, D. K., Wang, H., McCutcheon, J. P., Sundquist, W. I., and Hill, C. P. 1997. Structure of the carboxyl-terminal dimerization domain of the HIV-1 capsid protein. Science, 278(5339), 849-853.

Ganser-Pornillos, B. K., Cheng, A., and Yeager, M. 2007. Structure of full-length HIV-1 CA: a model for the mature capsid lattice. Cell, 131(1), 70-79.

Gao, F., Bailes, E., Robertson, D. L., Chen, Y., Rodenburg, C. M., Michael, S. F., Cummins, L. B., Arthur, L. O., Peeters, M., Shaw, G. M., Sharp, P. M., and Hahn, B. H. 1999. Origin of HIV-1 in the chimpanzee Pan troglodytes troglodytes. Nature, 397(6718), 436-441.

Gao, F., Morrison, S. G., Robertson, D. L., Thornton, C. L., Craig, S., Karlsson, G., Sodroski, J., Morgado, M., Galvao-Castro, B., von Briesen, H., Beddows, S., Weber, J., Sharp, P. M., Shaw, G. M., and Hahn, B. H. 1996. Molecular cloning and analysis of functional envelope genes from human immunodeficiency virus type 1 sequence subtypes A through G. The WHO and NIAID Networks for HIV Isolation and Characterization. J Virol, 70(3), 1651-1667.

Gao, F., Yue, L., White, A. T., Pappas, P. G., Barchue, J., Hanson, A. P., Greene, B. M., Sharp, P. M., Shaw, G. M., and Hahn, B. H. 1992. Human infection by genetically diverse SIVSM-related HIV-2 in west Africa. Nature, 358(6386), 495-499.

Garcia, J. V., and Miller, A. D. 1992. Downregulation of cell surface CD4 by nef. Res Virol, 143(1), 52-55.

Gartner, S., Markovits, P., Markovitz, D. M., Kaplan, M. H., Gallo, R. C., and Popovic, M. 1986. The role of mononuclear phagocytes in HTLV-III/LAV infection. Science, 233(4760), 215-219.

Gelmann, E. P., Franchini, G., Manzari, V., Wong-Staal, F., and Gallo, R. C. 1984. Molecular cloning of a unique human T-cell leukemia virus (HTLV-IIMo). Proc Natl Acad Sci U S A, 81(4), 993-997.

Gettings, K. B., Aponte, R. A., Vallone, P. M., and Butler, J. M. 2015. STR allele sequence variation: Current knowledge and future issues. Forensic Sci Int Genet, 18, 118-130.

Gilbert, M. T., Rambaut, A., Wlasiuk, G., Spira, T. J., Pitchenik, A. E., and Worobey, M. 2007. The emergence of HIV/AIDS in the Americas and beyond. Proc Natl Acad Sci U S A, 104(47), 18566-18570.

Gomes, M. J., Neves, J., and Sarmento, B. 2014. Nanoparticle-based drug delivery to improve the efficacy of antiretroviral therapy in the central nervous system. Int J Nanomedicine, 9, 1757-1769.

Gonzalez-Perez, M. P., O'Connell, O., Lin, R., Sullivan, W. M., Bell, J., Simmonds, P., and Clapham, P. R. 2012. Independent evolution of macrophage-tropism and increased charge between HIV-1 R5 envelopes present in brain and immune tissue. Retrovirology, 9, 20.

Goodenow, M., Huet, T., Saurin, W., Kwok, S., Sninsky, J., and Wain-Hobson, S. 1989. HIV-1 isolates are rapidly evolving quasispecies: evidence for viral mixtures and preferred nucleotide substitutions. J Acquir Immune Defic Syndr, 2(4), 344-352.

Goodenow, M. M., and Collman, R. G. 2006. HIV-1 coreceptor preference is distinct from target cell tropism: a dual-parameter nomenclature to define viral phenotypes. J Leukoc Biol, 80(5), 965-972.

Gorny, M. K., Conley, A. J., Karwowska, S., Buchbinder, A., Xu, J. Y., Emini, E. A., Koenig, S., and Zolla-Pazner, S. 1992. Neutralization of diverse human immunodeficiency virus type 1 variants by an anti-V3 human monoclonal antibody. J Virol, 66(12), 7538-7542.

Gorny, M. K., VanCott, T. C., Hioe, C., Israel, Z. R., Michael, N. L., Conley, A. J., Williams, C., Kessler, J. A., 2nd, Chigurupati, P., Burda, S., and Zolla-Pazner, S. 1997. Human monoclonal antibodies to the V3 loop of HIV-1 with intra- and interclade cross-reactivity. J Immunol, 159(10), 5114-5122.

Gorny, M. K., Xu, J. Y., Karwowska, S., Buchbinder, A., and Zolla-Pazner, S. 1993. Repertoire of neutralizing human monoclonal antibodies specific for the V3 domain of HIV-1 gp120. J Immunol, 150(2), 635-643.

Gorry, P. R., Bristol, G., Zack, J. A., Ritola, K., Swanstrom, R., Birch, C. J., Bell, J. E., Bannert, N., Crawford, K., Wang, H., Schols, D., De Clercq, E., Kunstman, K., Wolinsky, S. M., and Gabuzda, D. 2001. Macrophage tropism of human

immunodeficiency virus type 1 isolates from brain and lymphoid tissues predicts neurotropism independent of coreceptor specificity. J Virol, 75(21), 10073-10089.

Gorry, P. R., Taylor, J., Holm, G. H., Mehle, A., Morgan, T., Cayabyab, M., Farzan, M., Wang, H., Bell, J. E., Kunstman, K., Moore, J. P., Wolinsky, S. M., and Gabuzda, D. 2002. Increased CCR5 affinity and reduced CCR5/CD4 dependence of a neurovirulent primary human immunodeficiency virus type 1 isolate. J Virol, 76(12), 6277-6292.

Gottlieb, M. S., Schroff, R., Schanker, H. M., Weisman, J. D., Fan, P. T., Wolf, R. A., and Saxon, A. 1981. Pneumocystis carinii pneumonia and mucosal candidiasis in previously healthy homosexual men: evidence of a new acquired cellular immunodeficiency. N Engl J Med, 305(24), 1425-1431.

Gottlinger, H. G., Dorfman, T., Cohen, E. A., and Haseltine, W. A. 1993. Vpu protein of human immunodeficiency virus type 1 enhances the release of capsids produced by gag gene constructs of widely divergent retroviruses. Proc Natl Acad Sci U S A, 90(15), 7381-7385.

Gottlinger, H. G., Dorfman, T., Sodroski, J. G., and Haseltine, W. A. 1991. Effect of mutations affecting the p6 gag protein on human immunodeficiency virus particle release. Proc Natl Acad Sci U S A, 88(8), 3195-3199.

Gottlinger, H. G., Sodroski, J. G., and Haseltine, W. A. 1989. Role of capsid precursor processing and myristoylation in morphogenesis and infectivity of human immunodeficiency virus type 1. Proc Natl Acad Sci U S A, 86(15), 5781-5785.

Graham, F. L., Smiley, J., Russell, W. C., and Nairn, R. 1977. Characteristics of a human cell line transformed by DNA from human adenovirus type 5. J Gen Virol, 36(1), 59-74.

Gray, L., Roche, M., Churchill, M. J., Sterjovski, J., Ellett, A., Poumbourios, P., Sherieff, S., Wang, B., Saksena, N., Purcell, D. F., Wesselingh, S., Cunningham, A. L., Brew, B. J., Gabuzda, D., and Gorry, P. R. 2009. Tissue-specific sequence alterations in the human immunodeficiency virus type 1 envelope favoring CCR5 usage contribute to persistence of dual-tropic virus in the brain. J Virol, 83(11), 5430-5441.

Gray, L., Sterjovski, J., Churchill, M., Ellery, P., Nasr, N., Lewin, S. R., Crowe, S. M., Wesselingh, S. L., Cunningham, A. L., and Gorry, P. R. 2005. Uncoupling coreceptor usage of human immunodeficiency virus type 1 (HIV-1) from macrophage tropism reveals biological properties of CCR5-restricted HIV-1

isolates from patients with acquired immunodeficiency syndrome. Virology, 337(2), 384-398.

Guadalupe, M., Reay, E., Sankaran, S., Prindiville, T., Flamm, J., McNeil, A., and Dandekar, S. 2003. Severe CD4+ T-cell depletion in gut lymphoid tissue during primary human immunodeficiency virus type 1 infection and substantial delay in restoration following highly active antiretroviral therapy. J Virol, 77(21), 11708-11717.

Guindon, S., Dufayard, J. F., Lefort, V., Anisimova, M., Hordijk, W., and Gascuel, O. 2010. New algorithms and methods to estimate maximum-likelihood phylogenies: assessing the performance of PhyML 3.0. Syst Biol, 59(3), 307-321.

Gurtler, L. G., Hauser, P. H., Eberle, J., von Brunn, A., Knapp, S., Zekeng, L., Tsague, J. M., and Kaptue, L. 1994. A new subtype of human immunodeficiency virus type 1 (MVP-5180) from Cameroon. J Virol, 68(3), 1581-1585.

Guttman, M., Cupo, A., Julien, J. P., Sanders, R. W., Wilson, I. A., Moore, J. P., and Lee, K. K. 2015. Antibody potency relates to the ability to recognize the closed, pre-fusion form of HIV Env. Nat Commun, 6, 6144.

Haffar, O. K., Dowbenko, D. J., and Berman, P. W. 1988. Topogenic analysis of the human immunodeficiency virus type 1 envelope glycoprotein, gp160, in microsomal membranes. J Cell Biol, 107(5), 1677-1687.

Hallenberger, S., Bosch, V., Angliker, H., Shaw, E., Klenk, H. D., and Garten, W. 1992. Inhibition of furin-mediated cleavage activation of HIV-1 glycoprotein gp160. Nature, 360(6402), 358-361.

Harris, R. S., Bishop, K. N., Sheehy, A. M., Craig, H. M., Petersen-Mahrt, S. K., Watt, I. N., Neuberger, M. S., and Malim, M. H. 2003. DNA deamination mediates innate immunity to retroviral infection. Cell, 113(6), 803-809.

Harrison, G. P., and Lever, A. M. 1992. The human immunodeficiency virus type 1 packaging signal and major splice donor region have a conserved stable secondary structure. J Virol, 66(7), 4144-4153.

Heinzinger, N. K., Bukrinsky, M. I., Haggerty, S. A., Ragland, A. M., Kewalramani, V., Lee, M. A., Gendelman, H. E., Ratner, L., Stevenson, M., and Emerman, M. 1994. The Vpr protein of human immunodeficiency virus type 1 influences nuclear localization of viral nucleic acids in nondividing host cells. Proc Natl Acad Sci U S A, 91(15), 7311-7315.

Hioe, C. E., Wrin, T., Seaman, M. S., Yu, X., Wood, B., Self, S., Williams, C., Gorny, M. K., and Zolla-Pazner, S. 2010. Anti-V3 monoclonal antibodies display broad neutralizing activities against multiple HIV-1 subtypes. PLoS One, 5(4).

Hirsch, V. M., Olmsted, R. A., Murphey-Corb, M., Purcell, R. H., and Johnson, P. R. 1989. An African primate lentivirus (SIVsm) closely related to HIV-2. Nature, 339(6223), 389-392.

Ho, D. D., Neumann, A. U., Perelson, A. S., Chen, W., Leonard, J. M., and Markowitz, M. 1995. Rapid turnover of plasma virions and CD4 lymphocytes in HIV-1 infection. Nature, 373(6510), 123-126.

Hoffman, N. G., Seillier-Moiseiwitsch, F., Ahn, J., Walker, J. M., and Swanstrom, R. 2002. Variability in the human immunodeficiency virus type 1 gp120 Env protein linked to phenotype-associated changes in the V3 loop. J Virol, 76(8), 3852-3864.

Hoglund, S., Ohagen, A., Lawrence, K., and Gabuzda, D. 1994. Role of vif during packing of the core of HIV-1. Virology, 201(2), 349-355.

Huang, M., Orenstein, J. M., Martin, M. A., and Freed, E. O. 1995. p6Gag is required for particle production from full-length human immunodeficiency virus type 1 molecular clones expressing protease. J Virol, 69(11), 6810-6818.

Huang, W., Eshleman, S. H., Toma, J., Fransen, S., Stawiski, E., Paxinos, E. E., Whitcomb, J. M., Young, A. M., Donnell, D., Mmiro, F., Musoke, P., Guay, L. A., Jackson, J. B., Parkin, N. T., and Petropoulos, C. J. 2007. Coreceptor tropism in human immunodeficiency virus type 1 subtype D: high prevalence of CXCR4 tropism and heterogeneous composition of viral populations. J Virol, 81(15), 7885-7893.

Huang, X., Jin, W., Hu, K., Luo, S., Du, T., Griffin, G. E., Shattock, R. J., and Hu, Q. 2012. Highly conserved HIV-1 gp120 glycans proximal to CD4-binding region affect viral infectivity and neutralizing antibody induction. Virology, 423(1), 97-106.

Huet, T., Cheynier, R., Meyerhans, A., Roelants, G., and Wain-Hobson, S. 1990. Genetic organization of a chimpanzee lentivirus related to HIV-1. Nature, 345(6273), 356-359.

Hunter, E., and Swanstrom, R. 1990. Retrovirus envelope glycoproteins. Curr Top Microbiol Immunol, 157, 187-253.

Hwang, S. S., Boyle, T. J., Lyerly, H. K., and Cullen, B. R. 1991. Identification of the envelope V3 loop as the primary determinant of cell tropism in HIV-1. Science, 253(5015), 71-74.

Imamichi, H., Degray, G., Dewar, R. L., Mannon, P., Yao, M., Chairez, C., Sereti, I., and Kovacs, J. A. 2011. Lack of compartmentalization of HIV-1 quasispecies between the gut and peripheral blood compartments. J Infect Dis, 204(2), 309-314.

Imamichi, H., Igarashi, T., Imamichi, T., Donau, O. K., Endo, Y., Nishimura, Y., Willey, R. L., Suffredini, A. F., Lane, H. C., and Martin, M. A. 2002. Amino acid deletions are introduced into the V2 region of gp120 during independent pathogenic simian immunodeficiency virus/HIV chimeric virus (SHIV) infections of rhesus monkeys generating variants that are macrophage tropic. Proc Natl Acad Sci U S A, 99(21), 13813-13818.

Immonen, T. T., Conway, J. M., Romero-Severson, E. O., Perelson, A. S., and Leitner, T. 2015. Recombination Enhances HIV-1 Envelope Diversity by Facilitating the Survival of Latent Genomic Fragments in the Plasma Virus Population. PLoS Comput Biol, 11(12).

Immonen, T. T., and Leitner, T. 2014. Reduced evolutionary rates in HIV-1 reveal extensive latency periods among replicating lineages. Retrovirology, 11(1), 81.

Ince, W. L., Harrington, P. R., Schnell, G. L., Patel-Chhabra, M., Burch, C. L., Menezes, P., Price, R. W., Eron, J. J., Jr., and Swanstrom, R. I. 2009. Major coexisting human immunodeficiency virus type 1 env gene subpopulations in the peripheral blood are produced by cells with similar turnover rates and show little evidence of genetic compartmentalization. J Virol, 83(9), 4068-4080.

Irlbeck, D. M., Amrine-Madsen, H., Kitrinos, K. M., Labranche, C. C., and Demarest, J. F. 2008. Chemokine (C-C motif) receptor 5-using envelopes predominate in dual/mixed-tropic HIV from the plasma of drug-naive individuals. AIDS, 22(12), 1425-1431.

Jacks, T., Power, M. D., Masiarz, F. R., Luciw, P. A., Barr, P. J., and Varmus, H. E. 1988. Characterization of ribosomal frameshifting in HIV-1 gag-pol expression. Nature, 331(6153), 280-283.

Jambo, K. C., Banda, D. H., Kankwatira, A. M., Sukumar, N., Allain, T. J., Heyderman, R. S., Russell, D. G., and Mwandumba, H. C. 2014. Small alveolar macrophages are infected preferentially by HIV and exhibit impaired phagocytic function. Mucosal Immunol, 7(5), 1116-1126.

Jensen, M. A., Li, F. S., van 't Wout, A. B., Nickle, D. C., Shriner, D., He, H. X., McLaughlin, S., Shankarappa, R., Margolick, J. B., and Mullins, J. I. 2003. Improved coreceptor usage prediction and genotypic monitoring of R5-to-X4 transition by motif analysis of human immunodeficiency virus type 1 env V3 loop sequences. J Virol, 77(24), 13376-13388.

Jetzt, A. E., Yu, H., Klarmann, G. J., Ron, Y., Preston, B. D., and Dougherty, J. P. 2000. High rate of recombination throughout the human immunodeficiency virus type 1 genome. J Virol, 74(3), 1234-1240.

Jowett, J. B., Planelles, V., Poon, B., Shah, N. P., Chen, M. L., and Chen, I. S. 1995. The human immunodeficiency virus type 1 vpr gene arrests infected T cells in the G2 + M phase of the cell cycle. J Virol, 69(10), 6304-6313.

Julien, J. P., Lee, J. H., Cupo, A., Murin, C. D., Derking, R., Hoffenberg, S., Caulfield, M. J., King, C. R., Marozsan, A. J., Klasse, P. J., Sanders, R. W., Moore, J. P., Wilson, I. A., and Ward, A. B. 2013. Asymmetric recognition of the HIV-1 trimer by broadly neutralizing antibody PG9. Proc Natl Acad Sci U S A, 110(11), 4351-4356.

Kabat, D., Kozak, S. L., Wehrly, K., and Chesebro, B. 1994. Differences in CD4 dependence for infectivity of laboratory-adapted and primary patient isolates of human immunodeficiency virus type 1. J Virol, 68(4), 2570-2577.

Kao, S. Y., Calman, A. F., Luciw, P. A., and Peterlin, B. M. 1987. Anti-termination of transcription within the long terminal repeat of HIV-1 by tat gene product. Nature, 330(6147), 489-493.

Karlsson, I., Antonsson, L., Shi, Y., Oberg, M., Karlsson, A., Albert, J., Olde, B., Owman, C., Jansson, M., and Fenyo, E. M. 2004. Coevolution of RANTES sensitivity and mode of CCR5 receptor use by human immunodeficiency virus type 1 of the R5 phenotype. J Virol, 78(21), 11807-11815.

Kearse, M., Moir, R., Wilson, A., Stones-Havas, S., Cheung, M., Sturrock, S., Buxton, S., Cooper, A., Markowitz, S., Duran, C., Thierer, T., Ashton, B., Mentjies, P., and Drummond, A. 2012. Geneious Basic: an integrated and extendable desktop software platform for the organization and analysis of sequence data. Bioinformatics, 28(12), 1647-1649.

Keele, B. F., Giorgi, E. E., Salazar-Gonzalez, J. F., Decker, J. M., Pham, K. T., Salazar, M. G., Sun, C., Grayson, T., Wang, S., Li, H., Wei, X., Jiang, C., Kirchherr, J. L., Gao, F., Anderson, J. A., Ping, L. H., Swanstrom, R., Tomaras, G. D., Blattner, W. A., Goepfert, P. A., Kilby, J. M., Saag, M. S., Delwart, E. L., Busch, M. P., Cohen, M. S., Montefiori, D. C., Haynes, B. F., Gaschen, B.,

Athreya, G. S., Lee, H. Y., Wood, N., Seoighe, C., Perelson, A. S., Bhattacharya, T., Korber, B. T., Hahn, B. H., and Shaw, G. M. 2008. Identification and characterization of transmitted and early founder virus envelopes in primary HIV-1 infection. Proc Natl Acad Sci U S A, 105(21), 7552-7557.

Keele, B. F., Van Heuverswyn, F., Li, Y., Bailes, E., Takehisa, J., Santiago, M. L., Bibollet-Ruche, F., Chen, Y., Wain, L. V., Liegeois, F., Loul, S., Ngole, E. M., Bienvenue, Y., Delaporte, E., Brookfield, J. F., Sharp, P. M., Shaw, G. M., Peeters, M., and Hahn, B. H. 2006. Chimpanzee reservoirs of pandemic and nonpandemic HIV-1. Science, 313(5786), 523-526.

Kestler, H. W., 3rd, Ringler, D. J., Mori, K., Panicali, D. L., Sehgal, P. K., Daniel, M. D., and Desrosiers, R. C. 1991. Importance of the nef gene for maintenance of high virus loads and for development of AIDS. Cell, 65(4), 651-662.

Kiernan, R. E., Ono, A., Englund, G., and Freed, E. O. 1998. Role of matrix in an early postentry step in the human immunodeficiency virus type 1 life cycle. J Virol, 72(5), 4116-4126.

Kim, S. Y., Byrn, R., Groopman, J., and Baltimore, D. 1989. Temporal aspects of DNA and RNA synthesis during human immunodeficiency virus infection: evidence for differential gene expression. J Virol, 63(9), 3708-3713.

Klimkait, T., Strebel, K., Hoggan, M. D., Martin, M. A., and Orenstein, J. M. 1990. The human immunodeficiency virus type 1-specific protein vpu is required for efficient virus maturation and release. J Virol, 64(2), 621-629.

Koito, A., Harrowe, G., Levy, J. A., and Cheng-Mayer, C. 1994. Functional role of the V1/V2 region of human immunodeficiency virus type 1 envelope glycoprotein gp120 in infection of primary macrophages and soluble CD4 neutralization. J Virol, 68(4), 2253-2259.

Kondo, E., Mammano, F., Cohen, E. A., and Gottlinger, H. G. 1995. The p6gag domain of human immunodeficiency virus type 1 is sufficient for the incorporation of Vpr into heterologous viral particles. J Virol, 69(5), 2759-2764.

Koning, F. A., Newman, E. N., Kim, E. Y., Kunstman, K. J., Wolinsky, S. M., and Malim, M. H. 2009. Defining APOBEC3 expression patterns in human tissues and hematopoietic cell subsets. J Virol, 83(18), 9474-9485.

Koot, M., Keet, I. P., Vos, A. H., de Goede, R. E., Roos, M. T., Coutinho, R. A., Miedema, F., Schellekens, P. T., and Tersmette, M. 1993. Prognostic value of HIV-1 syncytium-inducing phenotype for rate of CD4+ cell depletion and progression to AIDS. Ann Intern Med, 118(9), 681-688.

Koot, M., Vos, A. H., Keet, R. P., de Goede, R. E., Dercksen, M. W., Terpstra, F. G., Coutinho, R. A., Miedema, F., and Tersmette, M. 1992. HIV-1 biological phenotype in long-term infected individuals evaluated with an MT-2 cocultivation assay. AIDS, 6(1), 49-54.

Korber, B., Muldoon, M., Theiler, J., Gao, F., Gupta, R., Lapedes, A., Hahn, B. H., Wolinsky, S., and Bhattacharya, T. 2000. Timing the ancestor of the HIV-1 pandemic strains. Science, 288(5472), 1789-1796.

Kowalski, M., Potz, J., Basiripour, L., Dorfman, T., Goh, W. C., Terwilliger, E., Dayton, A., Rosen, C., Haseltine, W., and Sodroski, J. 1987. Functional regions of the envelope glycoprotein of human immunodeficiency virus type 1. Science, 237(4820), 1351-1355.

Koyanagi, Y., Miles, S., Mitsuyasu, R. T., Merrill, J. E., Vinters, H. V., and Chen, I. S. 1987. Dual infection of the central nervous system by AIDS viruses with distinct cellular tropisms. Science, 236(4803), 819-822.

Krachmarov, C. P., Honnen, W. J., Kayman, S. C., Gorny, M. K., Zolla-Pazner, S., and Pinter, A. 2006. Factors determining the breadth and potency of neutralization by V3-specific human monoclonal antibodies derived from subjects infected with clade A or clade B strains of human immunodeficiency virus type 1. J Virol, 80(14), 7127-7135.

Kuang, F., Wang, B. R., Zhang, P., Fei, L. L., Jia, Y., Duan, X. L., Wang, X., Xu, Z., Li, G. L., Jiao, X. Y., and Ju, G. 2004. Extravasation of blood-borne immunoglobulin G through blood-brain barrier during adrenaline-induced transient hypertension in the rat. Int J Neurosci, 114(6), 575-591.

Kwong, P. D., Doyle, M. L., Casper, D. J., Cicala, C., Leavitt, S. A., Majeed, S., Steenbeke, T. D., Venturi, M., Chaiken, I., Fung, M., Katinger, H., Parren, P. W., Robinson, J., Van Ryk, D., Wang, L., Burton, D. R., Freire, E., Wyatt, R., Sodroski, J., Hendrickson, W. A., and Arthos, J. 2002. HIV-1 evades antibody-mediated neutralization through conformational masking of receptor-binding sites. Nature, 420(6916), 678-682.

Kwong, P. D., Wyatt, R., Robinson, J., Sweet, R. W., Sodroski, J., and Hendrickson, W. A. 1998. Structure of an HIV gp120 envelope glycoprotein in complex with the CD4 receptor and a neutralizing human antibody. Nature, 393(6686), 648-659.

Lapadat-Tapolsky, M., De Rocquigny, H., Van Gent, D., Roques, B., Plasterk, R., and Darlix, J. L. 1993. Interactions between HIV-1 nucleocapsid protein and viral

DNA may have important functions in the viral life cycle. Nucleic Acids Res, 21(4), 831-839.

Lasky, L. A., Nakamura, G., Smith, D. H., Fennie, C., Shimasaki, C., Patzer, E., Berman, P., Gregory, T., and Capon, D. J. 1987. Delineation of a region of the human immunodeficiency virus type 1 gp120 glycoprotein critical for interaction with the CD4 receptor. Cell, 50(6), 975-985.

Lecossier, D., Bouchonnet, F., Clavel, F., and Hance, A. J. 2003. Hypermutation of HIV-1 DNA in the absence of the Vif protein. Science, 300(5622), 1112.

Lee, B., Sharron, M., Montaner, L. J., Weissman, D., and Doms, R. W. 1999. Quantification of CD4, CCR5, and CXCR4 levels on lymphocyte subsets, dendritic cells, and differentially conditioned monocyte derived macrophages. Proc Natl Acad Sci U S A, 96(9), 5215-5220.

Lee, C. N., Wang, W. K., Fan, W. S., Twu, S. J., Chen, S. C., Sheng, M. C., and Chen, M. Y. 2000. Determination of human immunodeficiency virus type 1 subtypes in Taiwan by vpu gene analysis. J Clin Microbiol, 38(7), 2468-2474.

Leonard, C. K., Spellman, M. W., Riddle, L., Harris, R. J., Thomas, J. N., and Gregory, T. J. 1990. Assignment of intrachain disulfide bonds and characterization of potential glycosylation sites of the type 1 recombinant human immunodeficiency virus envelope glycoprotein (gp120) expressed in Chinese hamster ovary cells. J Biol Chem, 265(18), 10373-10382.

Levin, J. G., Guo, J., Rouzina, I., and Musier-Forsyth, K. 2005. Nucleic acid chaperone activity of HIV-1 nucleocapsid protein: critical role in reverse transcription and molecular mechanism. Prog Nucleic Acid Res Mol Biol, 80, 217-286.

Li, G., Piampongsant, S., Faria, N. R., Voet, A., Pineda-Pena, A. C., Khouri, R., Lemey, P., Vandamme, A. M., and Theys, K. 2015. An integrated map of HIV genome-wide variation from a population perspective. Retrovirology, 12, 18.

Li, Q., Duan, L., Estes, J. D., Ma, Z. M., Rourke, T., Wang, Y., Reilly, C., Carlis, J., Miller, C. J., and Haase, A. T. 2005. Peak SIV replication in resting memory CD4+ T cells depletes gut lamina propria CD4+ T cells. Nature, 434(7037), 1148-1152.

Li, S., Juarez, J., Alali, M., Dwyer, D., Collman, R., Cunningham, A., and Naif, H. M. 1999. Persistent CCR5 utilization and enhanced macrophage tropism by primary blood human immunodeficiency virus type 1 isolates from advanced

stages of disease and comparison to tissue derived isolates. J Virol, 73(12), 9741-9755.

Lin, N. H., Becerril, C., Giguel, F., Novitsky, V., Moyo, S., Makhema, J., Essex, M., Lockman, S., Kuritzkes, D. R., Sagar, M. 2012. Env sequence determinants in CXCR4-using human immunodeficiency virus type-1 subtype C. Virology, 433(2):296-307.

Liu, H., Wu, X., Newman, M., Shaw, G. M., Hahn, B. H., and Kappes, J. C. 1995. The Vif protein of human and simian immunodeficiency viruses is packaged into virions and associates with viral core structures. J Virol, 69(12), 7630-7638.

Liu, Y., Curlin, M. E., Diem, K., Zhao, H., Ghosh, A. K., Zhu, H., Woodward, A. S., Maenza, J., Stevens, C. E., Stekler, J., Collier, A. C., Genowati, I., Deng, W., Zioni, R., Corey, L., Zhu, T., and Mullins, J. I. 2008. Env length and N-linked glycosylation following transmission of human immunodeficiency virus Type 1 subtype B viruses. Virology, 374(2), 229-233.

Lorello, G., la Porte, C., Pilon, R., Zhang, G., Karnauchow, T., and MacPherson, P. 2009. Discordance in HIV-1 viral loads and antiretroviral drug concentrations comparing semen and blood plasma. HIV Med, 10(9), 548-554.

Lorenzo-Redondo, R., Fryer, H. R., Bedford, T., Kim, E. Y., Archer, J., Kosakovsky Pond, S. L., Chung, Y. S., Penugonda, S., Chipman, J. G., Fletcher, C. V., Schacker, T. W., Malim, M. H., Rambaut, A., Haase, A. T., McLean, A. R., and Wolinsky, S. M. 2016. Persistent HIV-1 replication maintains the tissue reservoir during therapy. Nature, 530(7588), 51-56.

Los Alamos National Laboratoy. 2016. Variable region characteristics. Retrieved from: http://www.hiv.lanl.gov/content/sequence/VAR_REG_CHAR/variable_region_characterization_explanation.html.

Lu, M., Blacklow, S. C., and Kim, P. S. 1995. A trimeric structural domain of the HIV-1 transmembrane glycoprotein. Nat Struct Biol, 2(12), 1075-1082.

Lu, S. 2006. Combination DNA plus protein HIV vaccines. Springer Semin Immunopathol, 28(3), 255-265.

Luban, J. 1996. Absconding with the chaperone: essential cyclophilin-Gag interaction in HIV-1 virions. Cell, 87(7), 1157-1159.

Lyumkis, D., Julien, J. P., de Val, N., Cupo, A., Potter, C. S., Klasse, P. J., Burton, D. R., Sanders, R. W., Moore, J. P., Carragher, B., Wilson, I. A., and

Ward, A. B. 2013. Cryo-EM structure of a fully glycosylated soluble cleaved HIV-1 envelope trimer. Science, 342(6165), 1484-1490.

Maddon, P. J., Dalgleish, A. G., McDougal, J. S., Clapham, P. R., Weiss, R. A., and Axel, R. 1986. The T4 gene encodes the AIDS virus receptor and is expressed in the immune system and the brain. Cell, 47(3), 333-348.

Malim, M. H., Bohnlein, S., Hauber, J., and Cullen, B. R. 1989a. Functional dissection of the HIV-1 Rev trans-activator--derivation of a trans-dominant repressor of Rev function. Cell, 58(1), 205-214.

Malim, M. H., Hauber, J., Le, S. Y., Maizel, J. V., and Cullen, B. R. 1989b. The HIV-1 rev trans-activator acts through a structured target sequence to activate nuclear export of unspliced viral mRNA. Nature, 338(6212), 254-257.

Malim, M. H., Tiley, L. S., McCarn, D. F., Rusche, J. R., Hauber, J., and Cullen, B. R. 1990. HIV-1 structural gene expression requires binding of the Rev trans-activator to its RNA target sequence. Cell, 60(4), 675-683.

Mangeat, B., Turelli, P., Caron, G., Friedli, M., Perrin, L., and Trono, D. 2003. Broad antiretroviral defence by human APOBEC3G through lethal editing of nascent reverse transcripts. Nature, 424(6944), 99-103.

Mansky, L. M., and Temin, H. M. 1995. Lower in vivo mutation rate of human immunodeficiency virus type 1 than that predicted from the fidelity of purified reverse transcriptase. J Virol, 69(8), 5087-5094.

Marin, M., Rose, K. M., Kozak, S. L., and Kabat, D. 2003. HIV-1 Vif protein binds the editing enzyme APOBEC3G and induces its degradation. Nat Med, 9(11), 1398-1403.

Markosyan, R. M., Cohen, F. S., and Melikyan, G. B. 2003. HIV-1 envelope proteins complete their folding into six-helix bundles immediately after fusion pore formation. Mol Biol Cell, 14(3), 926-938.

Masur, H., Michelis, M. A., Greene, J. B., Onorato, I., Stouwe, R. A., Holzman, R. S., Wormser, G., Brettman, L., Lange, M., Murray, H. W., and Cunningham-Rundles, S. 1981. An outbreak of community-acquired Pneumocystis carinii pneumonia: initial manifestation of cellular immune dysfunction. N Engl J Med, 305(24), 1431-1438.

McCrossan, M., Marsden, M., Carnie, F. W., Minnis, S., Hansoti, B., Anthony, I. C., Brettle, R. P., Bell, J. E., and Simmonds, P. 2006. An immune control model

for viral replication in the CNS during presymptomatic HIV infection. Brain, 129(Pt 2), 503-516.

McCune, J. M., Rabin, L. B., Feinberg, M. B., Lieberman, M., Kosek, J. C., Reyes, G. R., and Weissman, I. L. 1988. Endoproteolytic cleavage of gp160 is required for the activation of human immunodeficiency virus. Cell, 53(1), 55-67.

McDougal, J. S., Kennedy, M. S., Sligh, J. M., Cort, S. P., Mawle, A., and Nicholson, J. K. 1986. Binding of HTLV-III/LAV to T4+ T cells by a complex of the 110K viral protein and the T4 molecule. Science, 231(4736), 382-385.

McLellan, J. S., Pancera, M., Carrico, C., Gorman, J., Julien, J. P., Khayat, R., Louder, R., Pejchal, R., Sastry, M., Dai, K., O'Dell, S., Patel, N., Shahzad-ul-Hussan, S., Yang, Y., Zhang, B., Zhou, T., Zhu, J., Boyington, J. C., Chuang, G. Y., Diwanji, D., Georgiev, I., Kwon, Y. D., Lee, D., Louder, M. K., Moquin, S., Schmidt, S. D., Yang, Z. Y., Bonsignori, M., Crump, J. A., Kapiga, S. H., Sam, N. E., Haynes, B. F., Burton, D. R., Koff, W. C., Walker, L. M., Phogat, S., Wyatt, R., Orwenyo, J., Wang, L. X., Arthos, J., Bewley, C. A., Mascola, J. R., Nabel, G. J., Schief, W. R., Ward, A. B., Wilson, I. A., and Kwong, P. D. 2011. Structure of HIV-1 gp120 V1/V2 domain with broadly neutralizing antibody PG9. Nature, 480(7377), 336-343.

Melikyan, G. B., Markosyan, R. M., Hemmati, H., Delmedico, M. K., Lambert, D. M., and Cohen, F. S. 2000. Evidence that the transition of HIV-1 gp41 into a six-helix bundle, not the bundle configuration, induces membrane fusion. J Cell Biol, 151(2), 413-423.

Mild, M., Esbjornsson, J., Fenyo, E. M., and Medstrand, P. 2007. Frequent intrapatient recombination between human immunodeficiency virus type 1 R5 and X4 envelopes: implications for coreceptor switch. J Virol, 81(7), 3369-3376.

Milich, L., Margolin, B. H., and Swanstrom, R. 1997. Patterns of amino acid variability in NSI-like and SI-like V3 sequences and a linked change in the CD4-binding domain of the HIV-1 Env protein. Virology, 239(1), 108-118.

Miller, M. D., Feinberg, M. B., and Greene, W. C. 1994. The HIV-1 nef gene acts as a positive viral infectivity factor. Trends Microbiol, 2(8), 294-298.

Miyauchi, K., Kim, Y., Latinovic, O., Morozov, V., and Melikyan, G. B. 2009. HIV enters cells via endocytosis and dynamin-dependent fusion with endosomes. Cell, 137(3), 433-444.

Mizutani, S., Boettiger, D., and Temin, H. M. 1970. A DNA-depenent DNA polymerase and a DNA endonuclease in virions of Rous sarcoma virus. Nature, 228(5270), 424-427.

Mori, K., Rosenzweig, M., and Desrosiers, R. C. 2000. Mechanisms for adaptation of simian immunodeficiency virus to replication in alveolar macrophages. J Virol, 74(22), 10852-10859.

Munoz-Barroso, I., Salzwedel, K., Hunter, E., and Blumenthal, R. 1999. Role of the membrane-proximal domain in the initial stages of human immunodeficiency virus type 1 envelope glycoprotein-mediated membrane fusion. J Virol, 73(7), 6089-6092.

Musich, T., Peters, P. J., Duenas-Decamp, M. J., Gonzalez-Perez, M. P., Robinson, J., Zolla-Pazner, S., Ball, J. K., Luzuriaga, K., and Clapham, P. R. 2011. A conserved determinant in the V1 loop of HIV-1 modulates the V3 loop to prime low CD4 use and macrophage infection. J Virol, 85(5), 2397-2405.

Neil, S. J., Zang, T., and Bieniasz, P. D. 2008. Tetherin inhibits retrovirus release and is antagonized by HIV-1 Vpu. Nature, 451(7177), 425-430.

Nelson, J. A., Baribaud, F., Edwards, T., and Swanstrom, R. 2000. Patterns of changes in human immunodeficiency virus type 1 V3 sequence populations late in infection. J Virol, 74(18), 8494-8501.

Nelson, J. A., Fiscus, S. A., and Swanstrom, R. 1997. Evolutionary variants of the human immunodeficiency virus type 1 V3 region characterized by using a heteroduplex tracking assay. J Virol, 71(11), 8750-8758.

NIH. 2016. HIV treatment. Retrieved from: https://aidsinfo.nih.gov/education-materials/fact-sheets/21/58/fda-approved-hiv-medicines.

Nowacek, A., and Gendelman, H. E. 2009. NanoART, neuroAIDS and CNS drug delivery. Nanomedicine (Lond), 4(5), 557-574.

Nowak, M. A., Bonhoeffer, S., Shaw, G. M., and May, R. M. 1997. Anti-viral drug treatment: dynamics of resistance in free virus and infected cell populations. J Theor Biol, 184(2), 203-217.

O'Brien, W. A., Koyanagi, Y., Namazie, A., Zhao, J. Q., Diagne, A., Idler, K., Zack, J. A., and Chen, I. S. 1990. HIV-1 tropism for mononuclear phagocytes can be determined by regions of gp120 outside the CD4-binding domain. Nature, 348(6296), 69-73.

Ochsenbauer, C., Edmonds, T. G., Ding, H., Keele, B. F., Decker, J., Salazar, M. G., Salazar-Gonzalez, J. F., Shattock, R., Haynes, B. F., Shaw, G. M., Hahn, B. H., and Kappes, J. C. 2012. Generation of transmitted/founder HIV-1 infectious molecular clones and characterization of their replication capacity in CD4 T lymphocytes and monocyte derived macrophages. J Virol, 86(5), 2715-2728.

O'Connell, O., Repik, A., Reeves, J. D., Gonzalez-Perez, M. P., Quitadamo, B., Anton, E. D., Duenas-Decamp, M., Peters, P., Lin, R., Zolla-Pazner, S., Corti, D., Wallace, A., Wang, S., Kong, X. P., Lu, S., and Clapham, P. R. 2013. Efficiency of bridging-sheet recruitment explains HIV-1 R5 envelope glycoprotein sensitivity to soluble CD4 and macrophage tropism. J Virol, 87(1), 187-198.

Olshevsky, U., Helseth, E., Furman, C., Li, J., Haseltine, W., and Sodroski, J. 1990. Identification of individual human immunodeficiency virus type 1 gp120 amino acids important for CD4 receptor binding. J Virol, 64(12), 5701-5707.

Paxton, W., Connor, R. I., and Landau, N. R. 1993. Incorporation of Vpr into human immunodeficiency virus type 1 virions: requirement for the p6 region of gag and mutational analysis. J Virol, 67(12), 7229-7237.

Pear, W. S., Nolan, G. P., Scott, M. L., and Baltimore, D. 1993. Production of high-titer helper-free retroviruses by transient transfection. Proc Natl Acad Sci U S A, 90(18), 8392-8396.

Peterlin, B. M., and Trono, D. 2003. Hide, shield and strike back: how HIV-infected cells avoid immune eradication. Nat Rev Immunol, 3(2), 97-107.

Peters, P. J., Bhattacharya, J., Hibbitts, S., Dittmar, M. T., Simmons, G., Bell, J., Simmonds, P., and Clapham, P. R. 2004. Biological analysis of human immunodeficiency virus type 1 R5 envelopes amplified from brain and lymph node tissues of AIDS patients with neuropathology reveals two distinct tropism phenotypes and identifies envelopes in the brain that confer an enhanced tropism and fusigenicity for macrophages. J Virol, 78(13), 6915-6926.

Peters, P. J., Duenas-Decamp, M. J., Sullivan, W. M., Brown, R., Ankghuambom, C., Luzuriaga, K., Robinson, J., Burton, D. R., Bell, J., Simmonds, P., Ball, J., and Clapham, P. R. 2008. Variation in HIV-1 R5 macrophage-tropism correlates with sensitivity to reagents that block envelope: CD4 interactions but not with sensitivity to other entry inhibitors. Retrovirology, 5, 5.

Peters, P. J., Duenas-Decamp, M. J., Sullivan, W. M., and Clapham, P. R. 2007. Variation of macrophage tropism among HIV-1 R5 envelopes in brain and other tissues. J Neuroimmune Pharmacol, 2(1), 32-41.

Peters, P. J., Sullivan, W. M., Duenas-Decamp, M. J., Bhattacharya, J., Ankghuambom, C., Brown, R., Luzuriaga, K., Bell, J., Simmonds, P., Ball, J., and Clapham, P. R. 2006. Non-macrophage-tropic human immunodeficiency virus type 1 R5 envelopes predominate in blood, lymph nodes, and semen: implications for transmission and pathogenesis. J Virol, 80(13), 6324-6332.

Pfaff, J. M., Wilen, C. B., Harrison, J. E., Demarest, J. F., Lee, B., Doms, R. W., and Tilton, J. C. 2010. HIV-1 resistance to CCR5 antagonists associated with highly efficient use of CCR5 and altered tropism on primary CD4+ T cells. J Virol, 84(13), 6505-6514.

Plantier, J. C., Leoz, M., Dickerson, J. E., De Oliveira, F., Cordonnier, F., Lemee, V., Damond, F., Robertson, D. L., and Simon, F. 2009. A new human immunodeficiency virus derived from gorillas. Nat Med, 15(8), 871-872.

Platt, E. J., Bilska, M., Kozak, S. L., Kabat, D., and Montefiori, D. C. 2009. Evidence that ecotropic murine leukemia virus contamination in TZM-bl cells does not affect the outcome of neutralizing antibody assays with human immunodeficiency virus type 1. J Virol, 83(16), 8289-8292.

Platt, E. J., Wehrly, K., Kuhmann, S. E., Chesebro, B., and Kabat, D. 1998. Effects of CCR5 and CD4 cell surface concentrations on infections by macrophagetropic isolates of human immunodeficiency virus type 1. J Virol, 72(4), 2855-2864.

Pollakis, G., Baan, E., van Werkhoven, M. B., Berkhout, B., Bakker, M., Jurriaans, S., and Paxton, W. A. 2015. Association between gp120 envelope V1V2 and V4V5 variable loop profiles in a defined HIV-1 transmission cluster. AIDS, 29(10), 1161-1171.

Pollakis, G., Kang, S., Kliphuis, A., Chalaby, M. I., Goudsmit, J., and Paxton, W. A. 2001. N-linked glycosylation of the HIV type-1 gp120 envelope glycoprotein as a major determinant of CCR5 and CXCR4 coreceptor utilization. J Biol Chem, 276(16), 13433-13441.

Popovic, M., Sarngadharan, M. G., Read, E., and Gallo, R. C. 1984. Detection, isolation, and continuous production of cytopathic retroviruses (HTLV-III) from patients with AIDS and pre-AIDS. Science, 224(4648), 497-500.

Poznansky, M., Lever, A., Bergeron, L., Haseltine, W., and Sodroski, J. 1991. Gene transfer into human lymphocytes by a defective human immunodeficiency virus type 1 vector. J Virol, 65(1), 532-536.

Preston, B. D., Poiesz, B. J., and Loeb, L. A. 1988. Fidelity of HIV-1 reverse transcriptase. Science, 242(4882), 1168-1171.

Reeves, J. D., Gallo, S. A., Ahmad, N., Miamidian, J. L., Harvey, P. E., Sharron, M., Pohlmann, S., Sfakianos, J. N., Derdeyn, C. A., Blumenthal, R., Hunter, E., and Doms, R. W. 2002. Sensitivity of HIV-1 to entry inhibitors correlates with envelope/coreceptor affinity, receptor density, and fusion kinetics. Proc Natl Acad Sci U S A, 99(25), 16249-16254.

Reeves, J. D., Miamidian, J. L., Biscone, M. J., Lee, F. H., Ahmad, N., Pierson, T. C., and Doms, R. W. 2004. Impact of mutations in the coreceptor binding site on human immunodeficiency virus type 1 fusion, infection, and entry inhibitor sensitivity. J Virol, 78(10), 5476-5485.

Refsland, E. W., and Harris, R. S. 2013. The APOBEC3 family of retroelement restriction factors. Curr Top Microbiol Immunol, 371:1-27.

Refsland, E. W., Stenglein, M. D., Shindo, K., Albin, J. S., Brown, W. L., and Harris, R. S. 2010. Quantitative profiling of the full APOBEC3 mRNA repertoire in lymphocytes and tissues: implications for HIV-1 restriction. Nucleic Acids Res, 38(13), 4274-4284.

Repits, J., Oberg, M., Esbjornsson, J., Medstrand, P., Karlsson, A., Albert, J., Fenyo, E. M., and Jansson, M. 2005. Selection of human immunodeficiency virus type 1 R5 variants with augmented replicative capacity and reduced sensitivity to entry inhibitors during severe immunodeficiency. J Gen Virol, 86(Pt 10), 2859-2869.

Repits, J., Sterjovski, J., Badia-Martinez, D., Mild, M., Gray, L., Churchill, M. J., Purcell, D. F., Karlsson, A., Albert, J., Fenyo, E. M., Achour, A., Gorry, P. R., and Jansson, M. 2008. Primary HIV-1 R5 isolates from end-stage disease display enhanced viral fitness in parallel with increased gp120 net charge. Virology, 379(1), 125-134.

Rerks-Ngarm, S., Pitisuttithum, P., Nitayaphan, S., Kaewkungwal, J., Chiu, J., Paris, R., Premsri, N., Namwat, C., de Souza, M., Adams, E., Benenson, M., Gurunathan, S., Tartaglia, J., McNeil, J. G., Francis, D. P., Stablein, D., Birx, D. L., Chunsuttiwat, S., Khamboonruang, C., Thongcharoen, P., Robb, M. L., Michael, N. L., Kunasol, P., Kim, J. H., and MOPH–TAVEG Investigators. 2009. Vaccination with ALVAC and AIDSVAX to prevent HIV-1 infection in Thailand. N Engl J Med, 361(23), 2209-2220.

Resch, W., Hoffman, N., and Swanstrom, R. 2001. Improved success of phenotype prediction of the human immunodeficiency virus type 1 from envelope variable loop 3 sequence using neural networks. Virology, 288(1), 51-62.

Revilla, A., Delgado, E., Christian, E. C., Dalrymple, J., Vega, Y., Carrera, C., Gonzalez-Galeano, M., Ocampo, A., de Castro, R. O., Lezaun, M. J., Rodriguez, R., Marino, A., Ordonez, P., Cilla, G., Cisterna, R., Santamaria, J. M., Prieto, S., Rakhmanova, A., Vinogradova, A., Rios, M., Perez-Alvarez, L., Najera, R., Montefiori, D. C., Seaman, M. S., and Thomson, M. M. 2011. Construction and phenotypic characterization of HIV type 1 functional envelope clones of subtypes G and F. AIDS Res Hum Retroviruses, 27(8), 889-901.

Rhodes, T., Wargo, H., and Hu, W. S. 2003. High rates of human immunodeficiency virus type 1 recombination: near-random segregation of markers one kilobase apart in one round of viral replication. J Virol, 77(20), 11193-11200.

Richman, D. D., and Bozzette, S. A. 1994. The impact of the syncytium-inducing phenotype of human immunodeficiency virus on disease progression. J Infect Dis, 169(5), 968-974.

Roben, P., Moore, J. P., Thali, M., Sodroski, J., Barbas, C. F., 3rd, and Burton, D. R. 1994. Recognition properties of a panel of human recombinant Fab fragments to the CD4 binding site of gp120 that show differing abilities to neutralize human immunodeficiency virus type 1. J Virol, 68(8), 4821-4828.

Robert, D., Sallafranque-Andreola, M. L., Bordier, B., Sarih-Cottin, L., Tarrago-Litvak, L., Graves, P. V., Barr, P. J., Fournier, M., and Litvak, S. 1990. Interactions with tRNA(Lys) induce important structural changes in human immunodeficiency virus reverse transcriptase. FEBS Lett, 277(1-2), 239-242.

Rogel, M. E., Wu, L. I., and Emerman, M. 1995. The human immunodeficiency virus type 1 vpr gene prevents cell proliferation during chronic infection. J Virol, 69(2), 882-888.

Rosa, A., Chande, A., Ziglio, S., De Sanctis, V., Bertorelli, R., Goh, S. L., McCauley, S. M., Nowosielska, A., Antonarakis, S. E., Luban, J., Santoni, F. A., and Pizzato, M. 2015. HIV-1 Nef promotes infection by excluding SERINC5 from virion incorporation. Nature, 526(7572), 212-217.

Rose, P. P., and Korber, B. T. 2000. Detecting hypermutations in viral sequences with an emphasis on G --> A hypermutation. Bioinformatics, 16(4), 400-401.

Roy, S., Delling, U., Chen, C. H., Rosen, C. A., and Sonenberg, N. 1990. A bulge structure in HIV-1 TAR RNA is required for Tat binding and Tat-mediated trans-activation. Genes Dev, 4(8), 1365-1373.

Ruben, S., Perkins, A., Purcell, R., Joung, K., Sia, R., Burghoff, R., Haseltine, W. A., and Rosen, C. A. 1989. Structural and functional characterization of human immunodeficiency virus tat protein. J Virol, 63(1), 1-8.

Sagar, M., Wu, X., Lee, S., and Overbaugh, J. 2006. Human immunodeficiency virus type 1 V1-V2 envelope loop sequences expand and add glycosylation sites over the course of infection, and these modifications affect antibody neutralization sensitivity. J Virol, 80(19), 9586-9598.

Salazar-Gonzalez, J. F., Bailes, E., Pham, K. T., Salazar, M. G., Guffey, M. B., Keele, B. F., Derdeyn, C. A., Farmer, P., Hunter, E., Allen, S., Manigart, O., Mulenga, J., Anderson, J. A., Swanstrom, R., Haynes, B. F., Athreya, G. S., Korber, B. T., Sharp, P. M., Shaw, G. M., and Hahn, B. H. 2008. Deciphering human immunodeficiency virus type 1 transmission and early envelope diversification by single-genome amplification and sequencing. J Virol, 82(8), 3952-3970.

Salazar-Gonzalez, J. F., Salazar, M. G., Keele, B. F., Learn, G. H., Giorgi, E. E., Li, H., Decker, J. M., Wang, S., Baalwa, J., Kraus, M. H., Parrish, N. F., Shaw, K. S., Guffey, M. B., Bar, K. J., Davis, K. L., Ochsenbauer-Jambor, C., Kappes, J. C., Saag, M. S., Cohen, M. S., Mulenga, J., Derdeyn, C. A., Allen, S., Hunter, E., Markowitz, M., Hraber, P., Perelson, A. S., Bhattacharya, T., Haynes, B. F., Korber, B. T., Hahn, B. H., and Shaw, G. M. 2009. Genetic identity, biological phenotype, and evolutionary pathways of transmitted/founder viruses in acute and early HIV-1 infection. J Exp Med, 206(6), 1273-1289.

Salzwedel, K., West, J. T., and Hunter, E. 1999. A conserved tryptophan-rich motif in the membrane-proximal region of the human immunodeficiency virus type 1 gp41 ectodomain is important for Env-mediated fusion and virus infectivity. J Virol, 73(3), 2469-2480.

Sanborn, K. B., Somasundaran, M., Luzuriaga, K., and Leitner, T. 2015. Recombination elevates the effective evolutionary rate and facilitates the establishment of HIV-1 infection in infants after mother-to-child transmission. Retrovirology, 12, 96.

Schiffner, T., Sattentau, Q. J., and Dorrell, L. 2013. Development of prophylactic vaccines against HIV-1. Retrovirology, 10, 72.

Schnell, G., Price, R. W., Swanstrom, R., and Spudich, S. 2010. Compartmentalization and clonal amplification of HIV-1 variants in the cerebrospinal fluid during primary infection. J Virol, 84(5), 2395-2407.

Schwartz, O., Marechal, V., Le Gall, S., Lemonnier, F., and Heard, J. M. 1996. Endocytosis of major histocompatibility complex class I molecules is induced by the HIV-1 Nef protein. Nat Med, 2(3), 338-342.

Seclen, E., Soriano, V., del Mar Gonzalez, M., Gonzalez-Lahoz, J., and Poveda, E. 2011. Short communication: severe immune suppression in patients infected with R5-tropic HIV-1 strains is associated with increased gp120 net charge at variable regions. AIDS Res Hum Retroviruses, 27(9), 965-967.

Sen, J., Jacobs, A., Jiang, H., Rong, L., and Caffrey, M. 2007. The disulfide loop of gp41 is critical to the furin recognition site of HIV gp160. Protein Sci, 16(6), 1236-1241.

Shankarappa, R., Margolick, J. B., Gange, S. J., Rodrigo, A. G., Upchurch, D., Farzadegan, H., Gupta, P., Rinaldo, C. R., Learn, G. H., He, X., Huang, X. L., and Mullins, J. I. 1999. Consistent viral evolutionary changes associated with the progression of human immunodeficiency virus type 1 infection. J Virol, 73(12), 10489-10502.

Sheehy, A. M., Gaddis, N. C., Choi, J. D., and Malim, M. H. 2002. Isolation of a human gene that inhibits HIV-1 infection and is suppressed by the viral Vif protein. Nature, 418(6898), 646-650.

Sheehy, A. M., Gaddis, N. C., and Malim, M. H. 2003. The antiretroviral enzyme APOBEC3G is degraded by the proteasome in response to HIV-1 Vif. Nat Med, 9(11), 1404-1407.

Shioda, T., Levy, J. A., and Cheng-Mayer, C. 1991. Macrophage and T cell-line tropisms of HIV-1 are determined by specific regions of the envelope gp120 gene. Nature, 349(6305), 167-169.

Siegal, F. P., Lopez, C., Hammer, G. S., Brown, A. E., Kornfeld, S. J., Gold, J., Hassett, J., Hirschman, S. Z., Cunningham-Rundles, C., Adelsberg, B. R., Parham, D. M., Siegal, M., Cunningham-Rundles, S., and Armstrong, D. 1981. Severe acquired immunodeficiency in male homosexuals, manifested by chronic perianal ulcerative herpes simplex lesions. N Engl J Med, 305(24), 1439-1444.

Simmons, G., Reeves, J. D., McKnight, A., Dejucq, N., Hibbitts, S., Power, C. A., Aarons, E., Schols, D., De Clercq, E., Proudfoot, A. E., and Clapham, P. R. 1998.

CXCR4 as a functional coreceptor for human immunodeficiency virus type 1 infection of primary macrophages. J Virol, 72(10), 8453-8457.

Simmons, G., Wilkinson, D., Reeves, J. D., Dittmar, M. T., Beddows, S., Weber, J., Carnegie, G., Desselberger, U., Gray, P. W., Weiss, R. A., and Clapham, P. R. 1996. Primary, syncytium-inducing human immunodeficiency virus type 1 isolates are dual-tropic and most can use either Lestr or CCR5 as coreceptors for virus entry. J Virol, 70(12), 8355-8360.

Simon, F., Mauclere, P., Roques, P., Loussert-Ajaka, I., Muller-Trutwin, M. C., Saragosti, S., Georges-Courbot, M. C., Barre-Sinoussi, F., and Brun-Vezinet, F. 1998. Identification of a new human immunodeficiency virus type 1 distinct from group M and group O. Nat Med, 4(9), 1032-1037.

Sing, T., Low, A. J., Beerenwinkel, N., Sander, O., Cheung, P. K., Domingues, F. S., Buch, J., Daumer, M., Kaiser, R., Lengauer, T., and Harrigan, P. R. 2007. Predicting HIV coreceptor usage on the basis of genetic and clinical covariates. Antivir Ther, 12(7), 1097-1106.

Slatkin, M., and Maddison, W.P. 1989 A cladistic measure of gene flow inferred from phylogenies of alleles. Genetics, 123(3), 603–613.

Stanfield, R. L., Gorny, M. K., Williams, C., Zolla-Pazner, S., and Wilson, I. A. 2004. Structural rationale for the broad neutralization of HIV-1 by human monoclonal antibody 447-52D. Structure, 12(2), 193-204.

Starcich, B. R., Hahn, B. H., Shaw, G. M., McNeely, P. D., Modrow, S., Wolf, H., Parks, E. S., Parks, W. P., Josephs, S. F., Gallo, R. C., and Wong-Staal, F. 1986. Identification and characterization of conserved and variable regions in the envelope gene of HTLV-III/LAV, the retrovirus of AIDS. Cell, 45(5), 637-648.

Staszewski, S., Loveday, C., Picazo, J. J., Dellarnonica, P., Skinhoj, P., Johnson, M. A., Danner, S. A., Harrigan, P. R., Hill, A. M., Verity, L., and McDade, H. 1996. Safety and efficacy of lamivudine-zidovudine combination therapy in zidovudine-experienced patients. A randomized controlled comparison with zidovudine monotherapy. Lamivudine European HIV Working Group. JAMA, 276(2), 111-117.

Stengel, R. F. 2008. Mutation and control of the human immunodeficiency virus. Math Biosci, 213(2), 93-102.

Strack, B., Calistri, A., Craig, S., Popova, E., and Gottlinger, H. G. 2003. AIP1/ALIX is a binding partner for HIV-1 p6 and EIAV p9 functioning in virus budding. Cell, 114(6), 689-699.

Strebel, K., Klimkait, T., and Martin, M. A. 1988. A novel gene of HIV-1, vpu, and its 16-kilodalton product. Science, 241(4870), 1221-1223.

Sturdevant, C. B., Joseph, S. B., Schnell, G., Price, R. W., Swanstrom, R., and Spudich, S. 2015. Compartmentalized replication of R5 T cell-tropic HIV-1 in the central nervous system early in the course of infection. PLoS Pathog, 11(3).

Sullivan, N., Sun, Y., Sattentau, Q., Thali, M., Wu, D., Denisova, G., Gershoni, J., Robinson, J., Moore, J., and Sodroski, J. 1998. CD4-Induced conformational changes in the human immunodeficiency virus type 1 gp120 glycoprotein: consequences for virus entry and neutralization. J Virol, 72(6), 4694-4703.

Takehisa, J., Kraus, M. H., Ayouba, A., Bailes, E., Van Heuverswyn, F., Decker, J. M., Li, Y., Rudicell, R. S., Learn, G. H., Neel, C., Ngole, E. M., Shaw, G. M., Peeters, M., Sharp, P. M., and Hahn, B. H. 2009. Origin and biology of simian immunodeficiency virus in wild-living western gorillas. J Virol, 83(4), 1635-1648.

Takeuchi, Y., McClure, M. O., and Pizzato, M. 2008. Identification of gammaretroviruses constitutively released from cell lines used for human immunodeficiency virus research. J Virol, 82(24), 12585-12588.

Tamura, K., Peterson, D., Peterson, N., Stecher, G., Nei, M., and Kumar, S. 2011. MEGA5: Molecular Evolutionary Genetics Analysis using Maximum Likelihood, Evolutionary Distance, and Maximum Parsimony Methods. Mol Biol Evol, 28: 2731-2739.

Tersmette, M., de Goede, R. E., Al, B. J., Winkel, I. N., Gruters, R. A., Cuypers, H. T., Huisman, H. G., and Miedema, F. 1988. Differential syncytium-inducing capacity of human immunodeficiency virus isolates: frequent detection of syncytium-inducing isolates in patients with acquired immunodeficiency syndrome (AIDS) and AIDS-related complex. J Virol, 62(6), 2026-2032.

Tersmette, M., Gruters, R. A., de Wolf, F., de Goede, R. E., Lange, J. M., Schellekens, P. T., Goudsmit, J., Huisman, H. G., and Miedema, F. 1989. Evidence for a role of virulent human immunodeficiency virus (HIV) variants in the pathogenesis of acquired immunodeficiency syndrome: studies on sequential HIV isolates. J Virol, 63(5), 2118-2125.

Thali, M., Bukovsky, A., Kondo, E., Rosenwirth, B., Walsh, C. T., Sodroski, J., and Gottlinger, H. G. 1994. Functional association of cyclophilin A with HIV-1 virions. Nature, 372(6504), 363-365.

Thali, M., Moore, J. P., Furman, C., Charles, M., Ho, D. D., Robinson, J., and Sodroski, J. 1993. Characterization of conserved human immunodeficiency virus

type 1 gp120 neutralization epitopes exposed upon gp120-CD4 binding. J Virol, 67(7), 3978-3988.

Thomas, E. R., Dunfee, R. L., Stanton, J., Bogdan, D., Taylor, J., Kunstman, K., Bell, J. E., Wolinsky, S. M., and Gabuzda, D. 2007. Macrophage entry mediated by HIV Envs from brain and lymphoid tissues is determined by the capacity to use low CD4 levels and overall efficiency of fusion. Virology, 360(1), 105-119.

Tilton, J. C., Amrine-Madsen, H., Miamidian, J. L., Kitrinos, K. M., Pfaff, J., Demarest, J. F., Ray, N., Jeffrey, J. L., Labranche, C. C., and Doms, R. W. 2010. HIV type 1 from a patient with baseline resistance to CCR5 antagonists uses drug-bound receptor for entry. AIDS Res Hum Retroviruses, 26(1), 13-24.

Todd, B. J., Kedar, P., and Pope, J. H. 1995. Syncytium induction in primary CD4+ T-cell lines from normal donors by human immunodeficiency virus type 1 isolates with non-syncytium-inducing genotype and phenotype in MT-2 cells. J Virol, 69(11), 7099-7105.

Triguero, D., Buciak, J. B., Yang, J., and Pardridge, W. M. 1989. Blood-brain barrier transport of cationized immunoglobulin G: enhanced delivery compared to native protein. Proc Natl Acad Sci U S A, 86(12), 4761-4765.

Trkola, A., Dragic, T., Arthos, J., Binley, J. M., Olson, W. C., Allaway, G. P., Cheng-Mayer, C., Robinson, J., Maddon, P. J., and Moore, J. P. 1996. CD4-dependent, antibody-sensitive interactions between HIV-1 and its co-receptor CCR-5. Nature, 384(6605), 184-187.

Tuttle, D. L., Anders, C. B., Aquino-De Jesus, M. J., Poole, P. P., Lamers, S. L., Briggs, D. R., Pomeroy, S. M., Alexander, L., Peden, K. W., Andiman, W. A., Sleasman, J. W., and Goodenow, M. M. 2002. Increased replication of non-syncytium-inducing HIV type 1 isolates in monocyte derived macrophages is linked to advanced disease in infected children. AIDS Res Hum Retroviruses, 18(5), 353-362.

Tyor, W., Fritz-French, C., and Nath, A. 2013. Effect of HIV clade differences on the onset and severity of HIV-associated neurocognitive disorders. J Neurovirol, 19(6), 515-522.

UNAIDS. 2016. 90–90–90 - An ambitious treatment target to help end the AIDS epidemic. Retrieved from: http://www.unaids.org/en/resources/documents/2014/90-90-90.

Usami, Y., Wu, Y., and Gottlinger, H. G. 2015. SERINC3 and SERINC5 restrict HIV-1 infectivity and are counteracted by Nef. Nature, 526(7572), 218-223.

Vallari, A., Bodelle, P., Ngansop, C., Makamche, F., Ndembi, N., Mbanya, D., Kaptue, L., Gurtler, L. G., McArthur, C. P., Devare, S. G., and Brennan, C. A. 2010. Four new HIV-1 group N isolates from Cameroon: Prevalence continues to be low. AIDS Res Hum Retroviruses, 26(1), 109-115.

Vallari, A., Holzmayer, V., Harris, B., Yamaguchi, J., Ngansop, C., Makamche, F., Mbanya, D., Kaptue, L., Ndembi, N., Gurtler, L., Devare, S., and Brennan, C. A. 2011. Confirmation of putative HIV-1 group P in Cameroon. J Virol, 85(3), 1403-1407.

Van Damme, N., Goff, D., Katsura, C., Jorgenson, R. L., Mitchell, R., Johnson, M. C., Stephens, E. B., and Guatelli, J. 2008. The interferon-induced protein BST-2 restricts HIV-1 release and is downregulated from the cell surface by the viral Vpu protein. Cell Host Microbe, 3(4), 245-252.

Van Heuverswyn, F., Li, Y., Neel, C., Bailes, E., Keele, B. F., Liu, W., Loul, S., Butel, C., Liegeois, F., Bienvenue, Y., Ngolle, E. M., Sharp, P. M., Shaw, G. M., Delaporte, E., Hahn, B. H., and Peeters, M. 2006. Human immunodeficiency viruses: SIV infection in wild gorillas. Nature, 444(7116), 164.

van't Wout, A. B., Ran, L. J., Kuiken, C. L., Kootstra, N. A., Pals, S. T., and Schuitemaker, H. 1998. Analysis of the temporal relationship between human immunodeficiency virus type 1 quasispecies in sequential blood samples and various organs obtained at autopsy. J Virol, 72(1), 488-496.

Varatharajan, L., and Thomas, S. A. 2009. The transport of anti-HIV drugs across blood-CNS interfaces: summary of current knowledge and recommendations for further research. Antiviral Res, 82(2), A99-109.

Vazquez-Santiago, F., Garcia, Y., Rivera-Roman, I., Noel, R. J., Jr., Wojna, V., Melendez, L. M., and Rivera-Amill, V. 2015. Longitudinal analysis of cerebrospinal fluid and plasma HIV-1 envelope sequences isolated from a single donor with HIV asymptomatic neurocognitive impairment. J Virol Antivir Res, 4(1).

Veazey, R. S., DeMaria, M., Chalifoux, L. V., Shvetz, D. E., Pauley, D. R., Knight, H. L., Rosenzweig, M., Johnson, R. P., Desrosiers, R. C., and Lackner, A. A. 1998. Gastrointestinal tract as a major site of CD4+ T cell depletion and viral replication in SIV infection. Science, 280(5362), 427-431.

von Schwedler, U., Song, J., Aiken, C., and Trono, D. 1993. Vif is crucial for human immunodeficiency virus type 1 proviral DNA synthesis in infected cells. J Virol, 67(8), 4945-4955.

Walker, L. M., Phogat, S. K., Chan-Hui, P. Y., Wagner, D., Phung, P., Goss, J. L., Wrin, T., Simek, M. D., Fling, S., Mitcham, J. L., Lehrman, J. K., Priddy, F. H., Olsen, O. A., Frey, S. M., Hammond, P. W., Protocol, G. P. I., Kaminsky, S., Zamb, T., Moyle, M., Koff, W. C., Poignard, P., and Burton, D. R. 2009. Broad and potent neutralizing antibodies from an African donor reveal a new HIV-1 vaccine target. Science, 326(5950), 285-289.

Walter, B. L., Wehrly, K., Swanstrom, R., Platt, E., Kabat, D., and Chesebro, B. 2005. Role of low CD4 levels in the influence of human immunodeficiency virus type 1 envelope V1 and V2 regions on entry and spread in macrophages. J Virol, 79(8), 4828-4837.

Wang, T. H., Donaldson, Y. K., Brettle, R. P., Bell, J. E., and Simmonds, P. 2001. Identification of shared populations of human immunodeficiency virus type 1 infecting microglia and tissue macrophages outside the central nervous system. J Virol, 75(23), 11686-11699.

Wang, W., Nie, J., Prochnow, C., Truong, C., Jia, Z., Wang, S., Chen, X. S., and Wang, Y. 2013. A systematic study of the N-glycosylation sites of HIV-1 envelope protein on infectivity and antibody-mediated neutralization. Retrovirology, 10, 14.

Wei, X., Decker, J. M., Liu, H., Zhang, Z., Arani, R. B., Kilby, J. M., Saag, M. S., Wu, X., Shaw, G. M., and Kappes, J. C. 2002. Emergence of resistant human immunodeficiency virus type 1 in patients receiving fusion inhibitor (T-20) monotherapy. Antimicrob Agents Chemother, 46(6), 1896-1905.

Wei, X., Decker, J. M., Wang, S., Hui, H., Kappes, J. C., Wu, X., Salazar-Gonzalez, J. F., Salazar, M. G., Kilby, J. M., Saag, M. S., Komarova, N. L., Nowak, M. A., Hahn, B. H., Kwong, P. D., and Shaw, G. M. 2003. Antibody neutralization and escape by HIV-1. Nature, 422(6929), 307-312.

Wei, X., Ghosh, S. K., Taylor, M. E., Johnson, V. A., Emini, E. A., Deutsch, P., Lifson, J. D., Bonhoeffer, S., Nowak, M. A., Hahn, B. H., Saag, M. S., and Shaw, G. M. 1995. Viral dynamics in human immunodeficiency virus type 1 infection. Nature, 373(6510), 117-122.

Weissenhorn, W., Dessen, A., Harrison, S. C., Skehel, J. J., and Wiley, D. C. 1997. Atomic structure of the ectodomain from HIV-1 gp41. Nature, 387(6631), 426-430.

Westby, M., Smith-Burchnell, C., Mori, J., Lewis, M., Mosley, M., Stockdale, M., Dorr, P., Ciaramella, G., and Perros, M. 2007. Reduced maximal inhibition in phenotypic susceptibility assays indicates that viral strains resistant to the CCR5

antagonist maraviroc utilize inhibitor-bound receptor for entry. J Virol, 81(5), 2359-2371.

WHO. 2016. HIV/AIDS. Retrieved from: http://www.who.int/mediacentre/factsheets/fs360/en/.

Wilen, C. B., Parrish, N. F., Pfaff, J. M., Decker, J. M., Henning, E. A., Haim, H., Petersen, J. E., Wojcechowskyj, J. A., Sodroski, J., Haynes, B. F., Montefiori, D. C., Tilton, J. C., Shaw, G. M., Hahn, B. H., and Doms, R. W. 2011. Phenotypic and immunologic comparison of clade B transmitted/founder and chronic HIV-1 envelope glycoproteins. J Virol, 85(17), 8514-8527.

Willey, R. L., Maldarelli, F., Martin, M. A., and Strebel, K. 1992. Human immunodeficiency virus type 1 Vpu protein induces rapid degradation of CD4. J Virol, 66(12), 7193-7200.

Willey, R. L., Rutledge, R. A., Dias, S., Folks, T., Theodore, T., Buckler, C. E., and Martin, M. A. 1986. Identification of conserved and divergent domains within the envelope gene of the acquired immunodeficiency syndrome retrovirus. Proc Natl Acad Sci U S A, 83(14), 5038-5042.

Wolinsky, S. M., Korber, B. T., Neumann, A. U., Daniels, M., Kunstman, K. J., Whetsell, A. J., Furtado, M. R., Cao, Y., Ho, D. D., and Safrit, J. T. 1996. Adaptive evolution of human immunodeficiency virus-type 1 during the natural course of infection. Science, 272(5261), 537-542.

Wong, J. K., Ignacio, C. C., Torriani, F., Havlir, D., Fitch, N. J., and Richman, D. D. 1997. In vivo compartmentalization of human immunodeficiency virus: evidence from the examination of pol sequences from autopsy tissues. J Virol, 71(3), 2059-2071.

Wood, A., and Armour, D. 2005. The discovery of the CCR5 receptor antagonist, UK-427,857, a new agent for the treatment of HIV infection and AIDS. Prog Med Chem, 43, 239-271.

Worobey, M., Gemmel, M., Teuwen, D. E., Haselkorn, T., Kunstman, K., Bunce, M., Muyembe, J. J., Kabongo, J. M., Kalengayi, R. M., Van Marck, E., Gilbert, M. T., and Wolinsky, S. M. 2008. Direct evidence of extensive diversity of HIV-1 in Kinshasa by 1960. Nature, 455(7213), 661-664.

Wyatt, R., Kwong, P. D., Desjardins, E., Sweet, R. W., Robinson, J., Hendrickson, W. A., and Sodroski, J. G. 1998. The antigenic structure of the HIV gp120 envelope glycoprotein. Nature, 393(6686), 705-711.

Wyatt, R., Moore, J., Accola, M., Desjardin, E., Robinson, J., and Sodroski, J. 1995. Involvement of the V1/V2 variable loop structure in the exposure of human immunodeficiency virus type 1 gp120 epitopes induced by receptor binding. J Virol, 69(9), 5723-5733.

Yang, C., Pieniazek, D., Owen, S. M., Fridlund, C., Nkengasong, J., Mastro, T. D., Rayfield, M. A., Downing, R., Biryawaho, B., Tanuri, A., Zekeng, L., van der Groen, G., Gao, F., and Lal, R. B. 1999. Detection of phylogenetically diverse human immunodeficiency virus type 1 groups M and O from plasma by using highly sensitive and specific generic primers. J Clin Microbiol, 37(8), 2581-2586.

Yi, Y., Chen, W., Frank, I., Cutilli, J., Singh, A., Starr-Spires, L., Sulcove, J., Kolson, D. L., and Collman, R. G. 2003. An unusual syncytia-inducing human immunodeficiency virus type 1 primary isolate from the central nervous system that is restricted to CXCR4, replicates efficiently in macrophages, and induces neuronal apoptosis. J Neurovirol, 9(4), 432-441.

Yi, Y., Isaacs, S. N., Williams, D. A., Frank, I., Schols, D., De Clercq, E., Kolson, D. L., and Collman, R. G. 1999. Role of CXCR4 in cell-cell fusion and infection of monocyte derived macrophages by primary human immunodeficiency virus type 1 (HIV-1) strains: two distinct mechanisms of HIV-1 dual tropism. J Virol, 73(9), 7117-7125.

Yu, X., Yu, Y., Liu, B., Luo, K., Kong, W., Mao, P., and Yu, X. F. 2003. Induction of APOBEC3G ubiquitination and degradation by an HIV-1 Vif-Cul5-SCF complex. Science, 302(5647), 1056-1060.

Zapp, M. L., and Green, M. R. 1989. Sequence-specific RNA binding by the HIV-1 Rev protein. Nature, 342(6250), 714-716.

Zhang, H., Yang, B., Pomerantz, R. J., Zhang, C., Arunachalam, S. C., and Gao, L. 2003. The cytidine deaminase CEM15 induces hypermutation in newly synthesized HIV-1 DNA. Nature, 424(6944), 94-98.

Zhang, M., Foley, B., Schultz, A. K., Macke, J. P., Bulla, I., Stanke, M., Morgenstern, B., Korber, B., and Leitner, T. 2010. The role of recombination in the emergence of a complex and dynamic HIV epidemic. Retrovirology, 7, 25.

Zhang, M., Gaschen, B., Blay, W., Foley, B., Haigwood, N., Kuiken, C., and Korber, B. 2004. Tracking global patterns of N-linked glycosylation site variation in highly variable viral glycoproteins: HIV, SIV, and HCV envelopes and influenza hemagglutinin. Glycobiology, 14(12), 1229-1246.

Zhang, Z., Schuler, T., Zupancic, M., Wietgrefe, S., Staskus, K. A., Reimann, K. A., Reinhart, T. A., Rogan, M., Cavert, W., Miller, C. J., Veazey, R. S., Notermans, D., Little, S., Danner, S. A., Richman, D. D., Havlir, D., Wong, J., Jordan, H. L., Schacker, T. W., Racz, P., Tenner-Racz, K., Letvin, N. L., Wolinsky, S., and Haase, A. T. 1999. Sexual transmission and propagation of SIV and HIV in resting and activated CD4+ T cells. Science, 286(5443), 1353-1357.

Zhu, T., Korber, B. T., Nahmias, A. J., Hooper, E., Sharp, P. M., and Ho, D. D. 1998. An African HIV-1 sequence from 1959 and implications for the origin of the epidemic. Nature, 391(6667), 594-597.

Zolla-Pazner, S., O'Leary, J., Burda, S., Gorny, M. K., Kim, M., Mascola, J., and McCutchan, F. 1995. Serotyping of primary human immunodeficiency virus type 1 isolates from diverse geographic locations by flow cytometry. J Virol, 69(6), 3807-3815.